Draft version August 3, 2020
Typeset using LaTeX **preprint** style in AASTeX62

Discovering New Strong Gravitational Lenses in the DESI Legacy Imaging Surveys

X. Huang,[1] C. Storfer,[1] A. Gu,[2,3] V. Ravi,[4] A. Pilon,[1] W. Sheu,[2,3] R. Venguswamy,[5] S. Banka,[3] A. Dey,[6] M. Landriau,[7] D. Lang,[8,9,10] A. Meisner,[6] J. Moustakas,[11] A.D. Myers,[12] R. Sajith,[2,3] E.F. Schlafly,[13] and D.J. Schlegel[7]

[1]*Department of Physics & Astronomy, University of San Francisco, San Francisco, CA 94117-1080*
[2]*Department of Physics, University of California, Berkeley, Berkeley, CA 94720*
[3]*Department of Electrical Engineering & Computer Sciences, University of California, Berkeley, Berkeley, CA 94720*
[4]*Department of Computer Science, University of San Francisco, San Francisco, CA 94117-1080*
[5]*Department of Computing, Data Science, and Society, University of California, Berkeley, Berkeley, CA 94720*
[6]*NSF's National Optical-Infrared Astronomy Research Laboratory, 950 N. Cherry Ave., Tucson, AZ 85719*
[7]*Physics Division, Lawrence Berkeley National Laboratory, 1 Cyclotron Road, Berkeley, CA, 94720*
[8]*Dunlap Institute, University of Toronto, Toronto, ON M5S 3H4, Canada*
[9]*Department of Astronomy & Astrophysics, University of Toronto, Toronto, ON M5S 3H4, Canada*
[10]*Perimeter Institute for Theoretical Physics, Waterloo, ON N2L 2Y5, Canada*
[11]*Department of Physics and Astronomy, Siena College, 515 Loudon Rd., Loudonville, NY 12211*
[12]*Department of Physics & Astronomy, University of Wyoming, 1000 E. University, Dept 3905, Laramie, WY 8207*
[13]*Lawrence Livermore National Laboratory, 7000 East Ave., Livermore, CA 94550-9234*

(Received July xx, 2020)

Submitted to ApJ

ABSTRACT

We have conducted a search for new strong gravitational lensing systems in the Dark Energy Spectroscopic Instrument Legacy Imaging Surveys Data Release 8. We use deep residual neural networks, building on previous work presented in Huang et al. (2020). These surveys together cover approximately one third of the sky visible from the northern hemisphere, reaching a z band AB magnitude of ~ 22.5. We compile a training sample that consists of known lensing systems as well as non-lenses in the Legacy Surveys and the Dark Energy Survey. After applying our trained neural networks to the survey data, we visually inspect and rank images with probabilities above a threshold. Here we present 1210 new strong lens candidates.

Keywords: galaxies: high-redshift – gravitational lensing: strong

1. INTRODUCTION

Strong gravitational lensing systems are a powerful tool for cosmology. They have been used to study how dark matter is distributed in galaxies and clusters (e.g., Kochanek 1991; Koopmans &

Corresponding author: Xiaosheng Huang
xhuang22@usfca.edu

Treu 2002; Bolton et al. 2006; Koopmans et al. 2006; Vegetti & Koopmans 2009; Tessore et al. 2016), and are uniquely suited to probe dark matter substructure in galaxies and to test the predictions of CDM beyond the local universe (e.g., Vegetti et al. 2014, 2018; Ritondale et al. 2019; Diaz Rivero & Dvorkin 2020). Multiply lensed supernovae (SNe) are ideal for measuring time delays and H_0 because of their well-characterized light curves, and in the case of Type Ia, with the added benefit of standardizable luminosity (Refsdal 1964; Treu 2010; Oguri & Marshall 2010). In recent years, strongly lensed supernovae, both core-collapse (Kelly et al. 2015; Rodney et al. 2016) and Type Ia (Quimby et al. 2014; Goobar et al. 2017), have been discovered. Time-delay H_0 measurements from multiply imaged supernovae (e.g., Goldstein & Nugent 2017; Goldstein et al. 2018a,b; Wojtak et al. 2019; Pierel & Rodney 2019; Suyu et al. 2020), combined with measurements from distance ladders (e.g., Riess et al. 2019; Freedman et al. 2019, 2020) and lensed quasars (e.g., Suyu et al. 2010, 2013; Treu & Marshall 2016; Bonvin et al. 2017; Wong et al. 2019) can be an important test of the tension between H_0 measured locally and the value inferred from the CMB.

The application of strong lensing to cosmology has been limited by the available sample size of the lenses. In the last few years, several groups have used convolutional neural networks to search for strong lensing systems in photometric surveys including, in increasing sky coverage, CFHTLS (Jacobs et al. 2017), KiDS (Petrillo et al. 2017, 2019; Li et al. 2020), DES (Jacobs et al. 2019a,b), and Pan-STARRS (Canameras et al. 2020).

Data release 8 (DR8) of the DESI Legacy Surveys[1] (Dey et al. 2019), for which at least z band is observed with a 4-m telescope, covers ∼14,000 deg^2, three times the size of the DES footprint. In Huang et al. (2020, H20), we identified hundreds of new strong lenses in the Legacy Surveys Data Release 7 (DR7) by using a residual neural network. In this paper, building on H20, we have significantly improved the efficiency of the neural network and report the discovery of new strong lensing systems in DESI Legacy Surveys DR8.

This paper is organized as follows. A brief description of the Legacy Surveys is given in § 2. In § 3, we describe our methodology, including the improvements we have made on H20. In § 4, we show the inference results and present our best strong lensing system candidates. We discuss our results in § 5, and conclude in § 6.

2. OBSERVATIONS

The Legacy Imaging Surveys consist of three projects: the Dark Energy Camera Legacy Survey (DECaLS), observed by the Dark Energy Camera (DECam; Flaugher et al. 2015) on the 4-m Blanco telescope at the Cerro Tololo Inter-American Observatory; the Beijing-Arizona Sky Survey (BASS), by the 90Prime camera (Williams et al. 2004) on the Bok 2.3-m telescope owned and operated by the University of Arizona located on Kitt Peak; and the Mayall z-band Legacy Survey (MzLS), by the Mosaic3 camera (Dey et al. 2016) on the 4-meter Mayall telescope at Kitt Peak National Observatory. Together they cover ∼14,000 deg^2 of the extragalactic sky visible from the northern hemisphere with at least three passes in each of the three bands, grz. The $5\,\sigma$ z-band median limiting AB magnitude is 22.5 mag for galaxies with an exponential disk profile with $r_{\rm half} = 0.45''$.

The combined survey footprint is split into two contiguous areas by the Galactic plane. DECaLS covers the ∼9000 deg^2 $\delta \lesssim +32^\circ$ sub-region of the Legacy Surveys, while BASS/MzLS the ∼ 5000 deg^2

[1] http://www.legacysurvey.org/

northern sub-region. Figure 1 shows the different regions in the the Legacy Surveys footprint and the depth of the z-band observation.

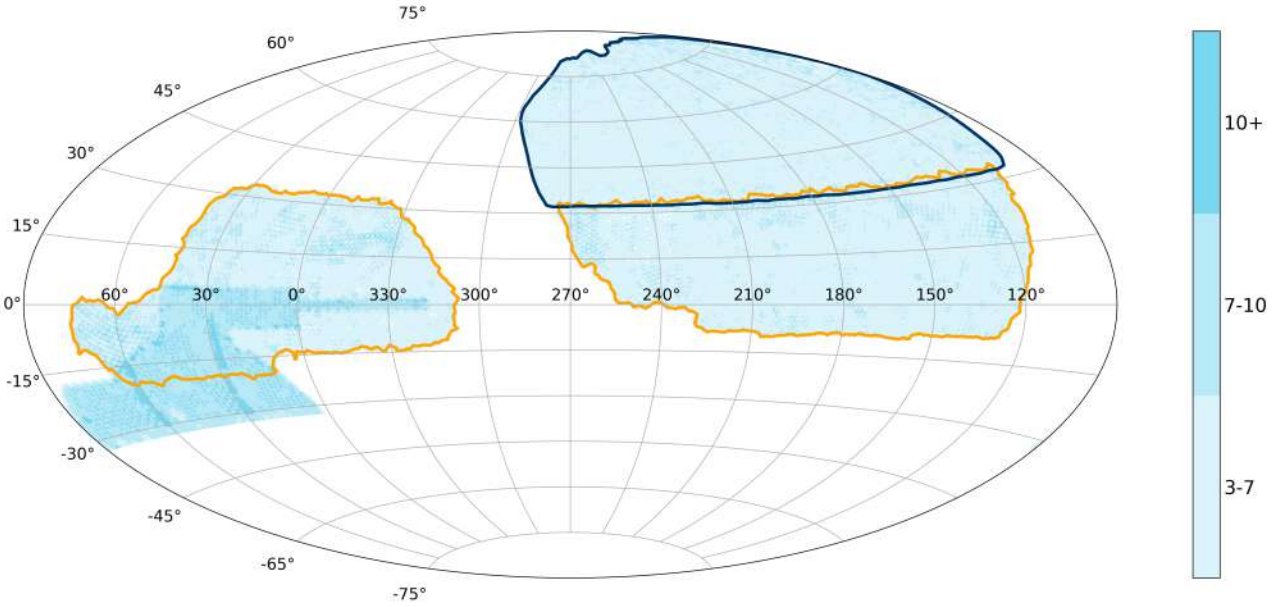

Figure 1. The DESI Legacy Imaging Surveys footprint in an equal area Aitoff projection in equatorial coordinates. The blue and gold borders approximately outline the north (coinciding with MzLS/BASS) and south (residing within DECaLS) regions of the spectroscopic survey, respectively. Slightly above $\delta = 32°$, there is a small amount of overlap between the imaging surveys. Patches with different shades of blue indicate the depth in z band: light for between three and seven passes; medium, between seven and ten, and dark, greater than ten. Note that DECaLS includes the DES footprint, but has incomplete coverage below $\delta \approx -32°$ in Data Release 8.

For DECaLS (gold outline in Figure 1), the delivered image quality has FWHM of approximately 1.29, 1.18, 1.11″ for g, r, and z bands, respectively. For the $\delta \gtrsim +32°$ (blue outline in Figure 1) footprint of the Legacy Surveys, MzLS has imaged in z-band that complemented the BASS g- and r-band observations in the same sub-region, with median delivered image quality of approximately 1.61″, 1.47″, and 1.01″ for g, r, and z bands, respectively.

The Legacy Surveys used *The Tractor* package (Lang et al. 2016) as a forward-modeling approach to perform source extraction on pixel-level data. *The Tractor* takes as input the individual images from multiple exposures in multiple bands, with different seeing in each. After source detection, the point source ("PSF") and spatially extended ("REX", round exponential galaxy) models are computed for every source and the better of these two is used when deciding whether to keep the source. The spatially extended sources (REX) are further classified if χ^2 is improved by 9 by treating it as a deVaucouleurs (DEV), an exponential (EXP) profile, or a composite of DEV + EXP, or COMP[2]. The same light profile (EXP, DEV, or COMP) is consistently fit to all images in order to determine the best-fit source shape parameters and photometry.

The categories of DEV and COMP indicate the classification of elliptical galaxies. Given that the vast majority of lensing events are caused by massive early type galaxies, we decided to first target

[2] http://legacysurvey.org/dr8/description/

objects with DEV and COMP classifications, and then REX, which tend to be smaller and/or fainter galaxies.

3. THE TRAINING SAMPLE AND RESIDUAL NEURAL NETWORKS

Deep convolutional neural networks (CNNs) and their variations have been shown to be highly effective in image recognition. In recent years, this technique has been successfully applied to recognize instances of strong lenses in simulations (e.g., Metcalf et al. 2018, and references therein). As mentioned in § 1, several groups have searched for and found strong lenses in existing imaging surveys. In all these efforts, at least the positive examples (lenses) in the training samples were constructed from simulated lenses, typically on the order of $\mathcal{O}(10^5)$. This is because the number of known lenses, on the order of several hundred, is thought to be too small to effectively train CNN models. Building on H20, we continue to use only *observed* data for lenses and non-lenses in our training sample. In this section (and § 4), we show we can train deep neural networks with a much smaller sample and far fewer positive examples and achieve comparable if not superior results. In § 3.1, we describe our training sample. We show the training results using the residual neural network from Lanusse et al. (2018) in § 3.2. Finally in § 3.3, we present an improved neural network model.

3.1. *Training Sample*

The Master Lens Database[3] (Moustakas et al. 2012), which contains hundreds of lensing events discovered prior to 2016, provided the initial list for the lens training sample. We have since added several hundred more lenses and lens candidates from more recent publications (Carrasco et al. 2017; Diehl et al. 2017; Pourrahmani et al. 2018; Sonnenfeld et al. 2018; Wong et al. 2018; Jacobs et al. 2017, 2019a,b; and H20). Initially our primary goal was to find lenses in DECaLS, part of which was observed by DES. Therefore in total we have identified 632 previously known lenses or lens candidates in DECaLS and DES, to be used in our training sample. For the lenses in the DES footprint, we only include grz bands. We also assemble $\sim 21,000$ non-lens image cutouts from DECaLS and DES, all with at least three passes in each of the grz bands, a z-band mag < 20.0, and typed as DEV or COMP, randomly distributed in the footprint. Given that on average we expect one strong lens in $\mathcal{O}(10^4)$ galaxies (e.g., Oguri & Marshall 2010), incidental inclusion of a lens or two in these randomly selected galaxies is not a significant concern.

In the training sample of H20, we found that the images for the lenses tend to be much deeper than the non-lenses. This led to the neural net during the inference stage preferentially assigning high probabilities to images with deeper observations whether they are lenses or not. To correct for this bias, given that many (359) of our lenses in the training sample are from DES south of $\delta = -18°$ with deeper observations (see Figure 2), we have included in the non-lens sample five thousand random cutout images from the same region.

As with H20, included in the non-lens sample are cutouts selected by eye so as to cover as many non-lens configurations as possible, especially cases that can potentially be confused by the neural net. These include spiral galaxies of different sizes and spiral arm configurations, elliptical galaxies, galaxy groups, images having objects with different colors (typically a blue galaxy next to a red one), cosmic rays appearing in different bands (some of which have curved trajectories), unusual arrangements of galaxies or stars, and finally certain data reduction artefacts.

[3] http://admin.masterlens.org/index.php

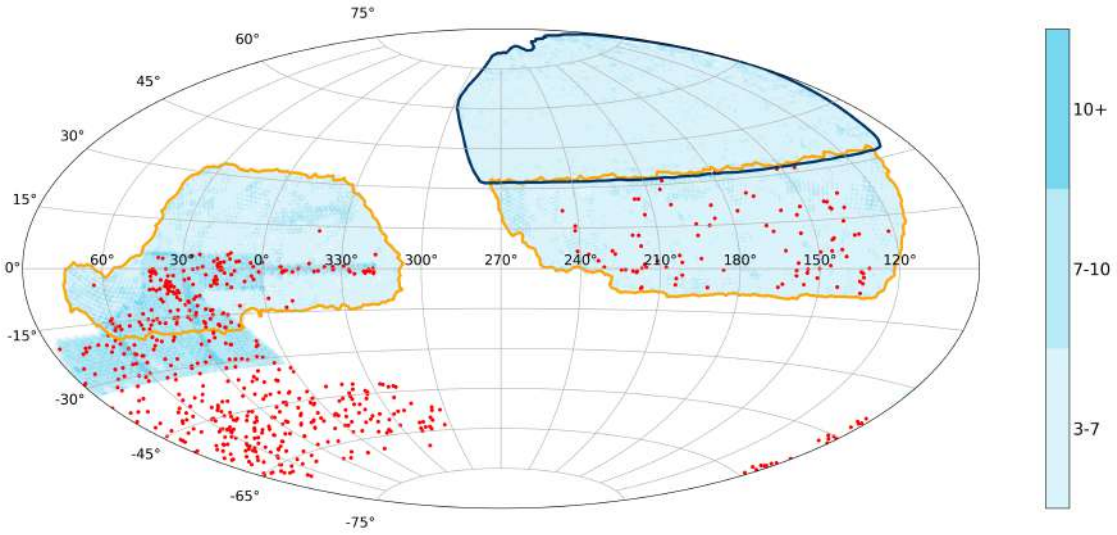

Figure 2. Previously known lenses or lens candidates in our training sample shown as red dots, against the background of the depth map of Legacy Surveys DR8 (see the caption for Figure 1). The lenses south of the DESI spectroscopic footprint (gold outline) are from DES.

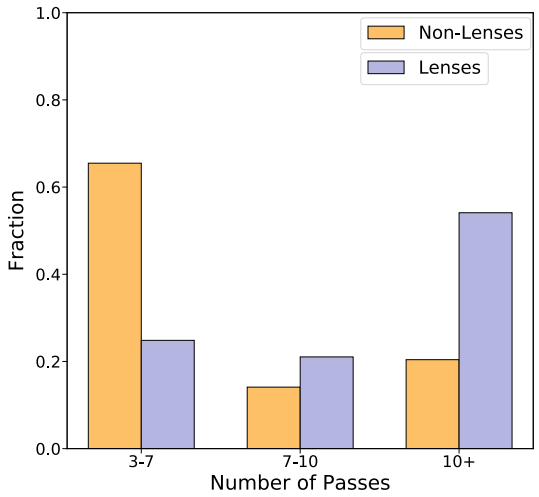

Figure 3. The yellow and violet columns show the fractions of lenses and non-lenses in the training sample, respectively, for the three bins of z-band depth.

The distribution of the lenses and non-lenses in our training sample is shown in Figure 3. While fractionally there are still more non-lenses in the shallowest bin and more lenses in the deepest bin, overall the disparity between the relative proportions of lenses and non-lenses in each depth bin is much improved compared with the training sample in H20.

3.2. *Residual Neural Networks*

We use the Residual Neural Network (ResNet) model of Lanusse et al. (2018, L18), after re-implementing it in TensorFlow[4]. We have left their architecture and hyperparameters unchanged (for details, see Section 3.3 of L18), except that we double the batch size to 256. The lens and non-lens images in the training sample are cutouts with a dimension of 101 × 101 pixels, following the specification in the Lens Challenge (Metcalf et al. 2018).

We split the training sample into training and validation *sets*, with a ratio of 7:3. We then train the ResNet on Google Colab[5] using a GPU (NVIDIA Tesla v100). The 120 epochs of training took 4 hours.

The ResNet attempts to minimize the cross entropy loss function:

$$-\sum_{i=1}^{N} y_i \log \hat{y}_i + (1 - y_i) \log(1 - \hat{y}_i) \tag{1}$$

where y_i is label for the ith image (1 for lens and 0 for non-lens), and $\hat{y}_i \in [0, 1]$ is the model predicted probability.

While the loss function is monitored during the training process to determine the point of termination, the overall performance of the trained model is typically assessed by the Receiver Operating Characteristic (ROC) curve. The ROC curve shows the True Positive Rate (TPR) vs. the False Positive Rate (FPR) for the validation set, where P(ositive) indicates a lens and N(egative), a non-lens. With the definitions True Positive (TP) = correctly identified as a lens, False Positive (FP) = incorrectly identified as a lens, True Negative (TN) = correctly rejected, and False Negative (FN) = incorrectly rejected,

$$\mathrm{TPR} = \frac{\mathrm{TP}}{\mathrm{P}} = \frac{\mathrm{TP}}{\mathrm{TP} + \mathrm{FN}}$$

and

$$\mathrm{FPR} = \frac{\mathrm{FP}}{\mathrm{N}} = \frac{\mathrm{FP}}{\mathrm{FP} + \mathrm{TN}}$$

The curve is generated by gradually increasing the threshold probability for a positive identification from 0 to 1. Random classifications will result in a diagonal line in this space with an area under the ROC curve (or AUC) equal 0.5. For a perfect classifier, AUC = 1.

In Figure 4, left panel, we show how the cross entropy loss functions vary as training progresses. For the validation set, we show the value at every epoch. For the training set, the cross entropy was reported for every step, which we have boxcar smoothed with a window size of 57. This is because the training set has a total of 14,725 images, with a batch size of 256 images, it takes approximately 57 steps to complete one full training epoch. Figure 4 shows that the AUC for the validation set has plateaued well within the 120 epochs of training. We achieve an AUC of 0.992 for the validation set (Figure 4, right panel). This is a significant improvement over an already high AUC of 0.977 from H20.

[4] https://www.tensorflow.org/
[5] https://colab.research.google.com/

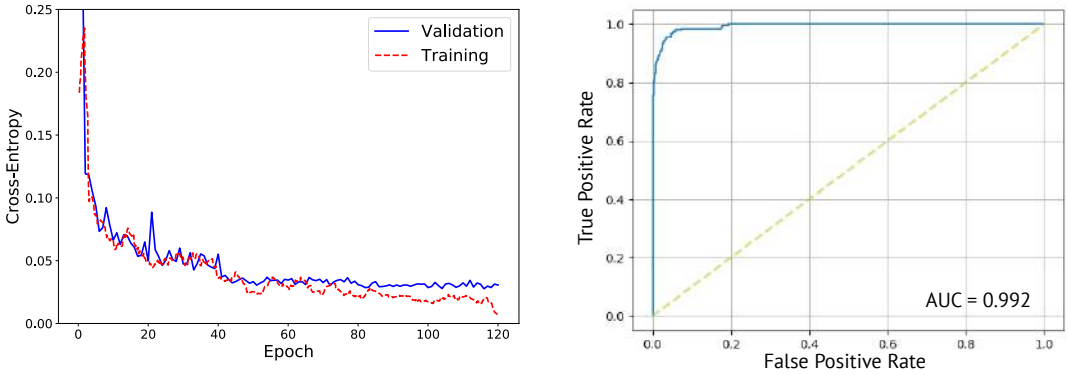

Figure 4. Left: The cross entropy loss functions for the training and validation sets over 120 epochs. Right: The receiver operative characteristic (ROC) curve for the validation set with the area under the curve (AUC) = 0.992.

3.3. *Improvement on the L18 Model*

We have experimented with a variety of ways to improve on the model in L18, including transfer learning and domain adaptation (e.g., Tzeng et al. 2017), among other techniques. We will provide the full results of the comparisons from these different approaches in a future publication.

So far we have run inference and visually inspected the results for one of the variants. In this modification on the original L18 model was the addition of "shielding" layers, inspired by the InceptionNet architecture of Szegedy et al. (2014). These "shields" are 1×1 convolutional layers inserted between every three blocks of the L18 architecture (see their Figure 4), so named because they have the effect of reducing dimensionality and mitigating the exponential increase in computational complexity present in the original architecture. With appropriate adjustments to the number of channels in the shielding layers, we reduce the number of trainable parameters by a factor of 50 (from 3 million to 60 thousand), thereby shortening the training time by 17%. Moreover, the validation AUC has increased from 0.992 (using the original L18 model; § 3.2) to 0.997. Thus the reduction in model complexity does not appear to have an adverse impact on performance, and in fact has improved it. This is likely because the problem at hand (to tell lenses apart from non-lenses) although complex, does not require a large number of dimensions in the underlying latent space. The addition of "shielding" layers compresses dimensionality by more than an order of magnitude, forcing the network to learn only the most salient features. For example, in the final block of the architecture in L18 (see their Figure 4) we experimented with reducing the output from 512 channels to 256, 128, 64, 32, and 16 channels. We find that "shields" that keep the output to 32 channels perform the best.

In § 4, we will show lens candidates from both the original model in L18 and the "shielded" model (the one with 32 output channels), to achieve greater completeness for the lens search in DR8 and to demonstrate that a different neural network model can identify new lens candidates.

4. RESULTS

In this section we present the lens candidates. In § 4.1, we present all the candidates found by using the ResNet model of L18, specifically: § 4.1.1, candidates that are DEV or COMP in DECaLS; § 4.1.2, candidates that are DEV or COMP found in BASS/MzLS, and § 4.1.3, candidates that are typed as REX in DECaLS and MzLS. In § 4.2, we show candidates that are found with the "shielded" model

(see § 3.3). To determine the probability threshold for human inspection, we consult the precision-recall curve (PRC), where precision = TP/(TP+FP) and recall = TP/(TP + FN), which is the same as TPR (§ 3.2). The PRC for the validation set, with probability threshold values marked, is shown in Figure 5.

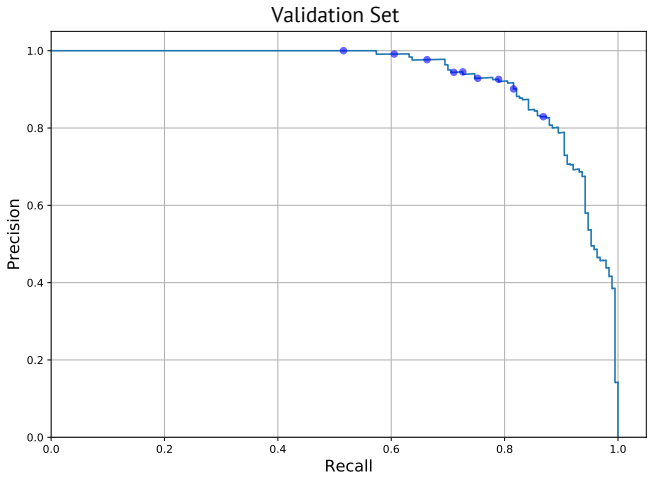

Figure 5. The precision-recall curve for the validation set. The blue points from left to right correspond to probability threshold values from 0.9 to 0.1 with an interval of 0.1.

We recognize that different terms have been used for the same quantities. To avoid confusion, in this paper:

$$\text{recall} = \text{TPR} = \text{completeness}$$

and

$$\text{precision} = \text{purity}$$

This redundancy in terminology in part stems from fairly standard usage (e.g., recall or TPR depending on the context) and in part from the difference in terminology between machine learning and astrophysics (recall or completeness, precision or purity).

While ideally we would like to identify all the lenses that are discoverable in the data set, there is a ceiling to the number of images that can be inspected in a reasonable amount of time. We choose the threshold of 0.1 because it seems to be a reasonable compromise between purity (precision) and completeness (recall). Keep in mind that the PRC provides completeness and purity for the validation set. For deployment on the whole data set, it is not possible to determine the completeness without inspecting the entire data set, which is infeasible. We will address the question of completeness in the context of comparing the results of different neural network models in a future publication (see § 3.3). Since our training sample has a lens to non-lens ratio ($\sim$ 1 in 33) that is much higher than expected for the data set as a whole ($\sim$ 1 in 10^4), we estimate the expected purity for deployment at our chosen probability threshold of 0.1 in the following way. Given the 7:3 training and validation split, there are approximately $N_l = 190$ lenses and $N_{nl} = 6300$ non-lenses in the validation set. The number of non-lenses misclassified as lenses is then $\sim 33 (= N_l \times r \times \frac{1-p}{p})$, where $r(= 0.87)$ and $p(= 0.83)$ are the recall (or, completeness) and precision (or, purity), respectively. The fraction of non-lenses that are misclassified as lenses is $33/N_{nl} \approx 0.00052$. With the expectation of one strong lens in

$\mathcal{O}(10^4)$ galaxies, this translates to a purity of 1 in 52, or 1.9%. We will refer to all cutout images with probabilities above this threshold as the ResNet "recommendations". Below, through human inspection, we will compare the percentage of lens candidates relative to the "recommendations" with this estimated purity for deployment. (Note that in H20, we used the term "human inspection efficiency" for this quantity).

Throughout this section, all objects we run inference on have ≥ 3 passes for all three bands and z-band mag < 20.0. For the ensuing human inspection, we follow this process. Co-authors S.B., A.G., A.P., V.R., C.S., W.S., and R.V. make the "first pass" selections, according to these criteria, erring on the generous side: small blue galaxy/galaxies (red galaxies are rare but certainly acceptable) next to the red galaxy/galaxies at the center that

- are typically 1 - 5″ away
- have low surface brightness
- curve toward the red galaxy/galaxies
- have counter/multiple images with similar colors (especially in Einstein-cross like configuration)
- are elongated (including semi- or nearly full circles)

Typically, most candidates do not have all these characteristics. In general, the greater the number of characteristics listed above an image has, the higher they are ranked by humans. For the "second pass", co-authors X.H. and A.D. examine all "first pass" selections and assign an integer score between 1 and 4. These two scores are averaged. We assign a letter grade according to the average:

- ≥ 3.5: Grade A. We have a high level of confidence of these candidates. Many of them have one or more prominent arcs, usually blue. The rest have one or more clear arclets, sometimes arranged in multiple-image configurations with similar colors (again, typically blue). However, there are clear cases with red arcs.
- $= 3.0$: Grade B. They have similar characteristics as the Grade A's. For the cutout images where there appear to be giant arcs they tend to be fainter than those for the Grade A's. Likewise, the putative arclets tend to be smaller and/or fainter, or isolated (without counter images).
- $= 2.5$ or 2.0: Grade C. They generally have features that are even fainter and/or smaller than what is typical for Grade B candidates, but that are nevertheless suggestive of lensed arclets. Counter images are often not present or indiscernible. In a number of cases, the deflection angles are comparable to or only slightly larger than the seeing. Therefore, for some of these candidates, to attain a higher level of certainty, higher spatial resolution or deeper data would be required.

For Grade B and C candidates, we have included a small percentage of cases where it is difficult to judge whether it is a lensing event vs. a coincidental placement of galaxies, a spiral galaxy, a ring galaxy, or tidal features associated with galaxy interactions.

4.1. *Lens Candidates from the L18 ResNet*

Below we present all the strong lens candidates found by using the ResNet model in L18.

4.1.1. *Candidates from DEV and COMP in DECaLS*

Searching for strong lenses among the DEV and COMP objects in the DECaLS region originally was our primary goal. Our training sample is selected from the same region (see Figure 2). We deploy our model on $\sim$ 10 million cutouts centered on galaxies typed as DEV or COMP. With the probability threshold set at 0.1, in total we have examined 22,879 ResNet recommendations.

We have found 115 Grade A, 110 Grade B, and 501 Grade C candidates. The locations of these candidates in the sky are shown in Figure 6. In total, we have identified 726 candidates, achieving a purity of approximately 1 in 31 ResNet recommendations.

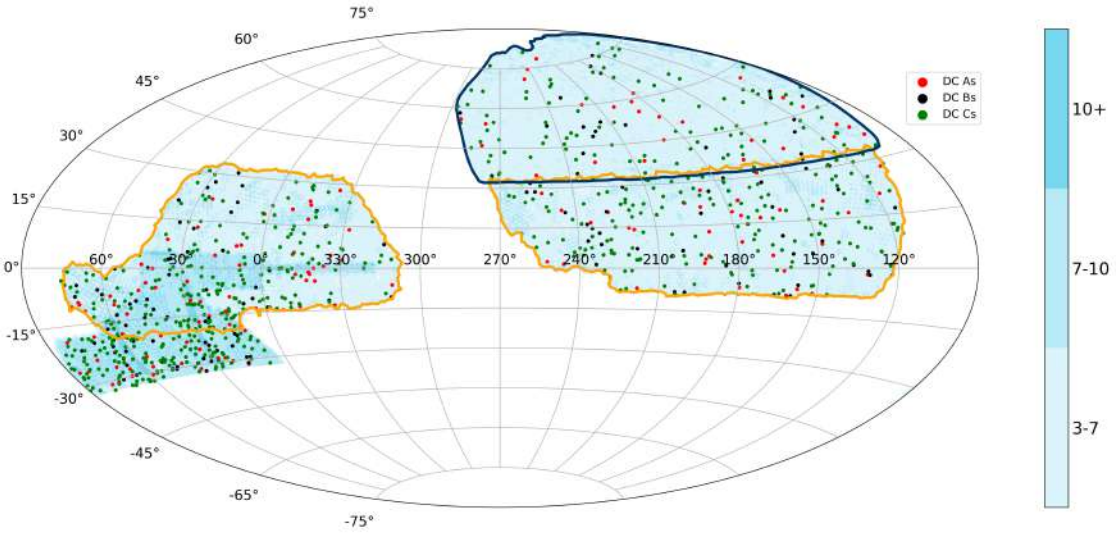

Figure 6. The new candidate lensing systems typed as DEV and COMP by *The Tractor* in the DECaLS and BASS/MzLS regions (see Figure 1 caption) are shown as red (Grade A), black (Grade B), and yellow (Grade C) circles.

We now briefly discuss the purity of the ResNet results thus far, since this is the primary data set in which we originally planned to search for lenses.

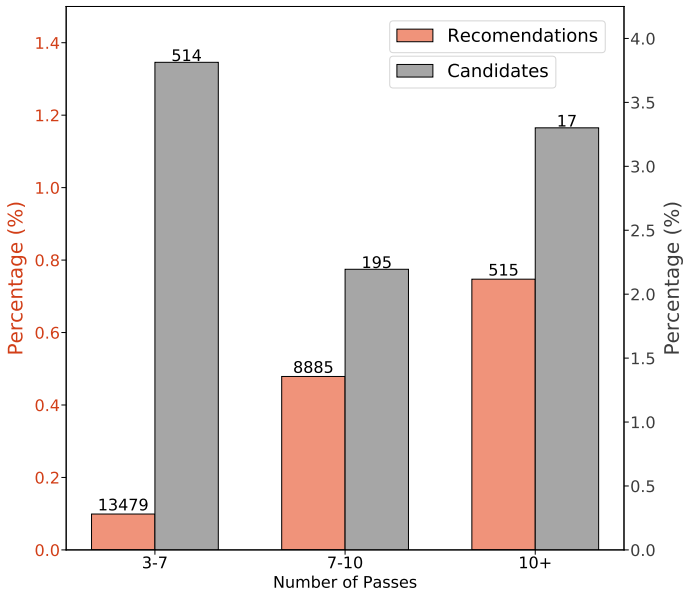

Figure 7. The orange columns (left y-axis) show the percentages of objects given a greater than 0.1 probability by our ResNet model (or "recommendations") for the three bins of z-band depth. The gray columns (right y-axis) show the percentages of ResNet recommendations that are selected as lens candidates through human inspection, or, the purity. The number of recommendations or candidates for each bin is shown atop the corresponding column.

In H20, we noted that due to the composition of our training sample (comparatively smaller number of non-lens images with deep observations), the neural net showed a preference for images with deep observations, whether they contain lensing systems or not. For the inference results in this paper, Figure 7 shows how a) the percentage of the ResNet recommendations relative to the objects and b) the percentage of candidates (determined by human inspection) relative to recommendations depend on the observational depth (see Figure 1). For the three depth bins, the percentages of lens candidates relative to the neural net recommendations are similar, approximately between 2.2 - 3.8%. This indicates that the neural net now makes recommendations largely free of bias with regard to depth. This is consistent with our expectation based on the composition of the training sample used in this paper. The orange columns show that 0.82% of the objects in the 10+ pass bin receive probability > 0.1 ("recommendations"), five times the value of 0.16% in the 3 - 7 passes bin. This trend in the ResNet recommendations indicates that, not surprisingly, there are more lenses to be discovered for deeper images. In fact, approximately one in 16,337, 8795, 3710 galaxies is a lens, from the shallowest to the deepest bin, assuming 100% completeness. These values are consistent with the expectation of one strong lens in $\mathcal{O}(10^4)$ galaxies.

Overall, our ResNet model achieves a purity of 3.2%, broadly consistent with our estimation of 1.9% (see the introduction to § 4). Compared with H20, this much improved purity likely stems from three factors: 1) a larger (by about $\sim 60\%$) training sample; 2) the lenses in the training sample are all well observed in DECaLS with clearly discernible lensing features; and 3) the non-lenses in the training sample includes a large number of images from DES that have observations with comparable depth as the lenses from DES in our training sample, which significantly reduced, if not eliminated, the ResNet's bias toward images with greater depth.

4.1.2. *Candidates from Deployment on DEV and COMP in BASS/MzLS*

For the northern MzLS/BASS region, the *gr* band observations have worse seeing. Given the success of the deployment in DECaLS, however, we decide to proceed with applying our trained ResNet model, without modification or re-training, to this region.

We run inference on 5.4 million cutouts centered on DEV and COMP objects, with z-band magnitude < 20.0. The inspection of 8761 ResNet recommendations finds 29 A's, 22 B's, and 103 C's. The locations of the candidates in the sky are shown, together with the candidates found in DECaLS, in Figure 6. In total, we have identified 154 candidates, approximately 1 in 57 ResNet recommendations. As expected, the purity of the ResNet recommendations is worse than for DECaLS, but is still competitive. Keep in mind that we used the same ResNet trained for DECaLS without any modification. Furthermore, as we mentioned in § 2, the *gr* band seeings are $1.61''$ and $1.47''$, respectively. To our knowledge, this is the first time a lens search has been attempted and successfully carried out, with competitive neural network recommendation purity, for a survey with seeing $\gtrsim 1.5''$. This is a remarkable result.

4.1.3. *Lens Candidates from Deployment on REX in Legacy Surveys*

The REX category contains an order of magnitude more objects than the DEV and COMP types combined, since most faint, extended galaxies are modeled by the REX profile (see § 2). This category likely includes many elliptical galaxies, though the percentage is unknown.

Given the success with DEV and COMP in both DECaLS and BASS/MzLS, without modification of the model or additional training, we deploy our trained ResNet on 6.7 million cutouts centered on REX (5 million in DECaLS and 1.7 million in BASS/MzLS), with z-band mag < 20.0. When we performed this inference run, the source extraction and typing by *The Tractor* became available for certain patches below $\delta = -32°$. These objects are included in the deployment.

In total, we have inspected 7039 (5861 in DECaLS and 1178 in BASS/MzLS) ResNet recommendations and identified 168 candidates. Of these, 156 are in DECaLS and 12 in BASS/MzLS, resulting in recommendations with purities of 1 in 38 and 1 in 98, respectively. The average purity is ~ 1 in 42. We have removed candidates that have already been found in DEV and COMP (these lensing systems are "discovered" again because the cutout images containing the same systems are centered on different objects this time).

In the end, we identify 15 A's (13 in DECaLS and 2 in BASS/MzLS), 7 B's (6 in DECaLS and 1 in BASS/MzLS), and 46 C's (42 in DECaLS and 4 in BASS/MzLS), for a total of 68 new candidates. The locations of the candidates in the sky are shown in Figure 8.

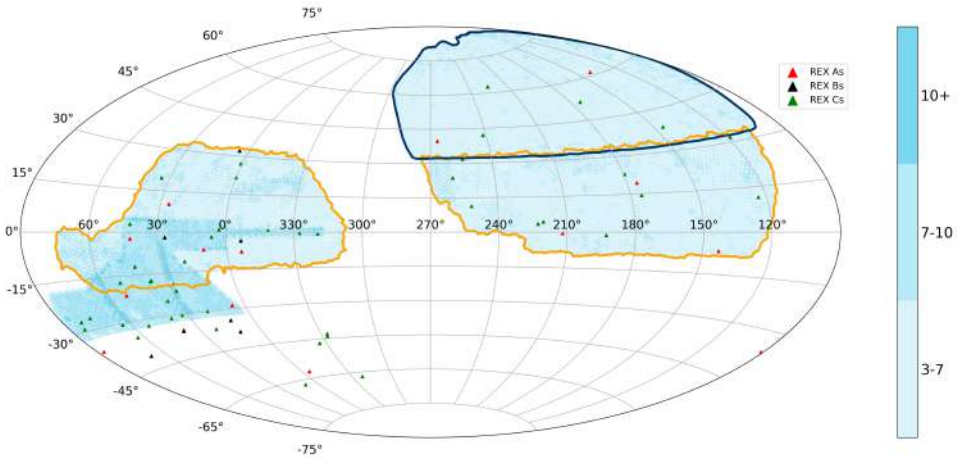

Figure 8. The new candidate lensing systems typed as REX by *The Tractor* in the Legacy Surveys are shown as red (Grade A), black (Grade B), and green (Grade C) triangles.

All the lens candidates found by the L18 model are summarized in Table 1.

Table 1. L18 Model

Grade	A	B	C		Total by Type (DECaLS,MzLS)
Human Score	≥ 3.5	3.0	2.5	2.0	
DC (DECaLS,MzLS)	144 (115,29)	132 (110,22)	280 (242,38)	324 (259,65)	880 (726,154)
REX (DECaLS,MzLS)	15 (13,2)	7 (6,1)	22 (20,2)	24 (22,2)	68 (61,7)
Total by Grade (DECaLS,MzLS)	159 (128,31)	139 (116,23)	302 (262,40)	348 (281,67)	948 (787,161)

4.2. *Candidates Found with the "Shielded" Model in Legacy Surveys*

As mentioned in § 3.3, we have experimented with modifications on the L18 ResNet model to optimize performance, but so far using the same training sample (although we will experiment with the makeup of the training sample as well). Here we present the lens candidates found by one of these attempts.

We deploy the "shielded" model on the entire Legacy Surveys footprint on objects that satisfy the same criteria as for the L18 ResNet model. We achieve a similar level of purity, and have found 364 *new* lens candidates, including 57 A's, 60 B's, and 247 C's. This demonstrates that a different neural network is capable of finding new lenses in the same footprint. These lens candidates are summarized in Table 2 with their locations on the sky shown in Figure 9.

Table 2. Shielded Model

Grade	A	B	C		Total by Type (DECaLS,MzLS)
Human Score	≥ 3.5	3.0	2.5	2.0	
DC (DECaLS,MzLS)	19 (16,3)	20 (19,1)	36 (34,2)	50 (45,5)	125 (114,11)
REX (DECaLS,MzLS)	38 (34,4)	40 (37,3)	49 (47,2)	112 (109,3)	239 (227,12)
Total by Grade (DECaLS,MzLS)	57 (50,7)	60 (56,4)	85 (81,4)	162 (154,8)	364 (341,23)

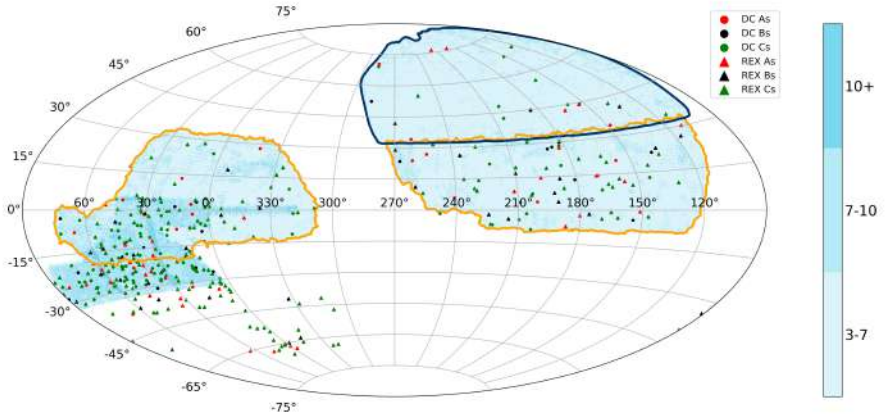

Figure 9. The new candidate lensing systems found by the "shielded" model are shown as red (Grade A), black (Grade B), and yellow (Grade C) circles (DEV or Comp) and triangles (REX).

4.3. *Summary of § 4*

Altogether, we have found 1312 strong lens candidates (Table 3). Of these, 102 have been found by other groups, none of which were included in our training sample. The citations for these systems are given in Tables 4 to 6. This leaves 1210 new lens candidates. Of these, there are 193 A's (Figures 11 - 13; Tables 4), 175 B's (Figures 14 - 16; Table 5), and 842 C's (Figures 17 - 25; Table 6). For each candidate presented in the figures, we report the average numerical scores from A.D. and X.H. and the absolute difference, the region where it is found, its type from *The Tractor*, and the neural network model used. The strong lens candidates discovered in this work are summarized in Table 3. We have checked our candidate list against the spectroscopic database from SDSS DR16[6] and found that for approximately half of them the putative lensing galaxy has a spectroscopic redshift. For the rest, we have found photometric redshifts from Zhou et al. (2020). The available spectrocopic or photomstric redshifts are included in Tables 4 to 6.

We believe we have held a high standard in grading our candidates. Many of our Grade C systems are in fact likely lensing candidates. Among our candidates, of the 102 systems that have been identified by other groups (but were not in our training sample), 55 are in Grade C, 27 of which have a score of 2.5 (see Table 3). This speaks to the quality of our Grade C candidates. We would like to note that 42% (360) of our Grade C candidates have a human inspection score of 2.5. As shown

[6] https://www.sdss.org/dr16/

in the examples in Figure 10 below, many of these systems are high likelihood candidates. In total, there are 728 new candidates with a score ≥ 2.5.

Many of our lens candidates have spectroscopic or photometric redshifts $z \gtrsim 0.8$, greater than the typical redshifts of 0.3 to 0.8 for the current known lensing sample (e.g., Brownstein et al. 2012; Wong et al. 2018). In fact, the highest spectroscopic redshift from SDSS DR16 is 0.8924 (DESI-241.7346+42.1102) and the highest photometric redshift is 1.232 (DESI-116.3092+33.6326). In addition, the deflection angles of our systems are typically between 1.5 - 5″ (see Figure 10), significantly larger than the typical value for previously known galaxy lensing systems ($\lesssim 1.5''$). This translates to longer time delays and a smaller relative uncertainty per system for quasars and supernova events in the background galaxy, and therefore higher precision in the measurement of H_0 (e.g., Suyu et al. 2020).

We end this section by highlighting in Figure 10 four examples each for four types of strong lens candidates that we have discovered. Among the 16 candidates shown, four have a average human inspection score of 2.5, and therefore are given a C grade, but they are nevertheless very likely lensing candidates.

Table 3. Lens Candidates

Grade	A	B	C		Total
Human Score	≥ 3.5	3.0	2.5	2.0	
L18+Shielded Models	216	199	387	510	1312
Known Lenses or Candidates	23	24	27	28	102
New Lens Candidates in this work	193	175	360	482	1210

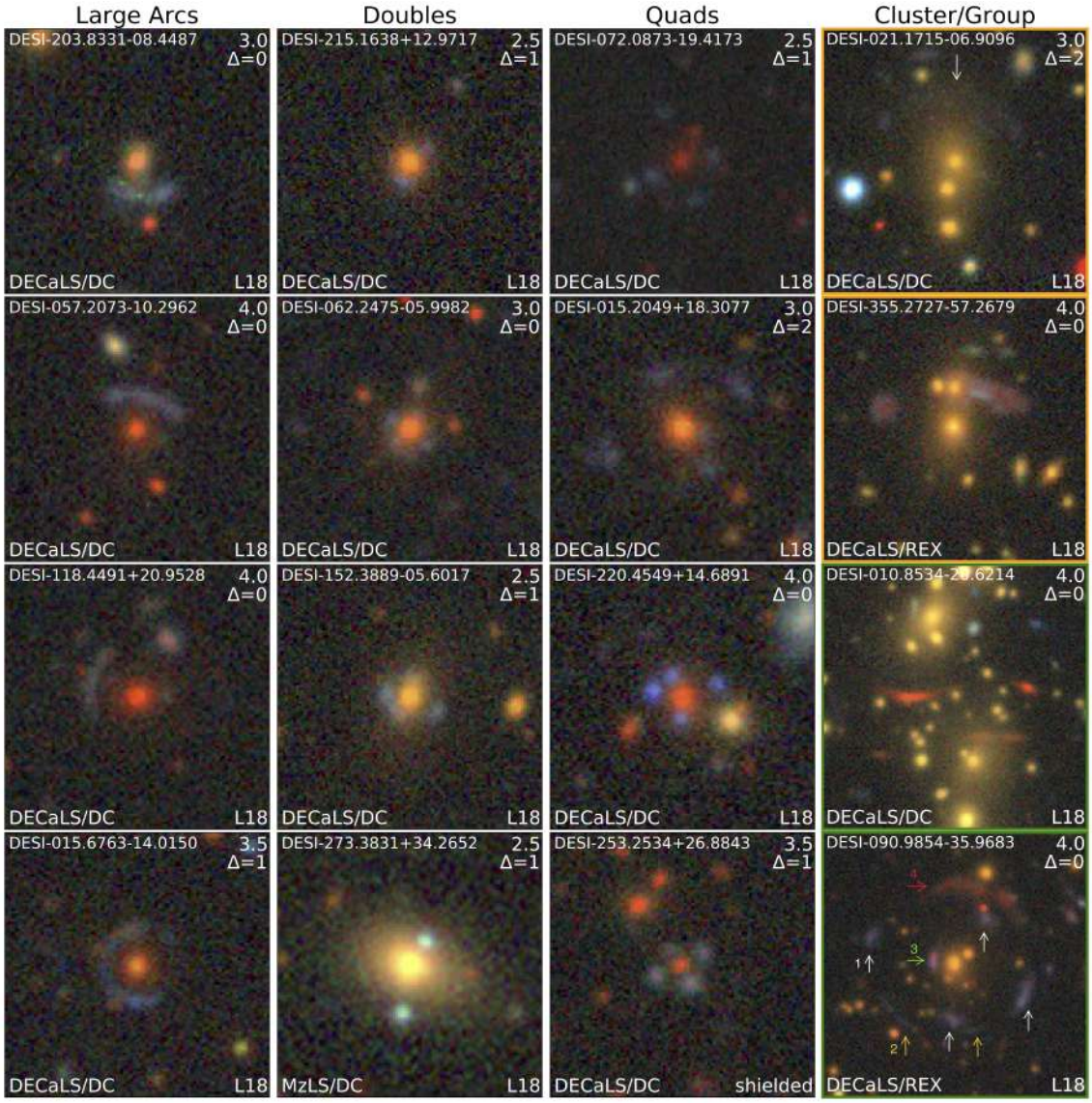

Figure 10. Sixteen of the 1210 new lensing candidates discovered in this paper. The naming convention is RA and Dec in decimal format. Top right corner of each image indicates the average human inspection score with Δ being the absolute difference; bottom left corner, the region and *The Tractor* type (REX or DC = DEV or COMP); and bottom right, the neural network model. North is up, and east to the left. The images without rims have a width of 101 pixels $\approx 26.5''$; with orange rims, 151 pixel $\approx 39.6''$; and green rims, 201 pixel $\approx 52.7''$. First Column: large arcs. The third system (DESI-118.4491+20.9528) clearly has a counter-image and the fourth one (DESI-015.6763-14.0150) is a near Einstein ring. Second Column: doubly lensed systems. The second (DESI-062.2475-05.9982) and third (DESI-152.3889-05.6017) systems hint at a possible Einstein cross (or a quad) and the fourth one (DESI-273.3831+34.2652) is a likely doubly lensed quasar system. Third column: quadruply lensed systems. These 12 systems have a single galaxy as the main lens. Fourth Column: cluster/group lensing systems. The first one (DESI-021.1715-06.9096) has a faint, giant blue arc (white arrow). The second (DESI-355.2727-57.2679) and third (DESI-010.8534-20.6214) systems show one and two sets of red arcs, respectively. The fourth one (DESI-010.9854-35.9683) is a spectacular system: at least four lensed sources at different redshifts are apparent, including a quad (1, white arrows), a "broken" long arc (2, yellow arrows), one red arc near the core of the group (3, green arrow), and a giant red arc at approximately $14''$ away from the lens center (4, red arrow). Note that the four candidates receiving a score of 2.5, and therefore a grade of C, are nevertheless very likely lensing candidates.

5. DISCUSSION

In our training sample there are 632 lenses. This is generally considered too small a number for training a neural network. Even our non-lens sample is much smaller than what is typically used (e.g., Jacobs et al. 2019a,b). Nevertheless, we have succeeded in finding 1210 new lens candidates in the three band Legacy Surveys with nonuniform depth (see Figure 1). The training sample was designed for searching among the DEV and COMP types in one of the two regions of the footprint, DECaLS, and our neural network model performed well for this category. The purity of our neural network recommendations is at least on par with the best in the literature. Compared with H20, using a larger training sample that includes a larger proportion of non-lenses with deep observations, we have improved the performance of our neural network model (as measured by recommendation purity) by a factor of 5 for DEV and COMP in DECaLS (from 1 in 150 to 1 in 31), where the majority of our lenses are found. For DEV and COMP in BASS/MzLS, which has inferior *gr* band seeing, and for REX in the entire Legacy Surveys footprint, we applied the exact same trained model, and the purities are only slightly lower: 1 in 57 and 1 in 42, respectively.

For future searches, there is still room for improvement, both in terms of the algorithm and the construction of the training sample. On the algorithm side, we have started experimenting with a variety of approaches (see § 3.3). In this paper we have shown the results from one of them, the "shielded" model, with 364 *new* candidates found in the same footprint. This is a promising sign that further exploration is warranted. In terms of the training sample, with the candidates reported in this paper and other recent discoveries (e.g., Canameras et al. 2020) we can add more lenses and lens candidates to our training sample. It is possible that further increasing the number of non-lenses in our training sample would help as well, as the current number of 21,000 is still relatively small.

6. CONCLUSIONS

We have carried out a search for strong gravitational lensing systems in the DESI Legacy Surveys data by using a deep residual neural network, developed by Lanusse et al. (2018), trained on observed lenses and non-lenses. We applied our trained neural network to a total of ~ 20 million cutout images in DR8 with at least three passes in each of the *grz* bands and a *z*-band magnitude cut of 20.0 for the galaxy at the center of each image. We have found 193 Grade A, 175 Grade B, and 842 Grade C new candidates. These include 364 candidates found by applying a modified neural network to the same data set. We believe we have held a high standard in grading these candidate systems. 728 of our candidates have a human inspection score ≥ 2.5, all of which are at least likely lensing systems.

We note that the candidates reported in this paper do not include the 335 strong lensing candidates (with 159 Grade A's and B's) we already found for Legacy Surveys DR7 (Huang et al. 2020).

Compared with efforts by other groups to search for strong lensing systems in other surveys, we use a much smaller training sample of 632 lenses and $\sim$21,000 non-lenses from observed data, for a survey that covers one third of the sky with nonuniform depth and seeing. We nevertheless have achieved competitive neural network recommendation purity and in this paper we report the discovery of 1210 new strong lens candidates.

7. ACKNOWLEDGEMENT

This research used resources of the National Energy Research Scientific Computing Center (NERSC), a U.S. Department of Energy Office of Science User Facility operated under Contract No. DE-AC02-05CH11231 and the Computational HEP program in The Department of Energy's

Science Office of High Energy Physics provided resources through the "Cosmology Data Repository" project (Grant #KA2401022). X.H. acknowledges the University of San Francisco Faculty Development Fund. A.D.'s research is supported by National Science Foundation's National Optical-Infrared Astronomy Research Laboratory, which is operated by the Association of Universities for Research in Astronomy (AURA) under cooperative agreement with the National Science Foundation.

This paper is based on observations at Cerro Tololo Inter-American Observatory, National Optical Astronomy Observatory (NOAO Prop. ID: 2014B-0404; co-PIs: D. J. Schlegel and A. Dey), which is operated by the Association of Universities for Research in Astronomy (AURA) under a cooperative agreement with the National Science Foundation.

This project used data obtained with the Dark Energy Camera (DECam), which was constructed by the Dark Energy Survey (DES) collaboration. Funding for the DES Projects has been provided by the U.S. Department of Energy, the U.S. National Science Foundation, the Ministry of Science and Education of Spain, the Science and Technology Facilities Council of the United Kingdom, the Higher Education Funding Council for England, the National Center for Supercomputing Applications at the University of Illinois at Urbana-Champaign, the Kavli Institute of Cosmological Physics at the University of Chicago, the Center for Cosmology and Astro-Particle Physics at the Ohio State University, the Mitchell Institute for Fundamental Physics and Astronomy at Texas A&M University, Financiadora de Estudos e Projetos, Fundação Carlos Chagas Filho de Amparo à Pesquisa do Estado do Rio de Janeiro, Conselho Nacional de Desenvolvimento Científico e Tecnológico and the Ministério da Ciência, Tecnologia e Inovacão, the Deutsche Forschungsgemeinschaft, and the Collaborating Institutions in the Dark Energy Survey. The Collaborating Institutions are Argonne National Laboratory, the University of California at Santa Cruz, the University of Cambridge, Centro de Investigaciones Enérgeticas, Medioambientales y Tecnológicas-Madrid, the University of Chicago, University College London, the DES-Brazil Consortium, the University of Edinburgh, the Eidgenössische Technische Hochschule (ETH) Zürich, Fermi National Accelerator Laboratory, the University of Illinois at Urbana-Champaign, the Institut de Ciències de l'Espai (IEEC/CSIC), the Institut de Física d'Altes Energies, Lawrence Berkeley National Laboratory, the Ludwig-Maximilians Universität München and the associated Excellence Cluster Universe, the University of Michigan, the National Optical Astronomy Observatory, the University of Nottingham, the Ohio State University, the OzDES Membership Consortium the University of Pennsylvania, the University of Portsmouth, SLAC National Accelerator Laboratory, Stanford University, the University of Sussex, and Texas A&M University.

REFERENCES

Bolton, A. S., Burles, S., Koopmans, L. V. E., Treu, T., & Moustakas, L. A. 2006, ApJ, 638, 703, doi: 10.1086/498884

Bonvin, V., Courbin, F., Suyu, S. H., et al. 2017, MNRAS, 465, 4914, doi: 10.1093/mnras/stw3006

Brownstein, J. R., Bolton, A. S., Schlegel, D. J., et al. 2012, ApJ, 744, 41, doi: 10.1088/0004-637X/744/1/41

Canameras, R., Schuldt, S., Suyu, S. H., et al. 2020, arXiv e-prints, arXiv:2004.13048. https://arxiv.org/abs/2004.13048

Carrasco, M., Barrientos, L. F., Anguita, T., et al. 2017, ApJ, 834, 210, doi: 10.3847/1538-4357/834/2/210

Dey, A., Rabinowitz, D., Karcher, A., et al. 2016, in Proc. SPIE, Vol. 9908, Ground-based and Airborne Instrumentation for Astronomy VI, 99082C

Dey, A., Schlegel, D. J., Lang, D., et al. 2019, AJ, 157, 168, doi: 10.3847/1538-3881/ab089d
Diaz Rivero, A., & Dvorkin, C. 2020, PhRvD, 101, 023515, doi: 10.1103/PhysRevD.101.023515
Diehl, H. T., Buckley-Geer, E. J., Lindgren, K. A., et al. 2017, ApJS, 232, 15, doi: 10.3847/1538-4365/aa8667
Flaugher, B., Diehl, H. T., Honscheid, K., et al. 2015, AJ, 150, 150, doi: 10.1088/0004-6256/150/5/150
Freedman, W. L., Madore, B. F., Hatt, D., et al. 2019, ApJ, 882, 34, doi: 10.3847/1538-4357/ab2f73
Freedman, W. L., Madore, B. F., Hoyt, T., et al. 2020, ApJ, 891, 57, doi: 10.3847/1538-4357/ab7339
Goldstein, D. A., & Nugent, P. E. 2017, ApJL, 834, L5, doi: 10.3847/2041-8213/834/1/L5
Goldstein, D. A., Nugent, P. E., & Goobar, A. 2018a, arXiv e-prints. https://arxiv.org/abs/1809.10147
Goldstein, D. A., Nugent, P. E., Kasen, D. N., & Collett, T. E. 2018b, ApJ, 855, 22, doi: 10.3847/1538-4357/aaa975
Goobar, A., Amanullah, R., Kulkarni, S. R., et al. 2017, Science, 356, 291, doi: 10.1126/science.aal2729
Huang, X., Storfer, C., Ravi, V., et al. 2020, The Astrophysical Journal, 894, 78, doi: 10.3847/1538-4357/ab7ffb
Inada, N., Becker, R. H., Burles, S., et al. 2003, AJ, 126, 666, doi: 10.1086/375906
Jacobs, C., Glazebrook, K., Collett, T., More, A., & McCarthy, C. 2017, MNRAS, 471, 167, doi: 10.1093/mnras/stx1492
Jacobs, C., Collett, T., Glazebrook, K., et al. 2019a, MNRAS, 484, 5330, doi: 10.1093/mnras/stz272
—. 2019b, ApJS, 243, 17, doi: 10.3847/1538-4365/ab26b6
Jaelani, A. T., More, A., Oguri, M., et al. 2020, MNRAS, 495, 1291, doi: 10.1093/mnras/staa1062
Kelly, P. L., Filippenko, A. V., Burke, D. L., et al. 2015, Science, 347, 1459, doi: 10.1126/science.1261475
Kochanek, C. S. 1991, ApJ, 373, 354, doi: 10.1086/170057
Koopmans, L. V. E., & Treu, T. 2002, ApJL, 568, L5, doi: 10.1086/340143
Koopmans, L. V. E., Treu, T., Bolton, A. S., Burles, S., & Moustakas, L. A. 2006, ApJ, 649, 599, doi: 10.1086/505696
Lang, D., Hogg, D. W., & Mykytyn, D. 2016, The Tractor: Probabilistic astronomical source detection and measurement, Astrophysics Source Code Library. http://ascl.net/1604.008
Lanusse, F., Ma, Q., Li, N., et al. 2018, MNRAS, 473, 3895, doi: 10.1093/mnras/stx1665
Lemon, C., Auger, M. W., McMahon, R., et al. 2020, MNRAS, 494, 3491, doi: 10.1093/mnras/staa652
Li, R., Napolitano, N. R., Tortora, C., et al. 2020, arXiv e-prints, arXiv:2004.02715. https://arxiv.org/abs/2004.02715
Metcalf, R. B., Meneghetti, M., Avestruz, C., et al. 2018, arXiv e-prints, arXiv:1802.03609. https://arxiv.org/abs/1802.03609
Moustakas, L. A., Brownstein, J., Fadely, R., et al. 2012, in American Astronomical Society Meeting Abstracts, Vol. 219, American Astronomical Society Meeting Abstracts #219, 146.01
Oguri, M., & Marshall, P. J. 2010, MNRAS, 405, 2579, doi: 10.1111/j.1365-2966.2010.16639.x
Petrillo, C. E., Tortora, C., Chatterjee, S., et al. 2017, MNRAS, 472, 1129, doi: 10.1093/mnras/stx2052
Petrillo, C. E., Tortora, C., Vernardos, G., et al. 2019, MNRAS, 484, 3879, doi: 10.1093/mnras/stz189
Pierel, J. D. R., & Rodney, S. 2019, ApJ, 876, 107, doi: 10.3847/1538-4357/ab164a
Pourrahmani, M., Nayyeri, H., & Cooray, A. 2018, ApJ, 856, 68, doi: 10.3847/1538-4357/aaae6a
Quimby, R. M., Oguri, M., More, A., et al. 2014, Science, 344, 396, doi: 10.1126/science.1250903
Refsdal, S. 1964, MNRAS, 128, 307, doi: 10.1093/mnras/128.4.307
Riess, A. G., Casertano, S., Yuan, W., Macri, L. M., & Scolnic, D. 2019, ApJ, 876, 85, doi: 10.3847/1538-4357/ab1422
Ritondale, E., Vegetti, S., Despali, G., et al. 2019, MNRAS, 485, 2179, doi: 10.1093/mnras/stz464
Rodney, S. A., Strolger, L. G., Kelly, P. L., et al. 2016, ApJ, 820, 50, doi: 10.3847/0004-637X/820/1/50
Sharon, K., Bayliss, M. B., Dahle, H., et al. 2020, ApJS, 247, 12, doi: 10.3847/1538-4365/ab5f13

Sonnenfeld, A., Gavazzi, R., Suyu, S. H., Treu, T., & Marshall, P. J. 2013, ApJ, 777, 97, doi: 10.1088/0004-637X/777/2/97

Sonnenfeld, A., Chan, J. H. H., Shu, Y., et al. 2018, PASJ, 70, S29, doi: 10.1093/pasj/psx062

Sonnenfeld, A., Verma, A., More, A., et al. 2020, arXiv e-prints, arXiv:2004.00634. https://arxiv.org/abs/2004.00634

Suyu, S. H., Marshall, P. J., Auger, M. W., et al. 2010, ApJ, 711, 201, doi: 10.1088/0004-637X/711/1/201

Suyu, S. H., Auger, M. W., Hilbert, S., et al. 2013, ApJ, 766, 70, doi: 10.1088/0004-637X/766/2/70

Suyu, S. H., Huber, S., Cañameras, R., et al. 2020, arXiv e-prints, arXiv:2002.08378. https://arxiv.org/abs/2002.08378

Szegedy, C., Liu, W., Jia, Y., et al. 2014, arXiv e-prints, arXiv:1409.4842. https://arxiv.org/abs/1409.4842

Tessore, N., Bellagamba, F., & Metcalf, R. B. 2016, MNRAS, 463, 3115, doi: 10.1093/mnras/stw2212

Treu, T. 2010, ARA&A, 48, 87, doi: 10.1146/annurev-astro-081309-130924

Treu, T., & Marshall, P. J. 2016, Astronomy and Astrophysics Review, 24, 11, doi: 10.1007/s00159-016-0096-8

Tzeng, E., Hoffman, J., Saenko, K., & Darrell, T. 2017, arXiv e-prints, arXiv:1702.05464. https://arxiv.org/abs/1702.05464

Vegetti, S., Despali, G., Lovell, M. R., & Enzi, W. 2018, MNRAS, 481, 3661, doi: 10.1093/mnras/sty2393

Vegetti, S., & Koopmans, L. V. E. 2009, MNRAS, 400, 1583, doi: 10.1111/j.1365-2966.2009.15559.x

Vegetti, S., Koopmans, L. V. E., Auger, M. W., Treu, T., & Bolton, A. S. 2014, MNRAS, 442, 2017, doi: 10.1093/mnras/stu943

Williams, G. G., Olszewski, E., Lesser, M. P., & Burge, J. H. 2004, in Proc. SPIE, Vol. 5492, Ground-based Instrumentation for Astronomy, ed. A. F. M. Moorwood & M. Iye, 787–798

Wojtak, R., Hjorth, J., & Gall, C. 2019, arXiv e-prints. https://arxiv.org/abs/1903.07687

Wong, K. C., Sonnenfeld, A., Chan, J. H. H., et al. 2018, ApJ, 867, 107, doi: 10.3847/1538-4357/aae381

Wong, K. C., Suyu, S. H., Chen, G. C. F., et al. 2019, arXiv e-prints, arXiv:1907.04869. https://arxiv.org/abs/1907.04869

Zhou, R., Newman, J. A., Mao, Y.-Y., et al. 2020, arXiv e-prints, arXiv:2001.06018. https://arxiv.org/abs/2001.06018

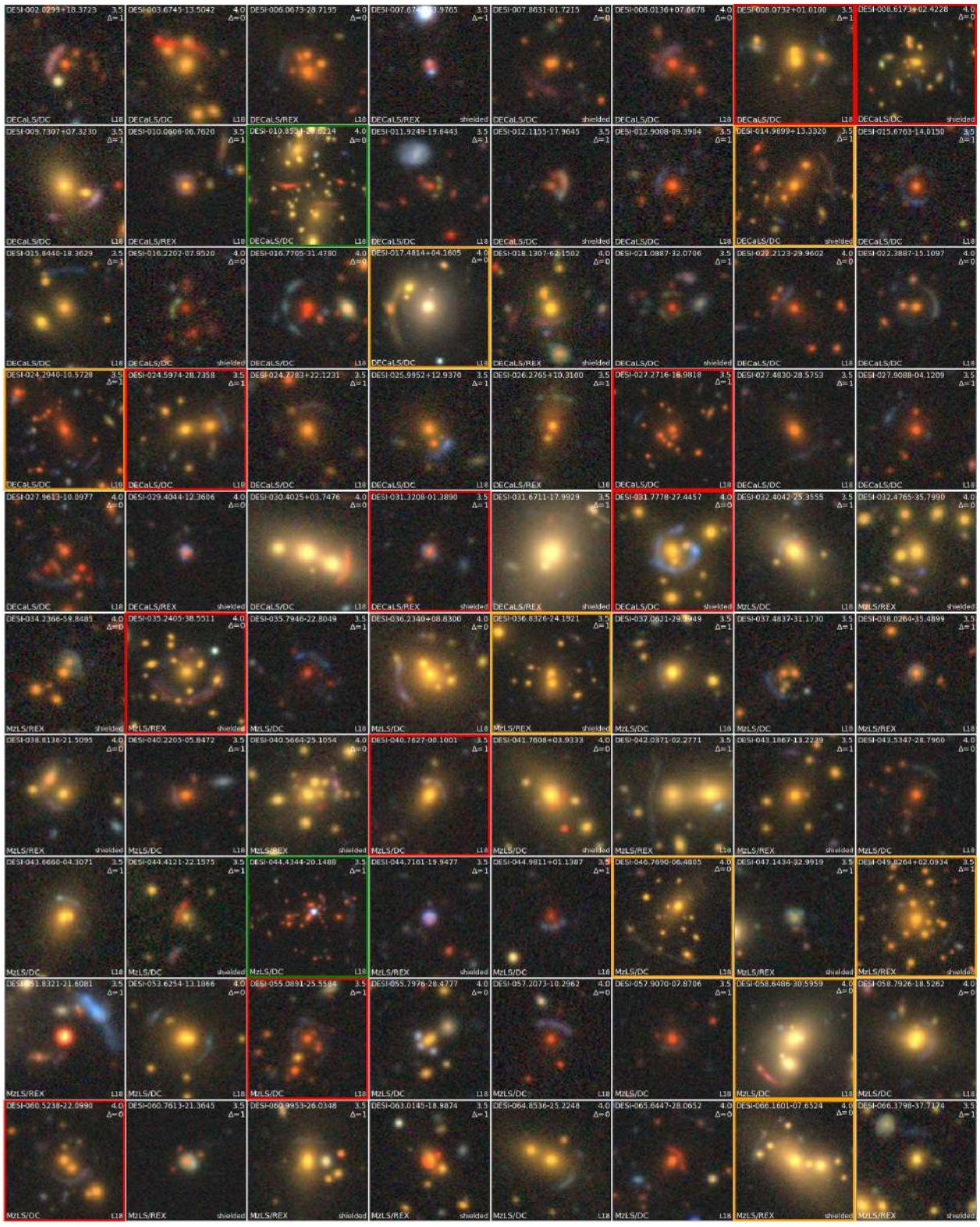

Figure 11. The 216 Grade A candidates arranged in ascending RA. Top right corner indicates the average human inspection score with Δ being the absolute difference; bottom left corner, the region and *The Tractor* type (REX or DC = DEV or COMP); and bottom right, the neural network model. For each image, N is up, and E to the left. For this and all figures that follow: images without rims have a width of 101 pixels (26.5″); with orange rims, 151 pixel (39.6″); green rims, 201 pixel (52.7″); blue rims, 251 pixel (65.8″); and purple rims, 351 pixel (92.0″). Images with red rims are known lenses but not included in our training sample, with citations given in Tables 4 - 6.

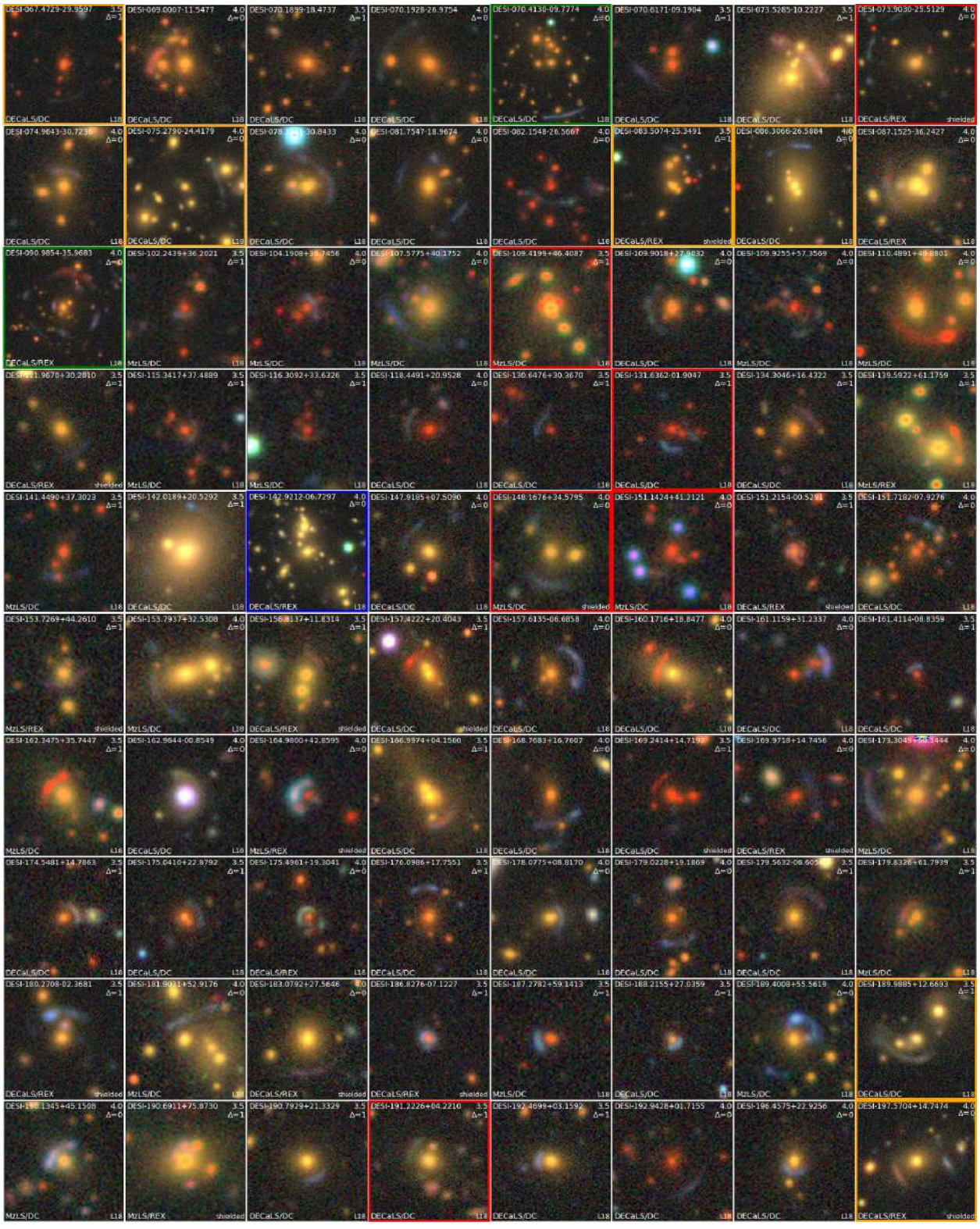

Figure 12. 216 Grade A candidates (continued; see caption of Figure 11).

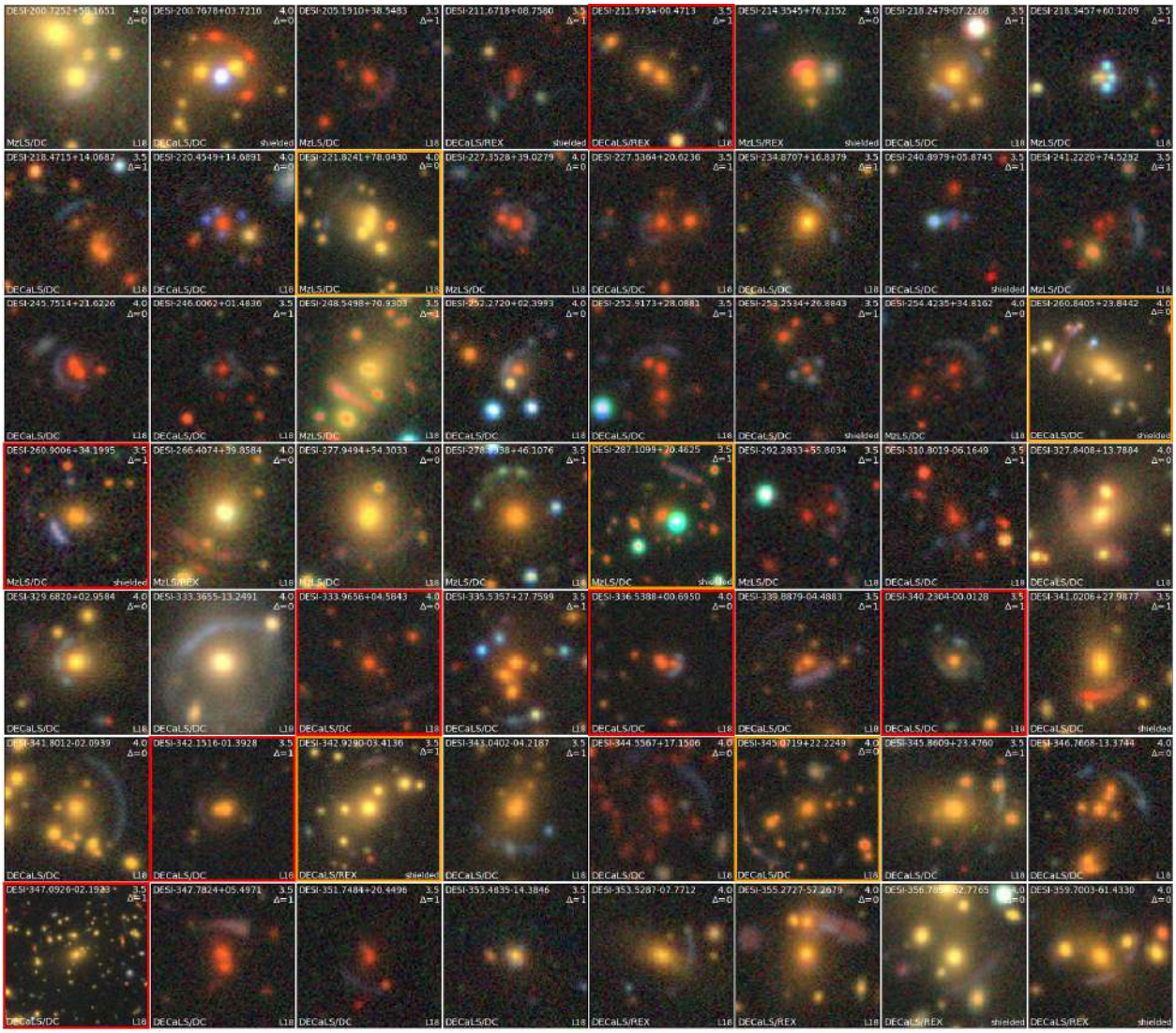

Figure 13. 216 Grade A candidates (continued; see caption of Figure 11).

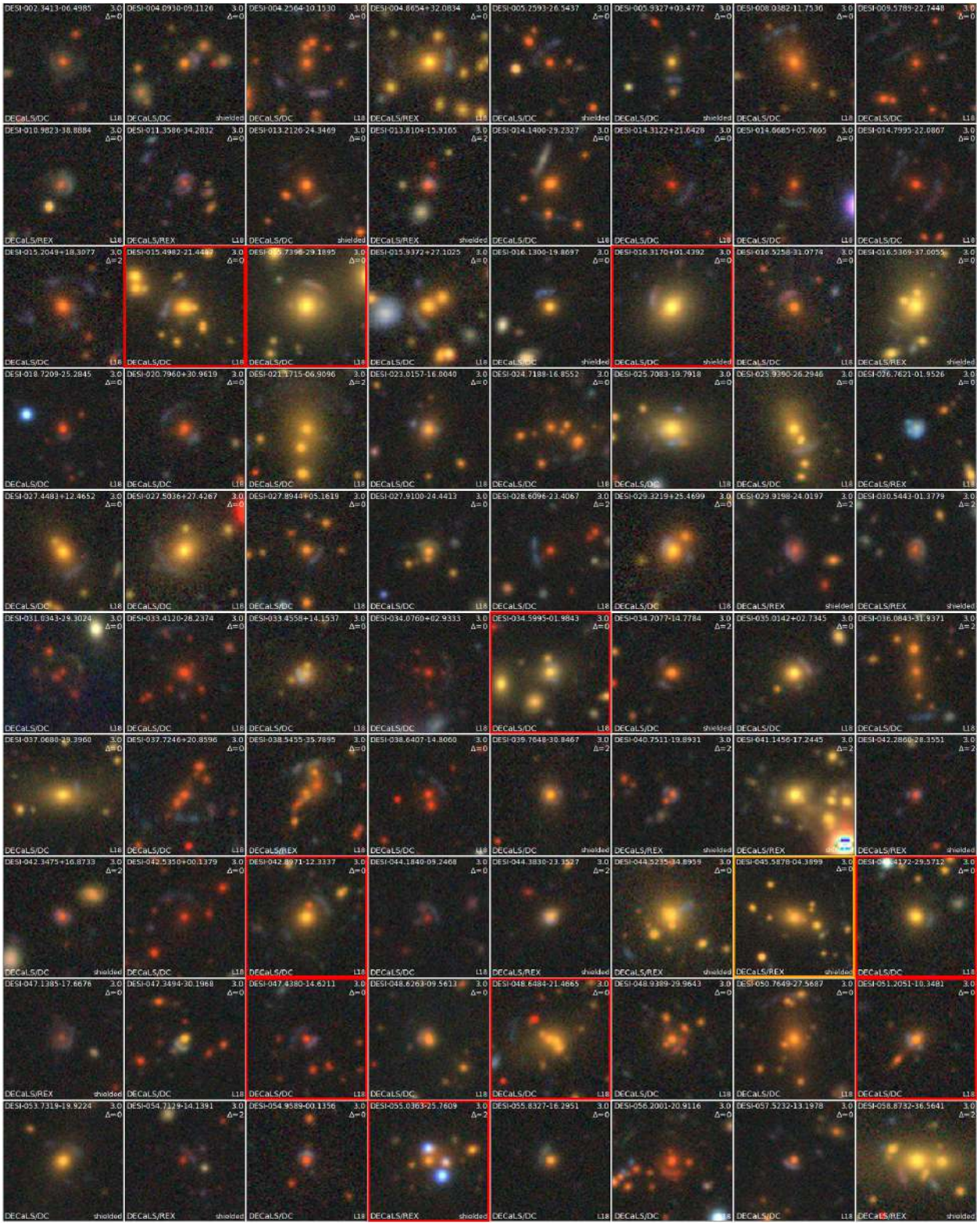

Figure 14. The 199 Grade B lens candidates arranged in ascending RA (see caption of Figure 11).

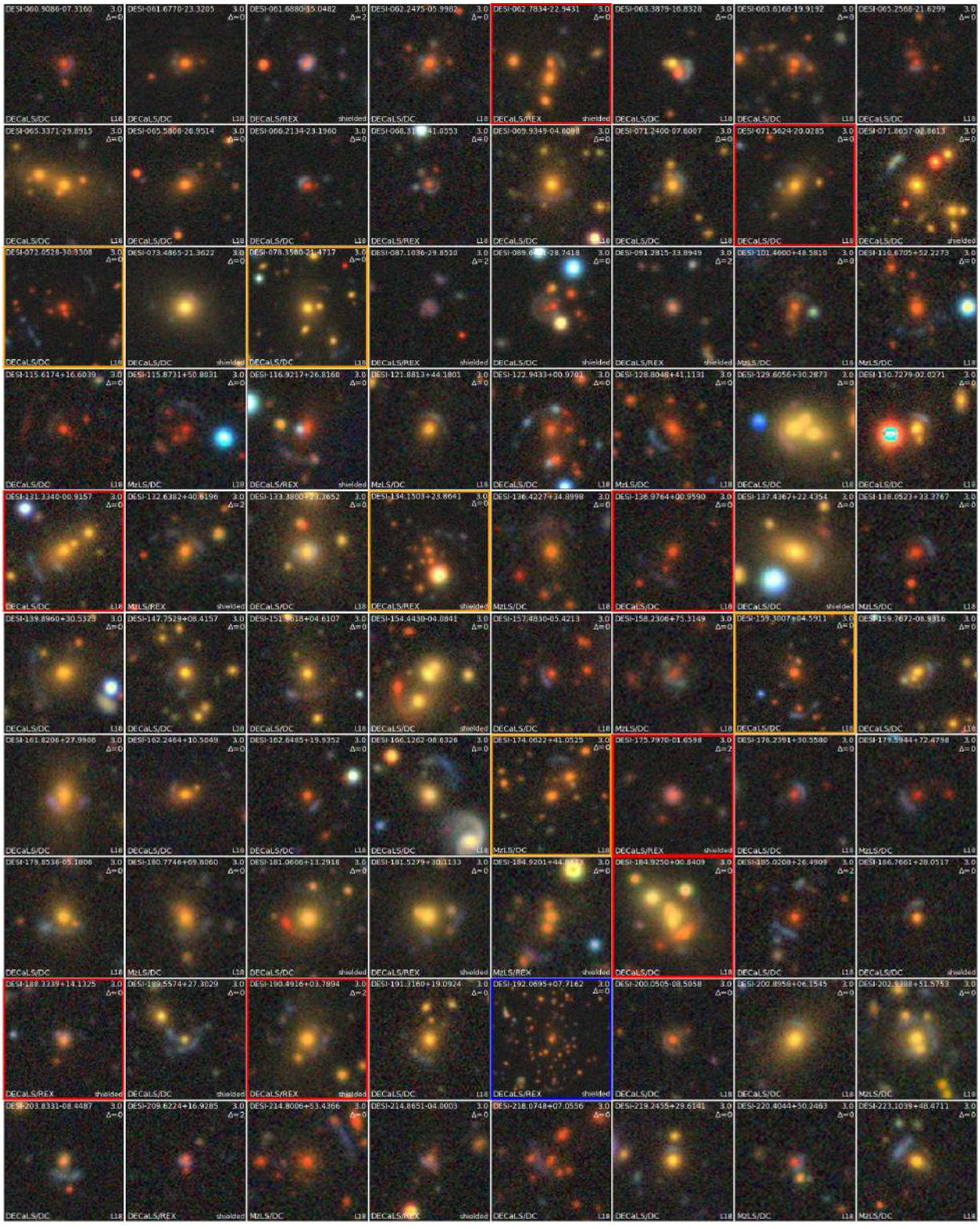

Figure 15. The 199 Grade B lens candidates (continued; see caption of Figure 11).

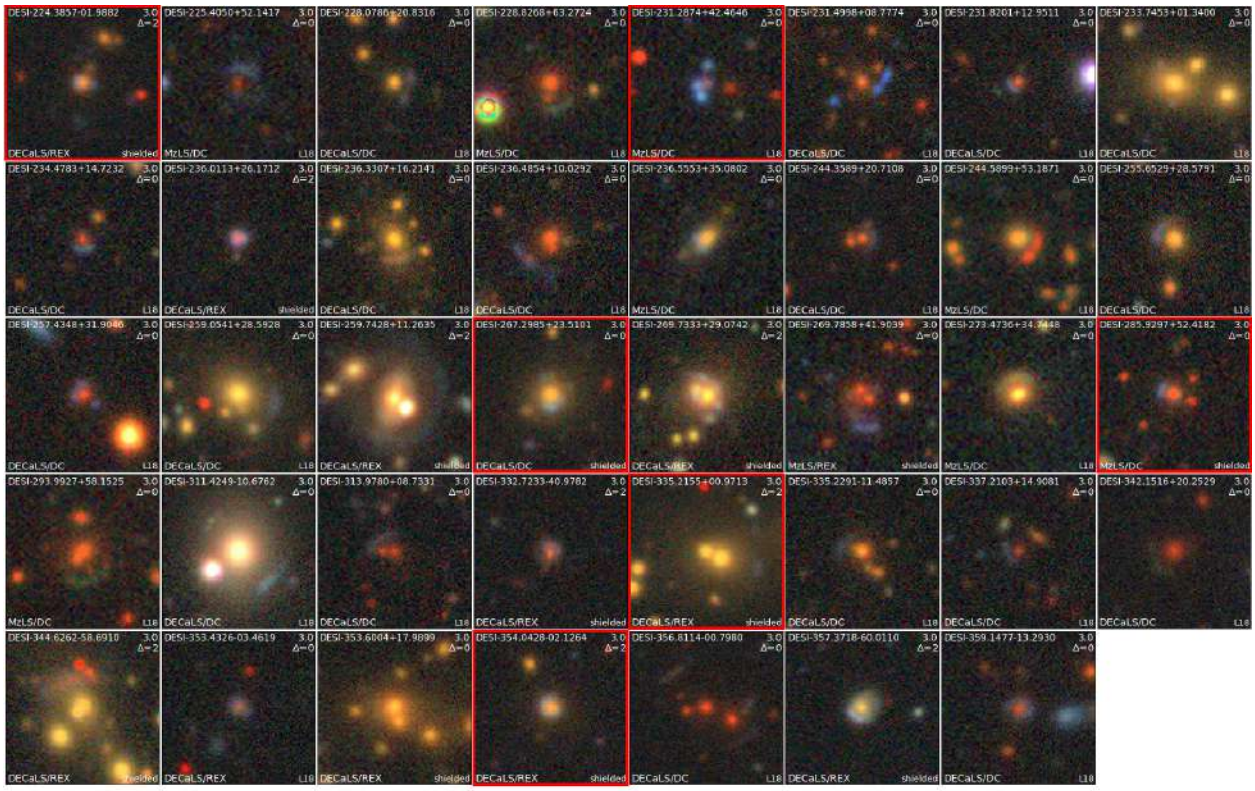

Figure 16. The 199 Grade B lens candidates (continued; see caption of Figure 11).

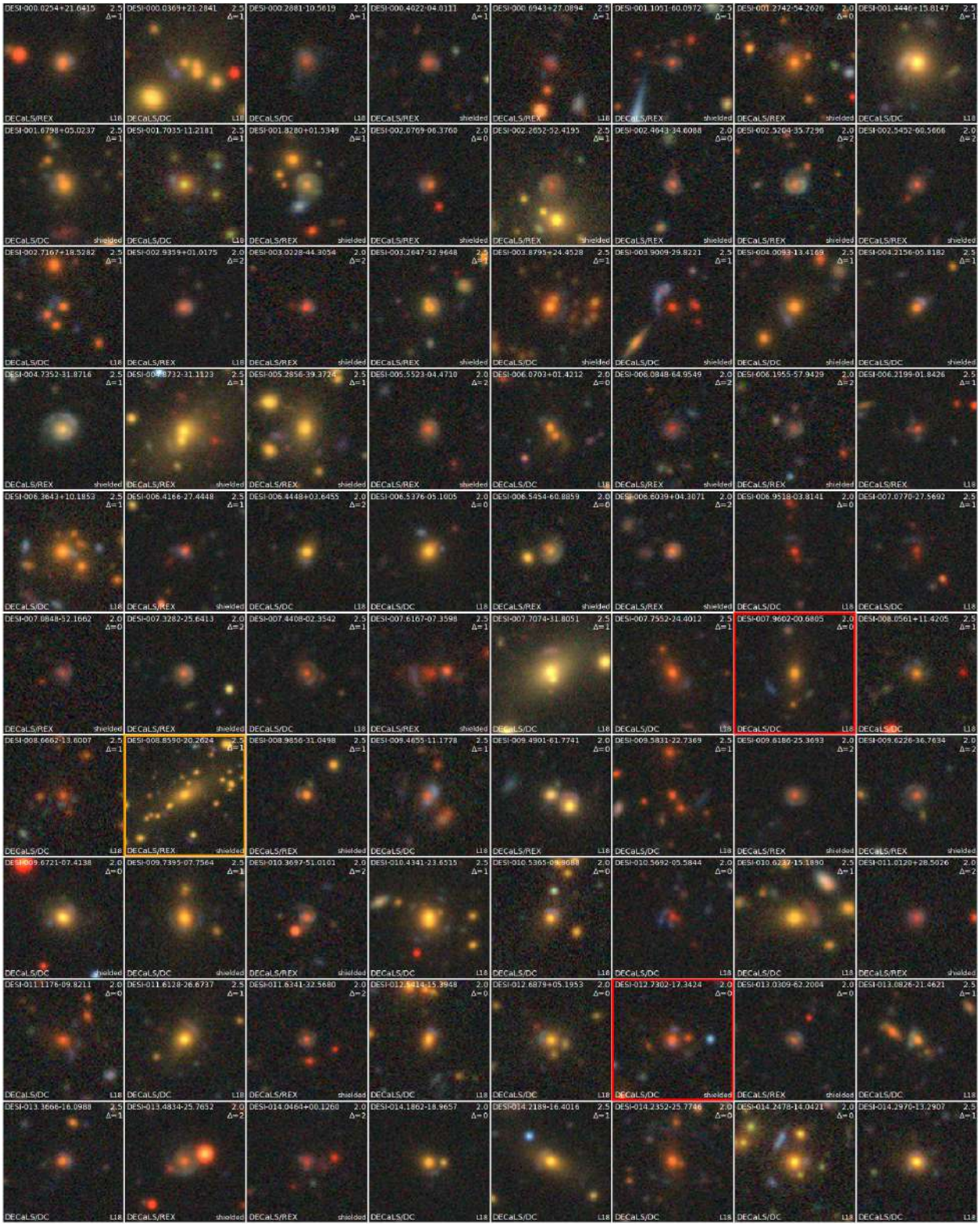

Figure 17. The 897 Grade C lens candidates arranged in ascending RA (see caption of Figure 11).

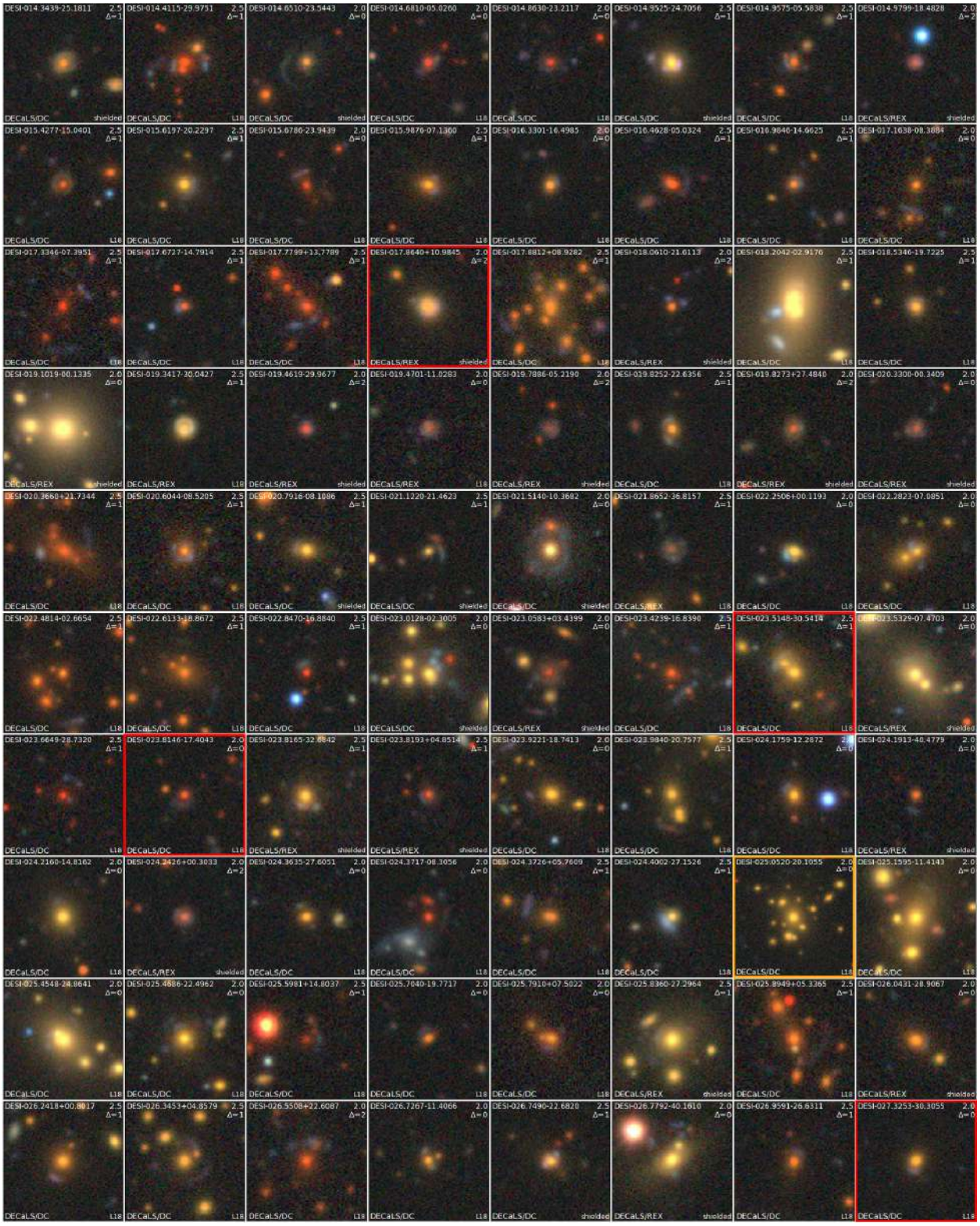

Figure 18. The 897 Grade C lens candidates (continued; see caption of Figure 11).

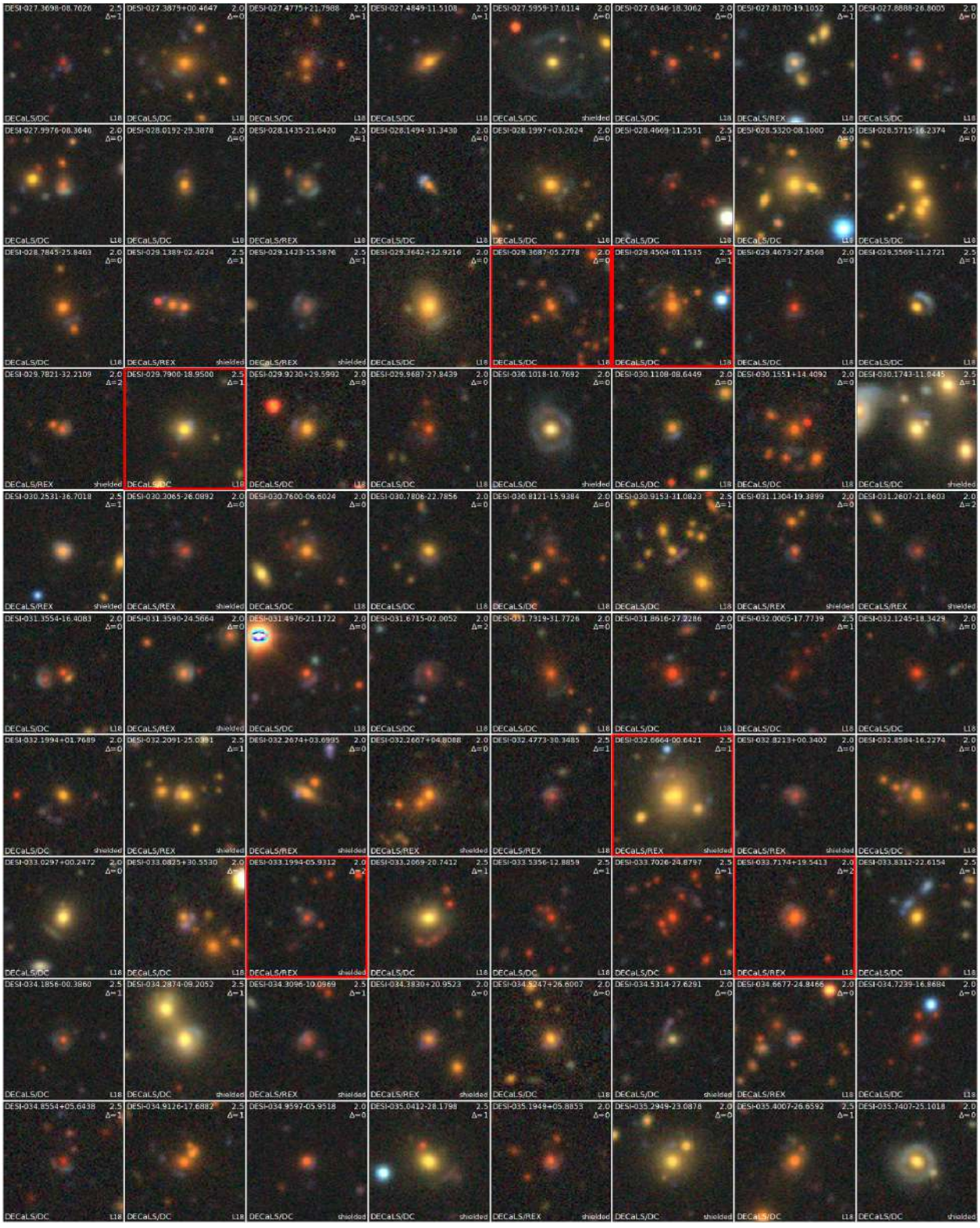

Figure 19. The 897 Grade C lens candidates (continued; see caption of Figure 11).

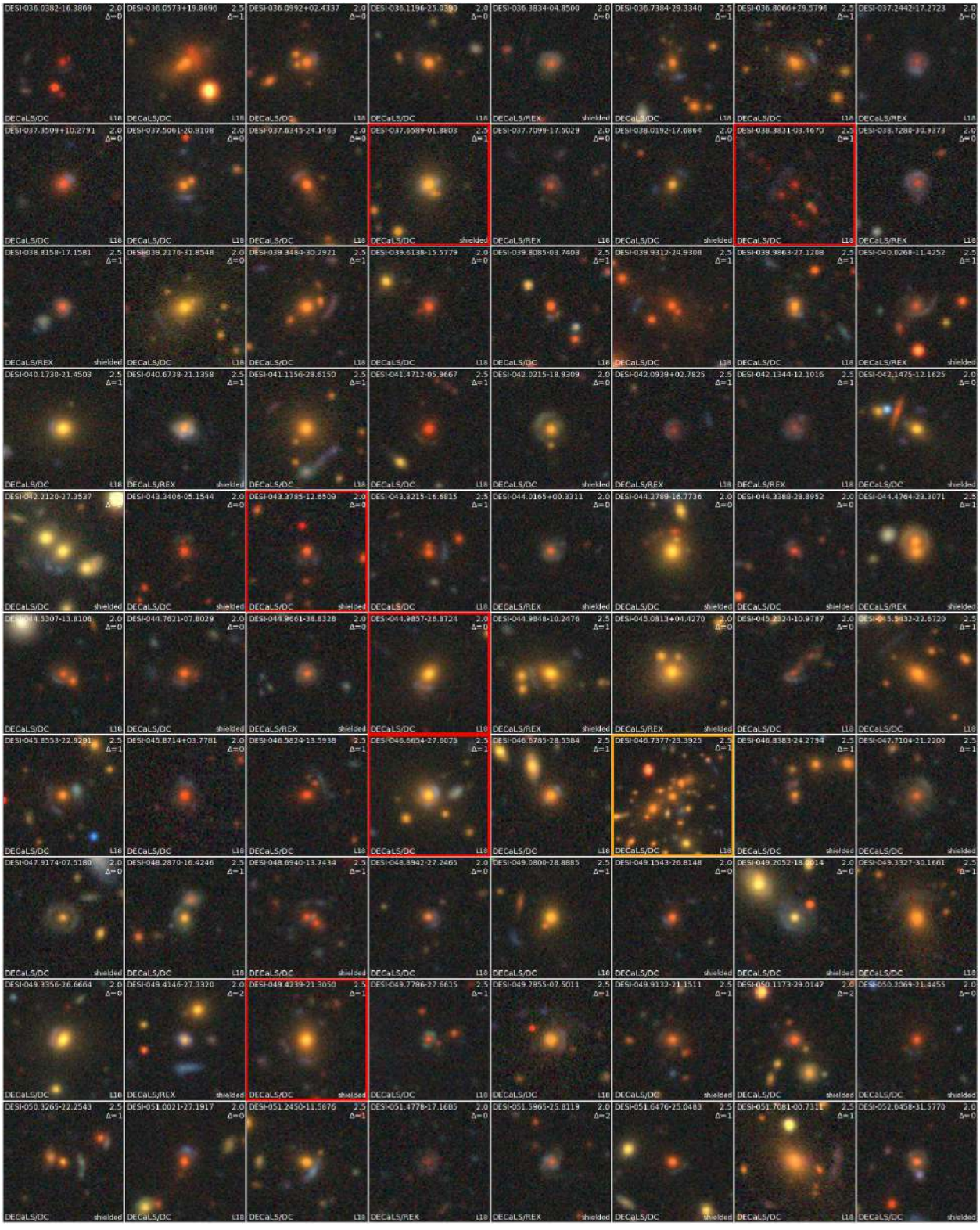

Figure 20. The 897 Grade C lens candidates (continued; see caption of Figure 11).

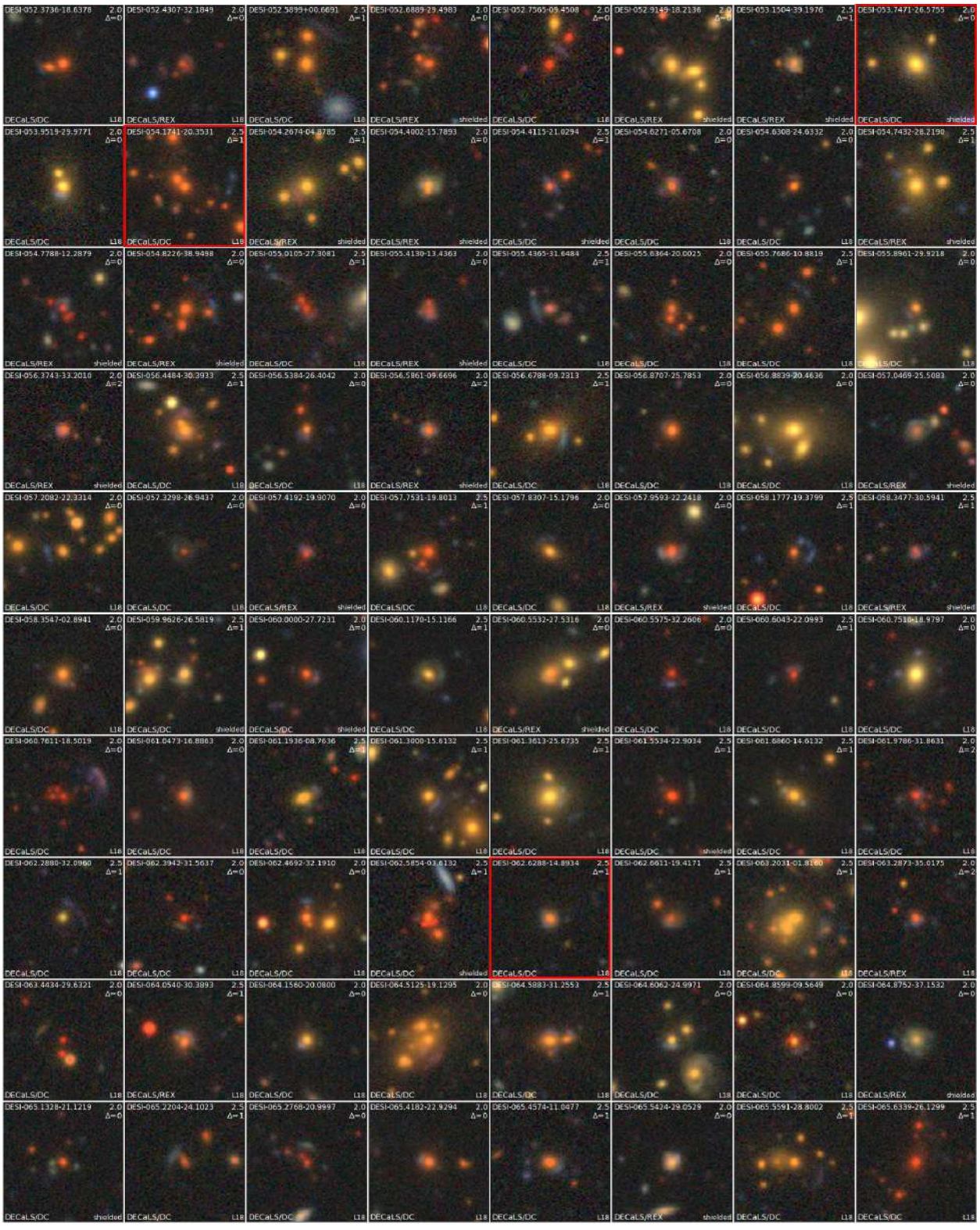

Figure 21. The 897 Grade C lens candidates (continued; see caption of Figure 11).

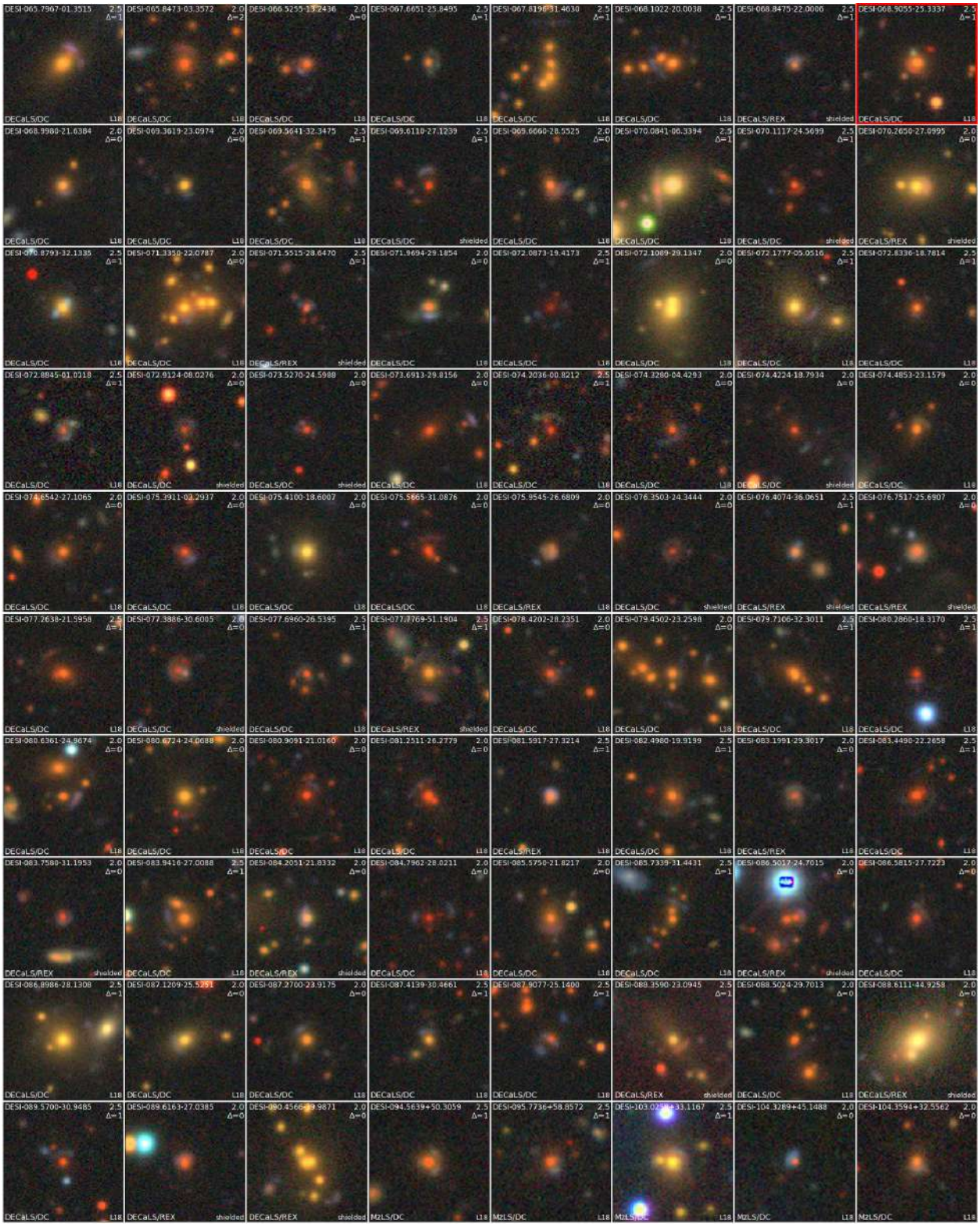

Figure 22. The 897 Grade C lens candidates (continued; see caption of Figure 11).

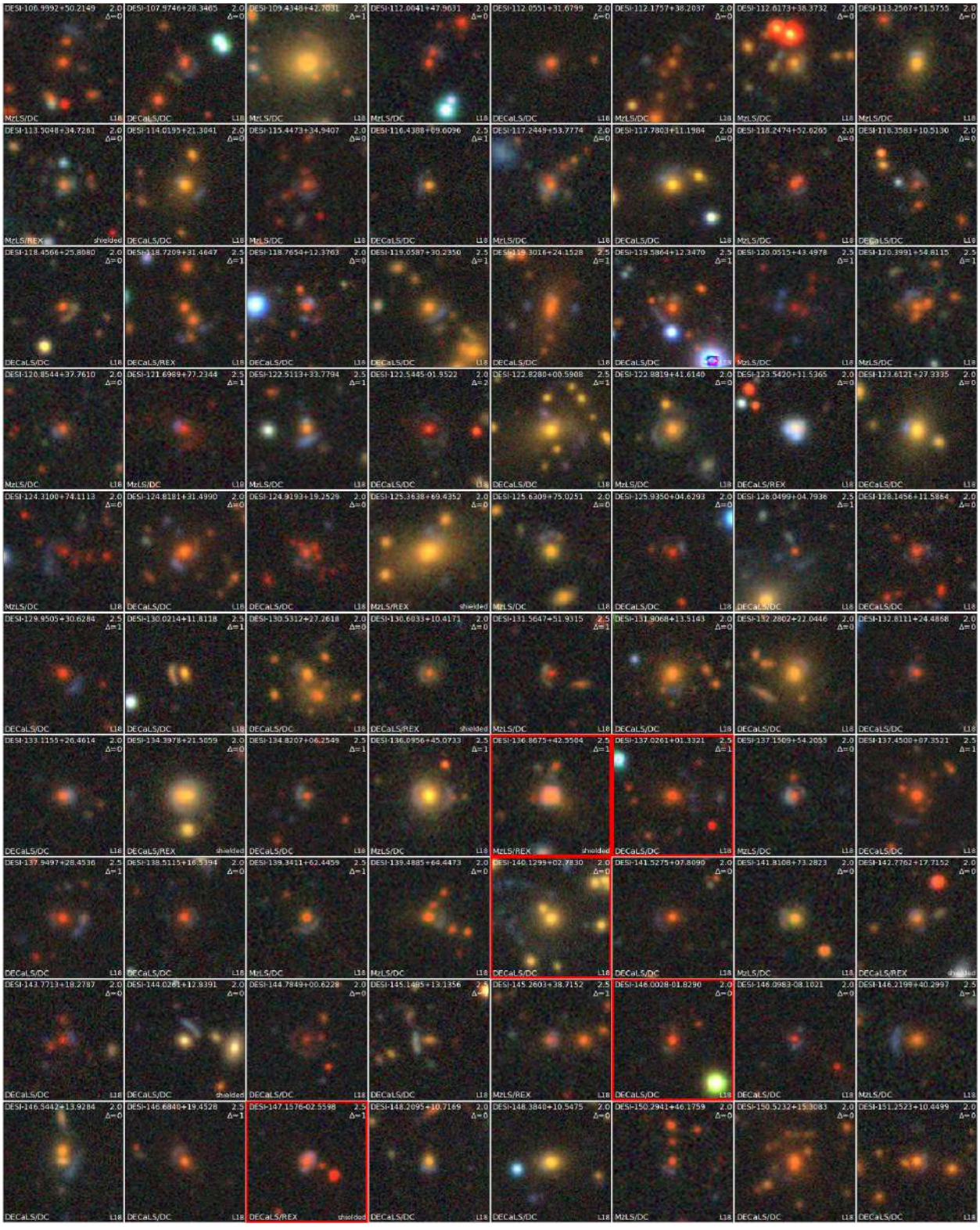

Figure 23. The 897 Grade C lens candidates (continued; see caption of Figure 11).

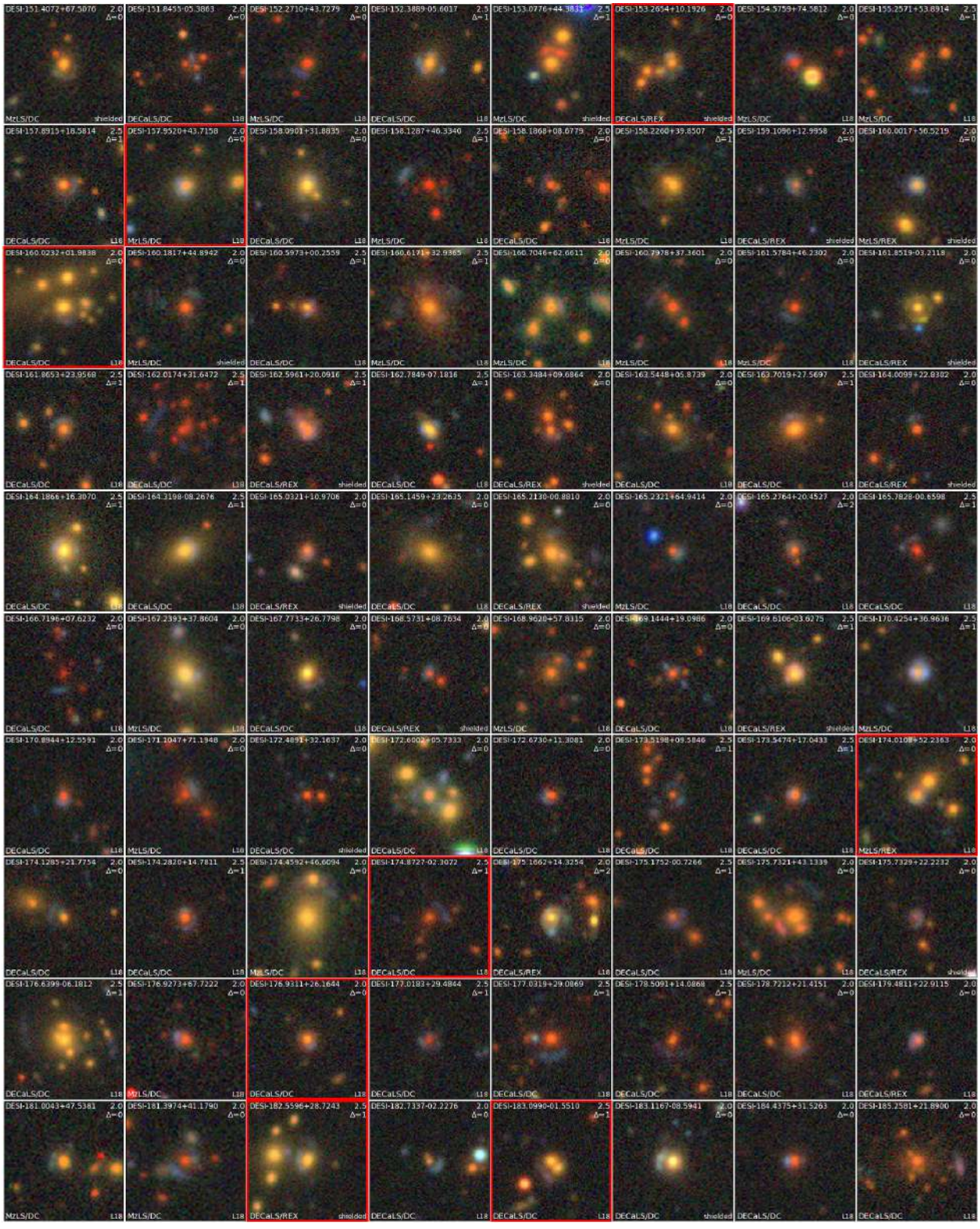

Figure 24. The 897 Grade C lens candidates (continued; see caption of Figure 11).

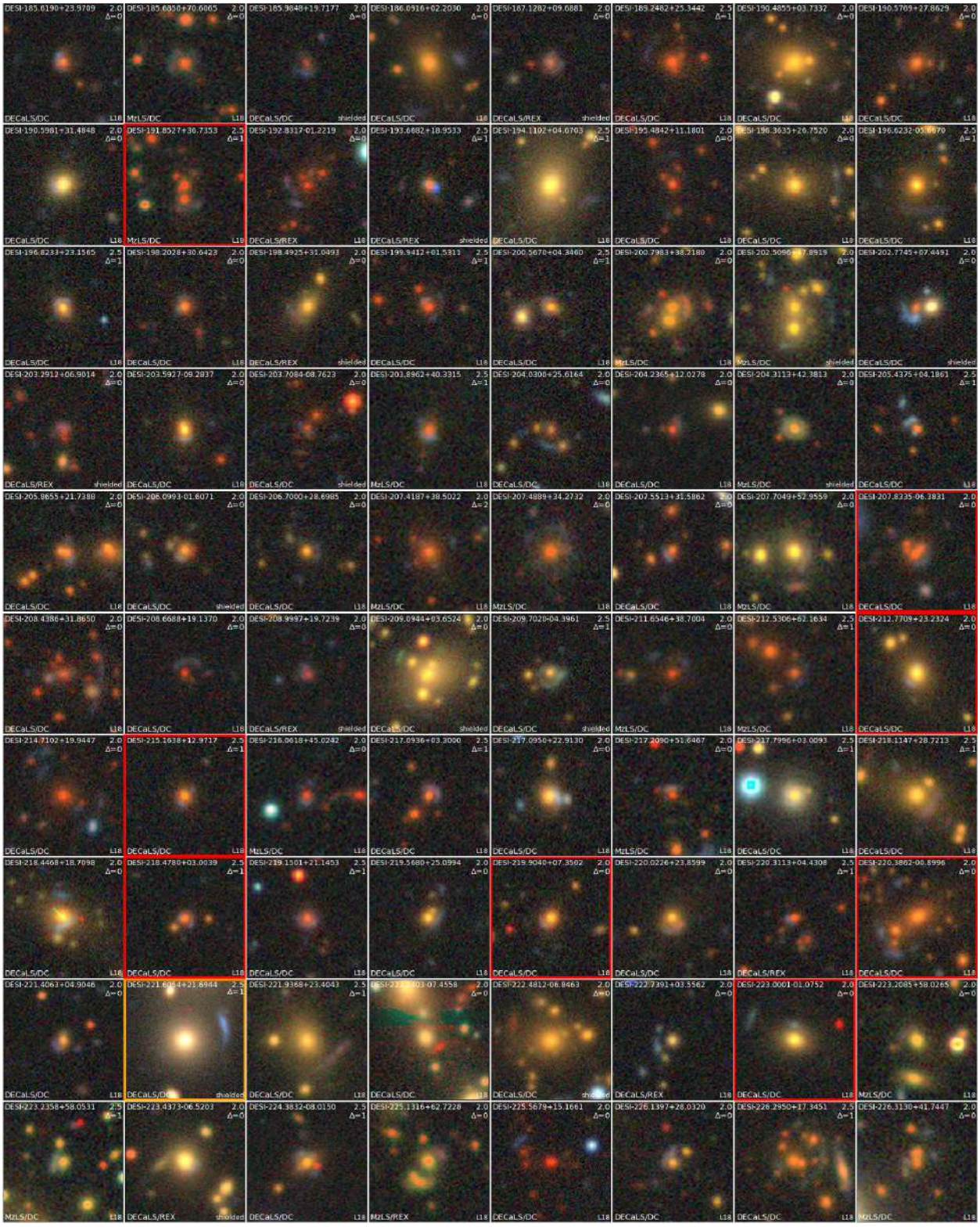

Figure 25. The 897 Grade C lens candidates (continued; see caption of Figure 11).

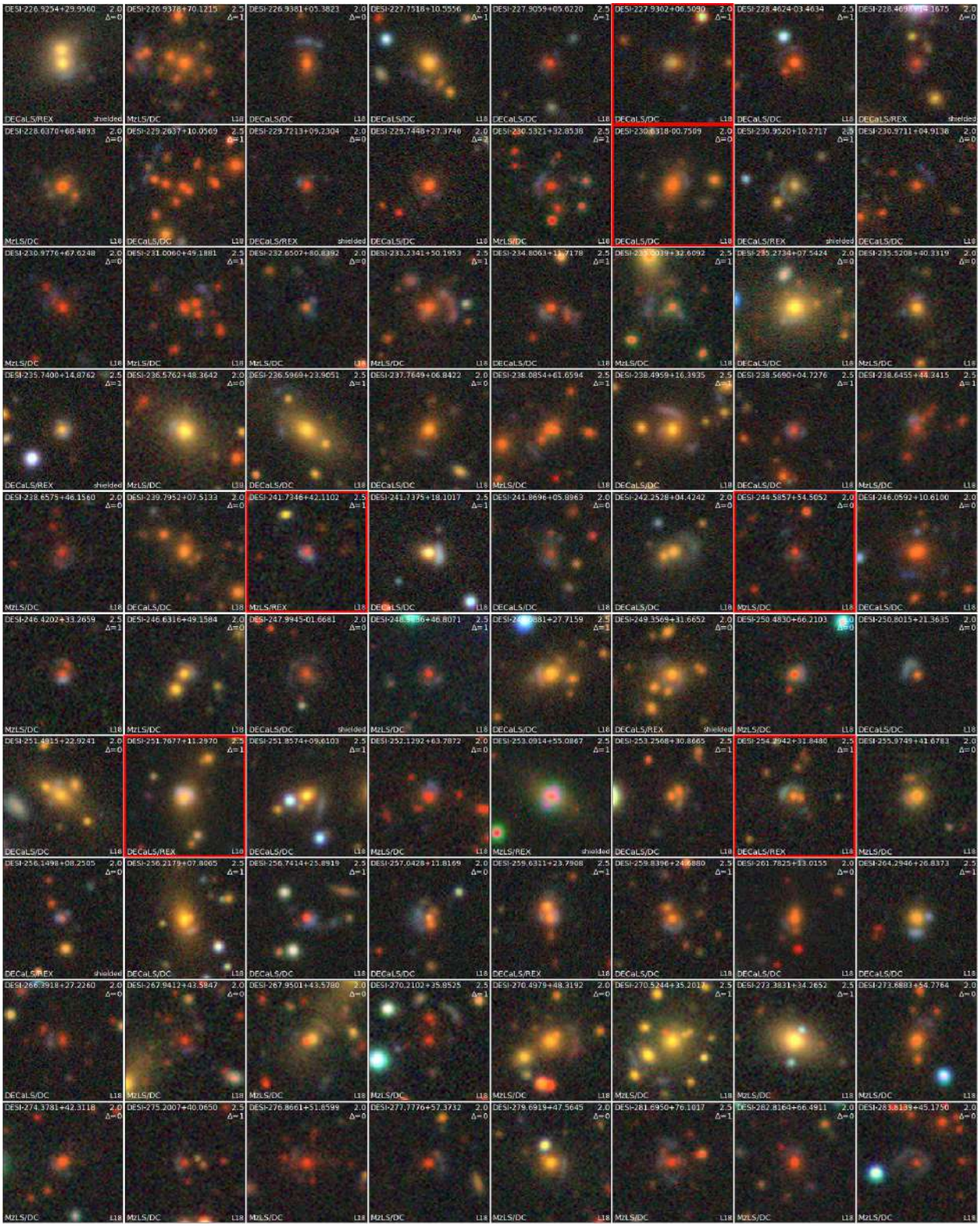

Figure 26. The 897 Grade C lens candidates (continued; see caption of Figure 11).

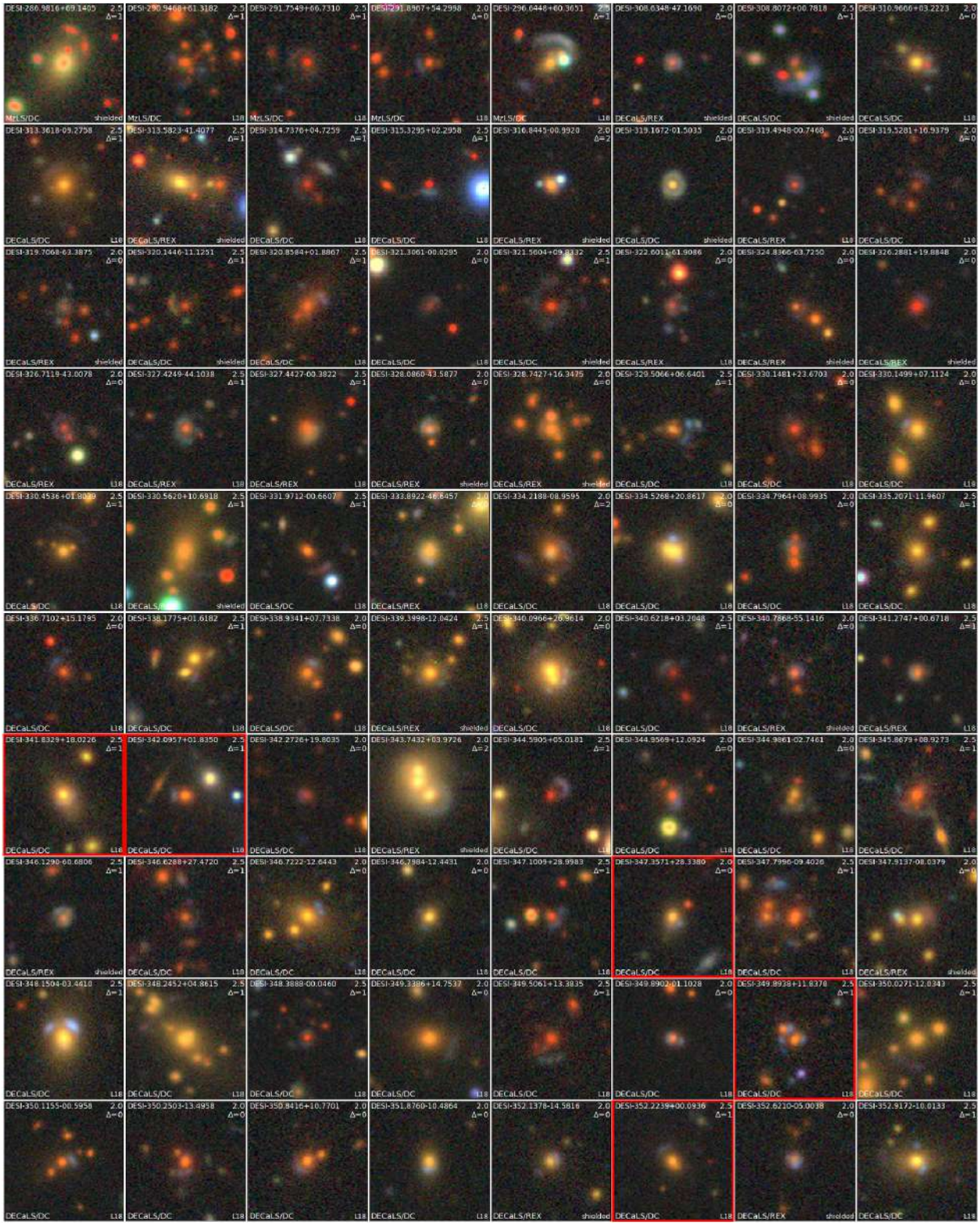

Figure 27. The 897 Grade C lens candidates (continued; see caption of Figure 11).

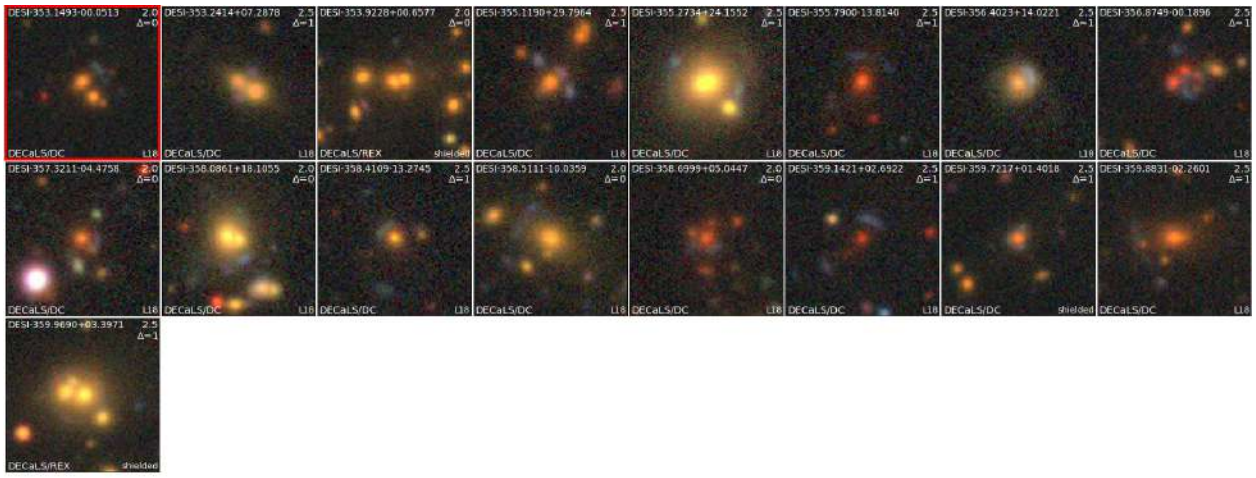

Figure 28. The 897 Grade C lens candidates (continued; see caption of Figure 11).

Table 4. Grade A Candidates

Name	Type	mag_g	mag_r	mag_z	Probability	z_{spec}	z_{phot}
DESI-002.0299+18.3723	DC	21.55	19.86	19.03	0.97	0.4724	
DESI-003.6745-13.5042	DC	21.01	19.43	18.58	0.01		0.406 ± 0.021
DESI-006.0673-28.7195	REX	21.51	20.15	19.31	0.97		0.533 ± 0.025
DESI-007.6741-33.9765	REX	22.07	20.83	19.69	0.20		0.858 ± 0.041
DESI-007.8631-01.7215	DC	20.95	19.33	18.48	0.53	0.5201	
DESI-008.0136+07.6678	DC	21.85	20.25	19.38	0.99	0.5566	
DESI-008.0732+01.0100[e]	DC	19.14	18.15	17.50	0.31		0.426 ± 0.091
DESI-008.6173+02.4228[b,e]	DC	21.72	19.84	18.72	0.54	0.4548	
DESI-009.7307+07.3230	DC	16.48	15.85	15.35	0.22	0.2547	
DESI-010.0606-06.7620	REX	19.76	19.25	18.94	1.00	0.6152	
DESI-010.8534-20.6214	DC	22.68	20.78	19.57	0.11	0.3381	
DESI-011.9249-19.6443	DC	22.30	21.22	19.82	0.84		0.688 ± 0.056
DESI-012.1155-17.9645	DC	20.37	18.95	18.23	0.90		0.735 ± 0.069
DESI-012.9008-09.3904	DC	23.68	21.59	19.94	1.00	0.4485	
DESI-014.9899+13.3320	DC	22.02	20.36	19.39	0.91	0.5163	
DESI-015.6763-14.0150	DC	18.26	17.29	16.62	1.00		0.658 ± 0.036
DESI-015.8440-18.3629	DC	22.15	20.57	19.67	1.00		0.364 ± 0.019
DESI-016.2202-07.9520	DC	20.94	19.38	18.57	0.48		0.764 ± 0.032
DESI-016.7705-31.4780	DC	22.18	20.53	19.71	1.00		0.772 ± 0.018
DESI-017.4814+04.1605	DC	21.21	19.49	18.63	0.19		0.281 ± 0.140
DESI-018.1307-62.1502	REX	20.54	20.04	19.79	0.98		0.427 ± 0.024
DESI-021.0887-32.0706	DC	22.61	20.79	19.63	0.82		0.754 ± 0.080
DESI-022.2123-29.9602	DC	20.90	19.26	18.36	1.00		0.649 ± 0.023
DESI-022.3887-15.1097	DC	17.68	16.76	16.08	1.00		0.524 ± 0.063
DESI-024.2940-10.5728	DC	22.04	20.30	19.38	0.87	0.4135	
DESI-024.5974-28.7358[d]	DC	23.20	21.18	19.92	1.00		0.414 ± 0.022
DESI-024.7783+22.1231	DC	20.20	18.86	18.01	0.13	0.4684	
DESI-025.9952+12.9370	DC	20.22	19.11	18.29	0.92	0.5114	
DESI-026.2765+10.3100	REX	22.65	20.92	19.99	0.28		0.462 ± 0.138
DESI-027.2716-16.9818[d]	DC	20.80	19.57	18.68	0.92	0.6916	
DESI-027.4830-28.5753	DC	20.76	19.03	18.08	0.97		0.557 ± 0.008
DESI-027.9088-04.1209	DC	22.47	20.72	19.39	0.81	0.6412	
DESI-027.9613-10.0977	DC	22.58	20.64	19.22	1.00	0.5234	
DESI-029.4044-12.3606	REX	21.29	20.41	19.91	0.95		0.747 ± 0.169
DESI-030.4025+03.7476	DC	22.52	20.73	19.74	0.64	0.1696	
DESI-031.3208-01.3890[d]	REX	19.18	18.24	17.57	1.00	0.6992	

Table 4 continued on next page

Table 4 *(continued)*

Name	Type	mag_g	mag_r	mag_z	Probability	z_{spec}	z_{phot}
DESI-031.6711-17.9929	REX	21.94	20.26	19.41	0.10	0.1548	
DESI-031.7778-27.4457[d]	DC	23.28	21.17	19.47	1.00		0.294 ± 0.018
DESI-032.4042-25.3555	DC	22.42	20.76	19.55	0.49		0.224 ± 0.015
DESI-032.4765-35.7990	REX	21.58	20.69	19.80	0.98		0.380 ± 0.076
DESI-034.2366-59.8485	REX	14.59	14.03	13.71	0.66		0.498 ± 0.017
DESI-035.2405-38.5511[d,d]	REX	21.35	19.95	19.01	0.45		0.407 ± 0.038
DESI-035.7946-22.8049	DC	22.95	21.20	19.67	1.00		0.890 ± 0.048
DESI-036.2340+08.8300	DC	21.19	19.91	19.08	1.00		0.326 ± 0.035
DESI-036.8326-24.1921	REX	20.14	19.21	18.53	0.39		0.405 ± 0.022
DESI-037.0621-29.3949	DC	19.54	18.21	17.46	0.93		0.312 ± 0.013
DESI-037.4837-31.1730	DC	19.48	18.18	17.33	0.99		0.466 ± 0.075
DESI-038.0264-35.4899	REX	22.01	20.53	19.61	1.00		0.550 ± 0.097
DESI-038.8136-21.5095	REX	21.25	19.70	18.73	0.94		0.328 ± 0.035
DESI-040.2205-05.8472	DC	22.47	20.53	19.26	0.97	0.5238	
DESI-040.5664-25.1054	REX	22.06	20.32	19.31	0.82		0.325 ± 0.045
DESI-040.7627-00.1001[d]	DC	23.51	21.49	20.00	1.00	0.4127	
DESI-041.7608+03.9333	DC	22.49	20.64	19.69	0.30	0.2603	
DESI-042.0371-02.2771	REX	21.97	20.64	19.80	0.93		0.247 ± 0.018
DESI-043.1867-13.2239	REX	21.91	20.35	19.49	0.67		0.431 ± 0.033
DESI-043.5347-28.7960	DC	22.21	20.44	19.47	0.93		0.632 ± 0.021
DESI-043.6660-04.3071	DC	22.04	20.18	18.97	1.00	0.2880	
DESI-044.4121-22.1575	DC	21.67	19.81	18.86	0.46		0.484 ± 0.070
DESI-044.4344-20.1488	DC	21.82	20.09	19.18	0.49		0.711 ± 0.025
DESI-044.7161-19.9477	REX	21.63	20.54	19.82	0.89		0.535 ± 0.327
DESI-044.9811+01.1387	DC	19.28	18.85	18.49	1.00		0.834 ± 0.079
DESI-046.7690-06.4805	DC	23.05	21.25	19.90	0.32		0.480 ± 0.105
DESI-047.1434-32.9919	REX	21.86	20.52	19.59	0.22		0.500 ± 0.091
DESI-049.8264+02.0934	REX	21.06	19.78	19.06	0.90	0.3189	
DESI-051.8321-21.6081	REX	21.71	20.60	19.87	0.16		0.502 ± 0.201
DESI-053.6254-13.1866	DC	22.40	20.63	19.67	1.00		0.362 ± 0.010
DESI-055.0891-25.5584[d]	DC	19.48	18.48	17.80	1.00		0.667 ± 0.047
DESI-055.7976-28.4777	DC	21.48	19.87	19.05	1.00		0.447 ± 0.049
DESI-057.2073-10.2962	DC	22.83	21.09	19.71	1.00		0.745 ± 0.075
DESI-057.9070-07.8706	DC	21.75	19.95	18.94	1.00		0.677 ± 0.051
DESI-058.6486-30.5959	DC	22.64	20.77	19.31	0.12		0.173 ± 0.021
DESI-058.7926-18.5262	DC	22.82	21.15	19.92	1.00		0.282 ± 0.011
DESI-060.5238-22.0990[d]	DC	19.50	18.43	17.70	1.00		0.367 ± 0.051
DESI-060.7613-21.3645	REX	22.89	21.01	19.89	0.28		0.455 ± 0.100

Table 4 continued on next page

Table 4 *(continued)*

Name	Type	mag_g	mag_r	mag_z	Probability	z_{spec}	z_{phot}
DESI-060.9953-26.0348	REX	21.55	20.28	19.61	0.80		0.289 ± 0.083
DESI-063.0145-18.9874	REX	22.56	21.28	19.93	0.18		0.572 ± 0.073
DESI-064.8536-25.2248	DC	18.04	16.86	16.12	0.98		0.360 ± 0.012
DESI-065.6447-28.0652	DC	19.47	18.29	17.53	0.53		0.641 ± 0.036
DESI-066.1601-07.6524	REX	24.06	21.89	19.84	0.79		0.278 ± 0.049
DESI-066.3798-37.7174	REX	21.07	19.99	19.21	0.23		0.290 ± 0.041
DESI-067.4729-29.9597	DC	22.07	20.39	19.37	0.24		0.716 ± 0.015
DESI-069.0007-11.5477	DC	19.43	18.96	18.69	0.91		0.425 ± 0.033
DESI-070.1899-18.4737	DC	19.12	18.28	17.71	0.63		0.526 ± 0.010
DESI-070.1928-26.9754	DC	19.50	18.41	17.69	0.82		0.500 ± 0.011
DESI-070.4130-09.7774	DC	22.67	20.84	19.59	1.00		0.437 ± 0.036
DESI-070.6171-09.1904	DC	22.83	20.92	19.80	0.55		0.588 ± 0.016
DESI-073.5285-10.2227	DC	23.37	21.38	19.77	0.89		0.311 ± 0.130
DESI-073.9030-25.5129[d]	REX	20.82	20.06	19.63	0.51		0.475 ± 0.051
DESI-074.9643-30.7236	DC	20.90	20.06	19.53	1.00		0.431 ± 0.017
DESI-075.2790-24.4179	DC	21.90	20.68	19.44	0.90		0.289 ± 0.106
DESI-078.3561-30.8433	DC	21.26	19.49	18.56	0.63		0.387 ± 0.021
DESI-081.7547-18.9674	DC	23.29	21.20	19.54	1.00		0.439 ± 0.013
DESI-082.1548-26.5667	DC	21.45	20.46	19.84	1.00		0.840 ± 0.043
DESI-083.5074-25.3491	REX	20.32	19.28	18.62	0.94		0.477 ± 0.064
DESI-086.3066-26.5884	DC	20.54	18.84	17.97	1.00		0.448 ± 0.083
DESI-087.1525-36.2427	REX	21.54	20.07	19.22	0.42		0.305 ± 0.036
DESI-090.9854-35.9683	REX	21.17	20.19	19.73	0.90		0.529 ± 0.115
DESI-102.2439+36.2021	DC	21.73	20.10	19.33	1.00		0.659 ± 0.047
DESI-104.1908+38.7456	DC	20.71	19.48	18.74	1.00	0.4549	
DESI-107.5775+40.1752	DC	22.26	20.64	19.78	1.00	0.2928	
DESI-109.4199+46.4087[a]	DC	22.42	20.57	19.46	0.90		0.429 ± 0.074
DESI-109.9018+27.9032	DC	21.02	19.32	18.42	0.63		0.533 ± 0.016
DESI-109.9255+57.3569	DC	21.11	19.73	18.89	0.21		0.747 ± 0.044
DESI-110.4891+49.8801	DC	20.37	18.78	17.93	0.16		0.430 ± 0.022
DESI-111.9670+30.2010	REX	20.08	19.37	18.85	0.23	0.1527	
DESI-115.3417+37.4889	DC	21.01	19.27	18.35	0.96	0.6031	
DESI-116.3092+33.6326	DC	22.05	20.42	19.57	0.33	0.5642	
DESI-118.4491+20.9528	DC	20.72	19.32	18.56	0.99	0.5866	
DESI-130.6476+30.3670	DC	21.73	19.80	18.36	0.33	0.5041	
DESI-131.6362-01.9047[e]	DC	19.95	18.79	18.08	1.00	0.5422	
DESI-134.3046+16.4322	DC	21.02	19.43	18.62	0.38	0.4441	
DESI-139.5922+61.1759	REX	22.25	20.64	19.79	0.29		0.242 ± 0.062

Table 4 continued on next page

Table 4 *(continued)*

Name	Type	mag_g	mag_r	mag_z	Probability	z_{spec}	z_{phot}
DESI-141.4490+37.3023	DC	22.74	20.82	19.61	0.65	0.5526	
DESI-142.0189+20.5292	DC	21.44	20.20	19.19	0.20		0.198 ± 0.006
DESI-142.9212-06.7297	REX	21.54	20.44	19.76	0.10		0.264 ± 0.032
DESI-147.9185+07.5090	DC	20.62	19.51	18.82	0.15	0.3527	
DESI-148.1676+34.5795[h]	DC	21.44	20.41	19.77	0.50	0.3963	
DESI-151.1424+41.2121[c]	DC	21.31	19.53	18.60	0.30	0.5934	
DESI-151.2154-00.5291	REX	22.51	20.76	19.75	1.00	0.6335	
DESI-151.7182-07.9276	DC	21.66	20.64	19.94	0.99		0.569 ± 0.025
DESI-153.7269+44.2610	REX	22.09	20.79	19.91	0.54	0.2971	
DESI-153.7937+32.5308	DC	19.81	18.21	17.37	0.30		0.243 ± 0.147
DESI-156.8137+11.8314	REX	21.69	20.58	19.83	0.28	0.2800	
DESI-157.4222+20.4043	DC	23.58	21.49	19.77	0.43		0.946 ± 0.324
DESI-157.6135-06.6858	DC	21.03	20.14	19.50	1.00		0.463 ± 0.029
DESI-160.1716+18.8477	DC	21.37	19.90	19.07	0.20		0.358 ± 0.039
DESI-161.1159+31.2337	DC	21.60	19.87	19.04	0.83	0.5291	
DESI-161.4114-08.8359	DC	21.51	19.64	18.59	0.98		0.813 ± 0.150
DESI-162.3475+35.7447	DC	21.71	20.63	19.98	0.29	0.2602	
DESI-162.9644-00.8549	DC	16.04	15.89	15.45	0.20		0.696 ± 0.245
DESI-164.9800+42.8595	REX	21.47	20.24	19.56	0.29		0.817 ± 0.036
DESI-166.9974+04.1560	DC	19.43	18.80	18.41	0.67	0.3359	
DESI-168.7683+16.7607	DC	20.38	19.32	18.66	0.96	0.6196	
DESI-169.2414+14.7197	DC	21.86	20.16	19.32	0.47	0.5424	
DESI-169.9718+14.7456	REX	19.74	19.40	19.12	0.16	0.1967	
DESI-173.3049+50.1444	DC	21.30	20.23	19.24	0.92	0.2426	
DESI-174.5481+14.7863	DC	20.68	19.29	18.55	0.96	0.5457	
DESI-175.0410+22.8792	DC	20.74	18.99	18.09	0.99	0.5426	
DESI-175.4961+19.3041	REX	17.72	17.17	16.80	1.00	0.5425	
DESI-176.0986+17.7551	DC	22.09	20.32	19.43	0.49	0.5273	
DESI-178.0775+08.8170	DC	21.70	20.01	18.99	1.00	0.3244	
DESI-179.0228+19.1869	DC	18.54	17.89	17.36	1.00	0.5689	
DESI-179.5632-06.6056	DC	22.73	21.04	19.88	0.74		0.430 ± 0.014
DESI-179.8326+61.7939	DC	22.58	20.99	19.66	0.99	0.3393	
DESI-180.2708-02.3681	REX	20.69	20.02	19.59	0.93	0.3667	
DESI-181.9031+52.9176	DC	18.62	17.98	17.48	1.00	0.3428	
DESI-183.0792+27.5646	REX	19.10	18.48	18.02	0.44	0.3364	
DESI-186.8276-07.1227	REX	22.00	20.63	19.66	1.00		0.617 ± 0.126
DESI-187.2782+59.1413	DC	21.54	19.86	18.91	0.98	0.5802	
DESI-188.2155+27.0359	DC	21.20	19.75	18.87	1.00	0.5566	

Table 4 continued on next page

Table 4 *(continued)*

Name	Type	mag_g	mag_r	mag_z	Probability	z_{spec}	z_{phot}
DESI-189.4008+55.5619	DC	22.84	21.04	19.62	1.00	0.4279	
DESI-189.9885+12.6693	DC	22.19	20.68	19.73	0.16	0.2183	
DESI-190.1345+45.1508	DC	22.35	21.04	19.83	1.00	0.2256	
DESI-190.6911+75.8730	REX	20.27	19.18	18.49	0.87		0.424 ± 0.031
DESI-190.7929+21.3329	DC	21.07	19.64	18.33	0.99	0.3106	
DESI-191.2226+04.2210[e]	DC	23.09	21.25	19.64	0.83	0.3260	
DESI-192.4699+03.1592	DC	21.58	19.94	19.08	1.00	0.3202	
DESI-192.9428+01.7155	DC	22.28	20.89	19.67	0.31	0.6730	
DESI-196.4575+22.9256	DC	20.61	19.17	18.43	1.00	0.2677	
DESI-197.5704+14.7474	REX	22.11	20.28	19.36	0.14	0.2943	
DESI-200.7252+58.1651	DC	20.22	19.08	18.36	0.68	0.2229	
DESI-200.7678+03.7216	DC	20.88	19.64	18.85	0.34		0.896 ± 0.078
DESI-205.1910+38.5483	DC	22.40	20.78	19.98	0.96	0.6334	
DESI-211.6718+08.7580	REX	21.21	20.02	19.36	0.38	0.1857	
DESI-211.9734-00.4713[k]	REX	20.80	19.87	19.23	0.15	0.4810	
DESI-214.3545+76.2152	REX	19.82	19.27	18.90	0.28		0.343 ± 0.386
DESI-218.2479-07.2268	DC	20.86	19.85	19.20	1.00		0.352 ± 0.043
DESI-218.3457+60.1209	DC	21.44	19.77	18.83	1.00		0.408 ± 0.072
DESI-218.4715+14.0687	DC	21.60	19.74	18.81	1.00	0.5512	
DESI-220.4549+14.6891	DC	21.39	19.56	18.54	1.00	0.6149	
DESI-221.8241+78.0430	DC	22.32	20.58	19.43	0.30		0.415 ± 0.281
DESI-227.3528+39.0279	DC	21.63	20.05	19.27	1.00	0.5975	
DESI-227.5364+20.6236	DC	21.98	20.23	19.39	1.00	0.5847	
DESI-234.8707+16.8379	DC	20.93	19.34	18.75	0.99	0.3979	
DESI-240.8979+05.8745	DC	21.48	20.55	19.93	0.97	0.6753	
DESI-241.2220+74.5292	DC	23.73	21.53	19.66	0.15		0.331 ± 0.021
DESI-245.7514+21.6226	DC	21.60	20.11	18.31	0.30		0.782 ± 0.062
DESI-246.0062+01.4836	DC	21.05	19.32	18.45	1.00		0.912 ± 0.105
DESI-248.5498+70.9303	DC	21.50	19.93	19.11	0.78		0.237 ± 0.017
DESI-252.2720+02.3993	DC	22.51	20.66	19.44	1.00		0.480 ± 0.139
DESI-252.9173+28.0881	DC	20.85	19.84	19.11	1.00		0.719 ± 0.130
DESI-253.2534+26.8843	DC	22.86	20.93	19.57	0.96	0.5214	
DESI-254.4235+34.8162	DC	21.56	20.42	19.65	1.00	0.5777	
DESI-260.8405+23.8442	DC	22.07	20.57	19.81	0.98		0.424 ± 0.155
DESI-260.9006+34.1995[h]	DC	22.53	20.86	19.88	0.85	0.4184	
DESI-266.4074+39.8584	REX	21.61	20.29	19.49	0.17		0.339 ± 0.050
DESI-277.9494+54.3033	DC	21.56	19.99	18.95	0.14		0.252 ± 0.009
DESI-278.8338+46.1076	DC	23.63	21.43	19.41	0.28		0.420 ± 0.016

Table 4 continued on next page

Table 4 *(continued)*

Name	Type	mag_g	mag_r	mag_z	Probability	z_{spec}	z_{phot}
DESI-287.1099+70.4625	DC	22.72	20.77	19.41	0.84		0.518 ± 0.049
DESI-292.2833+55.8034	DC	23.77	22.17	19.98	0.95		0.859 ± 0.067
DESI-310.8019-06.1649	DC	20.80	19.20	18.33	0.61	0.5076	
DESI-327.8408+13.7884	DC	20.17	19.13	18.30	0.10	0.2015	
DESI-329.6820+02.9584	DC	21.94	20.66	19.77	1.00	0.2886	
DESI-333.3655-13.2491	DC	22.57	20.77	19.75	1.00		0.110 ± 0.008
DESI-333.9656+04.5843[e]	DC	20.45	18.72	17.75	0.19	0.5863	
DESI-335.5357+27.7599	DC	20.67	19.52	18.88	0.55	0.4695	
DESI-336.5388+00.6950[j,d]	DC	20.66	19.07	18.21	1.00		0.649 ± 0.024
DESI-339.8879-04.4883	DC	22.54	20.66	19.55	1.00	0.5318	
DESI-340.2304-00.0128[e]	DC	20.62	19.23	18.42	0.58	0.4240	
DESI-341.0206+27.9877	DC	21.52	19.80	18.91	0.79	0.3373	
DESI-341.8012-02.0939	DC	20.46	18.94	18.07	1.00	0.3535	
DESI-342.1516-01.3928[d]	DC	19.69	18.68	18.01	0.99	0.6776	
DESI-342.9290-03.4136	REX	21.51	20.26	19.50	0.13	0.2580	
DESI-343.0402-04.2187	DC	20.00	18.57	17.73	0.97	0.4208	
DESI-344.5567+17.1506	DC	20.87	19.44	18.64	0.91	0.6646	
DESI-345.0719+22.2249	DC	20.96	19.38	18.52	0.44	0.4182	
DESI-345.8609+23.4760	DC	22.46	20.83	19.84	0.86	0.3252	
DESI-346.7668-13.3744	DC	21.50	20.03	19.22	0.96		0.575 ± 0.100
DESI-347.0926-02.1923[d]	DC	21.39	19.68	18.75	0.65	0.3578	
DESI-347.7824+05.4971	DC	22.44	20.55	19.57	0.17	0.5875	
DESI-351.7484+20.4496	DC	21.25	19.50	18.61	0.15	0.6529	
DESI-353.4835-14.3846	DC	23.06	21.17	19.74	0.57		0.372 ± 0.061
DESI-353.5287-07.7712	REX	21.31	20.34	19.66	0.13		0.522 ± 0.100
DESI-355.2727-57.2679	REX	20.09	19.42	19.02	0.95		0.447 ± 0.044
DESI-356.7894-62.7765	REX	20.62	19.23	18.44	0.29		0.252 ± 0.033
DESI-359.7003-61.4330	REX	21.89	20.51	19.65	0.94		0.730 ± 0.044

NOTE—Ninety-eight of the above 216 Grade A lens candidates have spectroscopic redshifts from SDSS DR16. All spectroscopic redshift uncertainties $< 3.7 \times 10^{-4}$. References for known lenses are as follows: [a]Canameras et al. (2020), [b]Carrasco et al. (2017), [c]Inada et al. (2003), [d]Jacobs et al. (2019b), [e]Jaelani et al. (2020), [f]Lemon et al. (2020), [g]Petrillo et al. (2019), [h]Sharon et al. (2020), [i]Sonnenfeld et al. (2013), [j]Sonnenfeld et al. (2018), [k]Sonnenfeld et al. (2020), [l]Wong et al. (2018).

Table 5. Grade B Candidates

Name	Type	mag_g	mag_r	mag_z	Probability	z_{spec}	z_{phot}
DESI-002.3413-06.4985	DC	23.05	21.20	19.99	0.05	0.4834	
DESI-004.0930-09.1126	DC	20.30	18.86	18.04	0.98	0.4545	
DESI-004.2564-10.1530	DC	22.24	20.26	19.12	0.60	0.5536	
DESI-004.8654+32.0834	REX	22.65	20.72	19.61	0.82		0.342 ± 0.049
DESI-005.2593-26.5437	DC	20.60	19.09	18.28	0.99		0.676 ± 0.027
DESI-005.9327+03.4772	DC	22.83	20.87	19.74	0.95	0.4088	
DESI-008.0382-11.7536	DC	20.68	19.48	18.75	0.70		0.542 ± 0.012
DESI-009.5789-22.7448	DC	21.69	20.25	19.46	0.95	0.6799	
DESI-010.9823-38.8884	REX	21.77	20.44	19.55	0.83		0.636 ± 0.041
DESI-011.3586-34.2832	REX	20.59	19.77	19.34	1.00		0.860 ± 0.078
DESI-013.2126-24.3469	DC	19.72	18.45	17.69	0.97		0.601 ± 0.011
DESI-013.8104-15.9165	REX	18.04	17.55	17.21	0.32		0.741 ± 0.055
DESI-014.1400-29.2327	DC	21.17	19.79	18.90	0.99		0.568 ± 0.010
DESI-014.3122+21.6428	DC	21.19	19.57	18.70	0.28	0.4444	
DESI-014.6685+05.7665	DC	20.05	18.81	17.90	0.44	0.5514	
DESI-014.7995-22.0867	DC	22.78	21.03	19.92	1.00		0.780 ± 0.057
DESI-015.2049+18.3077	DC	19.84	18.75	18.01	0.51	0.5987	
DESI-015.4982-21.4487[d]	DC	19.09	18.10	17.44	0.97		0.435 ± 0.027
DESI-015.7396-29.1895[d]	DC	22.64	21.17	19.88	1.00		0.266 ± 0.013
DESI-015.9372+27.1025	DC	17.94	17.04	16.39	0.69	0.3679	
DESI-016.1300-19.8697	DC	21.24	19.87	19.04	1.00		0.420 ± 0.024
DESI-016.3170+01.4392[e]	DC	21.21	19.46	18.58	0.61	0.2362	
DESI-016.5258-31.0774	DC	22.46	20.79	19.65	0.99		0.565 ± 0.031
DESI-016.5369-37.0055	REX	21.44	20.31	19.60	0.85		0.419 ± 0.081
DESI-018.7209-25.2845	DC	22.01	20.22	19.24	0.23		0.787 ± 0.034
DESI-020.7960+30.9619	DC	21.48	20.00	19.36	0.92	0.5345	
DESI-021.1715-06.9096	DC	22.54	20.67	19.64	0.32	0.3779	
DESI-023.0157-16.0040	DC	21.23	19.65	18.69	0.98		0.492 ± 0.047
DESI-024.7188-16.8552	DC	19.39	18.38	17.72	0.94		0.553 ± 0.016
DESI-025.7083-19.7918	DC	21.51	19.64	18.64	1.00		0.267 ± 0.016
DESI-025.9390-26.2946	DC	21.06	19.46	18.59	0.99		0.334 ± 0.019
DESI-026.7621-01.9526	REX	20.59	19.75	19.09	0.28	0.0748	
DESI-027.4483+12.4652	DC	22.66	20.81	19.80	0.64	0.3503	
DESI-027.5036+27.4267	DC	19.64	18.62	17.96	0.64	0.2872	
DESI-027.8944+05.1619	DC	21.67	20.21	19.43	1.00	0.4820	
DESI-027.9100-24.4413	DC	21.74	20.61	19.33	0.50		0.420 ± 0.040

Table 5 continued on next page

Table 5 *(continued)*

Name	Type	mag_g	mag_r	mag_z	Probability	z_{spec}	z_{phot}
DESI-028.6096-23.4067	DC	19.54	18.32	17.57	1.00		0.828 ± 0.067
DESI-029.3219+25.4699	DC	20.59	19.52	18.81	0.96	0.3456	
DESI-029.9198-24.0197	REX	21.39	20.40	19.81	0.88		0.813 ± 0.062
DESI-030.5443-01.3779	REX	18.96	18.07	17.54	0.96	0.5696	
DESI-031.0343-29.3024	DC	22.89	20.82	19.14	0.13		0.746 ± 0.208
DESI-033.4120-28.2374	DC	18.82	17.90	17.16	0.44		0.795 ± 0.030
DESI-033.4558+14.1537	DC	21.06	19.24	18.33	0.92	0.2604	
DESI-034.0760+02.9333	DC	19.97	18.75	18.00	0.20	0.6067	
DESI-034.5995-01.9843[e]	DC	20.85	19.46	18.68	0.11	0.2530	
DESI-034.7077-14.7784	DC	20.08	18.83	18.10	0.70		0.576 ± 0.011
DESI-035.0142+02.7345	DC	20.64	19.81	19.25	0.97	0.3234	
DESI-036.0843-31.9371	DC	21.36	20.07	19.34	0.93		0.510 ± 0.047
DESI-037.0680-29.3960	DC	22.52	20.68	19.39	0.45		0.292 ± 0.010
DESI-037.7246+20.8596	DC	22.25	20.48	19.47	0.98	0.4838	
DESI-038.5455-35.7895	REX	22.51	21.29	19.98	0.40		0.534 ± 0.069
DESI-038.6407-14.8060	DC	22.54	20.94	19.75	1.00		0.766 ± 0.018
DESI-039.7648-30.8467	DC	21.54	20.14	19.32	0.90		0.487 ± 0.041
DESI-040.7511-19.8931	REX	21.31	20.15	19.44	0.97		0.801 ± 0.044
DESI-041.1456-17.2445	REX	22.20	20.40	19.44	0.82		0.368 ± 0.043
DESI-042.2860-28.3551	REX	21.36	20.34	19.69	0.47		0.841 ± 0.098
DESI-042.3475+16.8733	DC	23.46	21.47	19.51	0.84		0.696 ± 0.087
DESI-042.5350+00.1379	DC	23.08	21.17	19.61	0.87		0.805 ± 0.024
DESI-042.8971-12.3337[d]	DC	20.91	19.35	18.38	1.00		0.440 ± 0.008
DESI-044.1840-09.2468	DC	22.63	20.77	19.54	1.00		0.885 ± 0.076
DESI-044.3830-23.3527	REX	22.80	20.95	19.87	0.40		0.463 ± 0.072
DESI-044.5235-34.8959	REX	20.82	19.53	18.83	0.81		0.442 ± 0.052
DESI-045.5878-04.3899	REX	21.11	20.11	19.48	0.20	0.1964	
DESI-046.4172-29.5712[g]	DC	22.33	20.66	19.72	0.24		0.358 ± 0.009
DESI-047.1385-17.6676	REX	21.25	20.18	19.49	0.78		0.802 ± 0.219
DESI-047.3494-30.1968	DC	22.54	20.80	19.75	0.89		0.362 ± 0.048
DESI-047.4380-14.6211[d]	DC	18.06	17.33	16.76	1.00		0.839 ± 0.098
DESI-048.6263-09.5613	DC	18.25	17.29	16.62	0.10		0.447 ± 0.071
DESI-048.6484-21.4665[d]	DC	22.04	20.20	19.24	0.45		0.445 ± 0.124
DESI-048.9389-29.9643	DC	23.24	21.38	19.85	0.51		0.552 ± 0.018
DESI-050.7649-27.5687	DC	22.94	20.80	19.13	0.65		0.540 ± 0.025
DESI-051.2051-10.3481[a]	DC	21.30	19.83	19.07	1.00		0.538 ± 0.041
DESI-053.7319-19.9224	DC	20.92	19.51	18.61	0.65		0.439 ± 0.017
DESI-054.7129-14.1391	REX	19.51	18.49	17.79	0.39		0.357 ± 0.043

Table 5 continued on next page

Table 5 *(continued)*

Name	Type	mag_g	mag_r	mag_z	Probability	z_{spec}	z_{phot}
DESI-054.9589-00.1356	DC	21.79	20.05	19.11	0.94	0.6045	
DESI-055.0363-25.7609[f]	REX	21.49	20.46	19.80	0.18		0.641 ± 0.082
DESI-055.8327-16.2951	DC	22.05	20.58	19.66	0.88		0.472 ± 0.051
DESI-056.2001-20.9116	DC	22.85	21.18	19.43	0.88		0.696 ± 0.017
DESI-057.5232-13.1978	DC	24.30	21.96	19.96	1.00	0.5220	
DESI-058.8732-36.5641	REX	21.45	20.23	19.46	0.91		0.327 ± 0.029
DESI-060.9086-07.3160	DC	22.27	20.83	19.78	0.29		0.785 ± 0.064
DESI-061.6770-23.3205	DC	23.44	21.38	19.43	1.00		0.566 ± 0.038
DESI-061.6880-15.0482	REX	21.29	20.51	20.00	1.00		0.561 ± 0.293
DESI-062.2475-05.9982	DC	19.67	18.68	17.87	1.00	0.5361	
DESI-062.7834-22.9431[d]	REX	22.33	20.66	19.71	0.93		0.562 ± 0.040
DESI-063.3879-16.8328	DC	19.75	18.64	17.95	0.87		0.306 ± 0.031
DESI-063.6168-19.9192	DC	23.33	21.51	19.99	1.00		0.571 ± 0.022
DESI-065.2568-21.6299	DC	21.94	20.07	18.51	1.00		0.927 ± 0.113
DESI-065.3371-29.8915	DC	20.17	19.12	18.38	0.12		0.419 ± 0.029
DESI-065.5808-26.9514	DC	17.87	16.93	16.26	0.66		0.524 ± 0.013
DESI-066.2134-23.1960	DC	23.09	21.09	19.47	0.82		0.854 ± 0.072
DESI-068.3176-41.0553	REX	20.98	20.10	19.50	0.99		0.721 ± 0.088
DESI-069.9349-04.6098	DC	18.57	17.74	17.17	0.98	0.5183	
DESI-071.2400-07.6007	DC	21.79	20.96	19.65	1.00		0.404 ± 0.029
DESI-071.5624-20.0285[d]	DC	22.13	20.10	18.97	0.97		0.404 ± 0.010
DESI-071.8657-02.8613	DC	20.99	19.49	18.68	0.78		0.416 ± 0.009
DESI-072.0528-30.3308	DC	18.54	17.35	16.49	0.78		0.765 ± 0.020
DESI-073.4865-21.3622	DC	20.97	19.36	18.52	0.27		0.258 ± 0.011
DESI-078.3580-21.4717	DC	21.69	20.18	19.38	0.96		0.362 ± 0.029
DESI-087.1036-29.8510	REX	22.48	20.65	19.51	0.89		0.838 ± 0.106
DESI-089.6411-28.7418	DC	22.24	20.48	19.60	0.84		0.447 ± 0.042
DESI-091.2815-33.8949	REX	22.42	20.69	19.80	0.10		0.704 ± 0.053
DESI-101.4600+48.5810	DC	22.17	20.46	19.56	0.56		0.499 ± 0.079
DESI-110.6705+52.2273	DC	21.46	19.70	18.66	0.83		0.619 ± 0.013
DESI-115.6174+16.6039	DC	21.33	20.15	19.35	0.28	0.6062	
DESI-115.8731+50.8031	DC	22.91	20.91	19.49	0.99		0.784 ± 0.024
DESI-116.9217+26.8160	REX	19.82	19.20	18.74	0.56		0.285 ± 0.096
DESI-121.8813+44.1801	DC	20.42	19.19	18.35	0.99	0.4489	
DESI-122.9433+00.9701	DC	22.97	21.07	19.50	0.79	0.6252	
DESI-128.8048+41.1131	DC	21.68	20.03	19.14	1.00	0.6091	
DESI-129.6056+30.2873	DC	21.14	19.61	18.79	0.95	0.3034	
DESI-130.7279-02.0271	DC	19.91	18.75	17.80	0.38	0.2687	

Table 5 continued on next page

Table 5 *(continued)*

Name	Type	mag_g	mag_r	mag_z	Probability	z_{spec}	z_{phot}
DESI-131.3340-00.9157[g,e]	DC	21.46	19.76	18.92	0.88	0.2562	
DESI-132.6382+40.6196	REX	20.35	19.74	19.31	0.70	0.4999	
DESI-133.3800+23.3652	DC	20.02	18.53	17.72	0.94	0.1916	
DESI-134.1503+23.8641	REX	21.56	20.00	18.96	0.19	0.6589	
DESI-136.4227+34.8998	DC	22.41	20.57	19.21	0.17	0.5283	
DESI-136.9764+00.9590[e]	DC	18.67	17.55	16.82	0.39	0.6282	
DESI-137.4367+22.4354	DC	21.51	19.83	18.96	0.49	0.3702	
DESI-138.0523+33.3767	DC	23.09	21.29	19.96	0.97	0.6039	
DESI-139.8960+30.5323	DC	22.61	20.61	19.25	0.13	0.3826	
DESI-147.7529+08.4157	DC	18.11	16.89	16.08	1.00	0.4292	
DESI-151.9618+04.6107	DC	21.88	20.36	19.61	0.33	0.3225	
DESI-154.4430-04.0841	DC	20.31	18.99	18.21	0.51		0.257 ± 0.008
DESI-157.4830-05.4213	DC	23.17	21.68	19.23	1.00		0.772 ± 0.102
DESI-158.2306+75.3149	DC	22.62	20.54	18.81	0.82		0.629 ± 0.059
DESI-159.3007+04.5911	DC	21.92	20.63	19.81	1.00	0.6405	
DESI-159.7672-08.9316	DC	23.44	21.58	19.79	0.89		0.397 ± 0.031
DESI-161.8206+27.9906	DC	22.08	20.37	19.26	1.00	0.4208	
DESI-162.2464+10.5049	DC	19.50	18.58	17.94	0.45		0.493 ± 0.023
DESI-162.6485+19.9352	DC	20.71	19.44	18.73	0.97	0.6174	
DESI-166.1262-08.6326	DC	22.95	21.19	19.84	0.23		0.292 ± 0.054
DESI-174.0622+41.0525	DC	19.41	18.38	17.57	0.29	0.5049	
DESI-175.7970-01.6598[l]	REX	20.80	20.02	19.52	0.96	0.6177	
DESI-176.2391+30.5580	DC	21.67	19.87	18.93	1.00	0.5219	
DESI-179.5944+72.4798	DC	21.63	20.00	19.19	0.98		0.797 ± 0.051
DESI-179.8536-05.1806	DC	21.43	19.54	18.54	0.97		0.417 ± 0.024
DESI-180.7746+69.8060	DC	22.00	20.23	19.07	0.98	0.4477	
DESI-181.0606+13.2918	DC	22.70	20.95	19.98	0.49		0.971 ± 0.227
DESI-181.5279+30.1133	REX	20.69	20.07	19.72	0.86	0.3438	
DESI-184.9201+44.8673	REX	19.36	18.83	18.43	0.41		0.491 ± 0.026
DESI-184.9250+00.8409[e]	DC	20.43	19.26	18.54	0.34	0.3405	
DESI-185.0208+26.4909	DC	20.50	19.11	18.36	0.98		0.710 ± 0.019
DESI-186.7661+28.0517	DC	22.95	21.03	19.50	0.59	0.5407	
DESI-188.3339+14.1325[a]	REX	22.61	20.98	19.68	0.86	0.5356	
DESI-189.5574+27.3029	DC	21.43	19.85	18.89	0.47	0.3314	
DESI-190.4916+03.7894[e]	REX	22.07	20.66	19.49	0.95	0.2921	
DESI-191.3160+19.0924	DC	22.25	21.03	19.71	0.12	0.3882	
DESI-192.0695+07.7162	REX	20.84	19.77	19.13	0.58	0.5753	
DESI-200.0505-08.5058	DC	22.17	20.59	19.75	0.98		0.611 ± 0.036

Table 5 continued on next page

Table 5 *(continued)*

Name	Type	mag_g	mag_r	mag_z	Probability	z_{spec}	z_{phot}
DESI-200.8958+06.1545	DC	22.33	20.96	19.97	0.31	0.3046	
DESI-202.9388+51.5753	DC	21.18	19.97	19.32	0.99	0.2806	
DESI-203.8331-08.4487	DC	23.06	21.02	19.61	0.16		0.486 ± 0.078
DESI-209.6224+16.9285	REX	19.97	18.94	18.32	0.93	0.7083	
DESI-214.8006+53.4366	DC	19.88	18.86	18.18	0.98	0.7039	
DESI-214.8651-04.0003	REX	20.90	19.60	18.77	0.77		0.701 ± 0.109
DESI-218.0748+07.0556	DC	22.08	20.32	19.41	0.79	0.5813	
DESI-219.2455+29.6141	DC	21.58	20.64	19.10	0.46	0.3037	
DESI-220.4044+50.2463	DC	20.84	19.78	19.11	1.00		0.812 ± 0.084
DESI-223.1039+48.4711	DC	21.95	20.45	19.67	0.56	0.4018	
DESI-224.3857-01.9882[j]	REX	21.82	20.10	19.16	0.79	0.6509	
DESI-225.4050+52.1417	DC	20.38	19.08	18.23	0.98	0.6694	
DESI-228.0786+20.8316	DC	22.51	20.97	19.58	0.19	0.3720	
DESI-228.8268+63.2724	DC	20.74	18.98	18.09	0.22		0.614 ± 0.015
DESI-231.2874+42.4646[e]	DC	21.52	19.68	18.58	0.17		0.820 ± 0.049
DESI-231.4998+08.7774	DC	21.04	19.81	19.03	0.80	0.6191	
DESI-231.8201+12.9511	DC	24.31	21.63	19.64	0.80	0.5240	
DESI-233.7453+01.3400	DC	22.17	20.27	19.17	0.34	0.2940	
DESI-234.4783+14.7232	DC	23.28	21.40	19.55	0.98	0.5206	
DESI-236.0113+26.1712	REX	22.02	20.82	19.68	0.29	0.7391	
DESI-236.3307+16.2141	DC	23.21	21.21	19.37	0.18	0.4049	
DESI-236.4854+10.0292	DC	21.86	20.67	19.97	0.95	0.5516	
DESI-236.5553+35.0802	DC	22.64	20.77	19.65	0.99	0.3242	
DESI-244.3589+20.7108	DC	22.87	21.02	19.82	1.00	0.5425	
DESI-244.5899+53.1871	DC	21.30	19.67	18.74	0.45	0.4164	
DESI-255.6529+28.5791	DC	23.54	21.68	19.90	1.00	0.3305	
DESI-257.4348+31.9046	DC	24.68	22.24	19.95	0.99		0.864 ± 0.071
DESI-259.0541+28.5928	DC	22.75	21.24	19.87	0.92	0.2245	
DESI-259.7428+11.2635	REX	21.96	20.61	19.85	0.18		0.160 ± 0.097
DESI-267.2985+23.5101[a]	DC	23.78	21.51	19.62	0.98		0.313 ± 0.027
DESI-269.7333+29.0742	REX	21.54	20.56	19.85	0.97		0.370 ± 0.041
DESI-269.7858+41.9039	REX	21.35	20.22	19.52	1.00	0.4203	
DESI-273.4736+34.7448	DC	21.84	19.94	18.76	0.50		0.297 ± 0.013
DESI-285.9297+52.4182[a]	DC	21.35	19.57	18.34	1.00		0.660 ± 0.049
DESI-293.9927+58.1525	DC	22.28	20.41	19.24	0.58		0.594 ± 0.016
DESI-311.4249-10.6762	DC	19.27	18.09	17.33	0.34		0.120 ± 0.006
DESI-313.9780+08.7331	DC	17.99	17.09	16.43	0.63		0.741 ± 0.052
DESI-332.7233-40.9782	REX	21.63	20.60	20.00	0.32		0.761 ± 0.053

Table 5 continued on next page

Table 5 *(continued)*

Name	Type	mag_g	mag_r	mag_z	Probability	z_{spec}	z_{phot}
DESI-335.2155+00.9713[e]	REX	21.91	20.73	19.84	0.32	0.2811	
DESI-335.2291-11.4857	DC	22.72	20.81	19.37	0.85		0.520 ± 0.009
DESI-337.2103+14.9081	DC	21.16	20.26	19.49	0.99		0.912 ± 0.067
DESI-342.1516+20.2529	DC	21.95	20.09	18.94	0.13	0.3960	
DESI-344.6262-58.6910	REX	22.77	21.00	19.96	0.94		0.311 ± 0.038
DESI-353.4326-03.4619	REX	20.45	19.46	18.77	0.94		0.756 ± 0.088
DESI-353.6004+17.9899	REX	22.26	20.59	19.84	0.23	0.4027	
DESI-354.0428-02.1264[a]	REX	21.58	20.33	19.51	0.99	0.2466	
DESI-356.8114-00.7980	DC	16.82	15.89	15.23	0.52	0.6000	
DESI-357.3718-60.0110	REX	22.12	20.46	19.64	0.14		0.370 ± 0.069
DESI-359.1477-13.2930	DC	20.50	18.67	17.72	1.00		0.782 ± 0.131

NOTE—Eighty-eight of the above 199 Grade B lens candidates have spectroscopic redshifts from SDSS DR16. All spectroscopic redshift uncertainties $< 3.6 \times 10^{-4}$. For references of known lenses, see NOTE for Table 4.

Table 6. Grade C Candidates

Name	Type	mag_g	mag_r	mag_z	Probability	z_{spec}	z_{phot}
DESI-000.0254+21.6415	REX	20.71	19.84	19.18	0.24	0.5030	
DESI-000.0369+21.2841	DC	21.08	19.53	18.75	1.00		0.357 ± 0.066
DESI-000.2881-10.5619	DC	20.87	19.35	18.56	0.18	0.4380	
DESI-000.4022-04.0111	REX	20.74	19.74	19.11	0.17	0.7237	
DESI-000.6943+27.0894	REX	18.80	18.23	17.78	0.39	0.5841	
DESI-001.1051-60.0972	REX	21.05	20.10	19.58	0.56		0.752 ± 0.072
DESI-001.2742-54.2626	REX	20.67	19.51	18.75	0.36		0.534 ± 0.047
DESI-001.4446+15.8147	DC	22.17	20.22	19.01	0.41	0.2141	
DESI-001.6798+05.0237	DC	22.23	20.38	19.37	0.90	0.4323	
DESI-001.7035-11.2181	DC	21.97	20.27	19.33	0.04	0.2862	
DESI-001.8280+01.5349	REX	19.81	19.28	18.93	0.88	0.3217	
DESI-002.0769-06.3760	REX	20.76	20.32	19.94	0.17	0.5890	
DESI-002.2652-52.4195	REX	22.12	20.65	19.69	0.78		0.275 ± 0.037
DESI-002.4643-34.6088	REX	20.64	19.43	18.71	0.17		0.775 ± 0.033
DESI-002.5204-35.7296	REX	22.36	20.65	19.72	0.17		0.567 ± 0.086
DESI-002.5452-60.5666	REX	22.20	20.63	19.83	0.19		0.774 ± 0.051
DESI-002.7167+18.5282	DC	23.66	21.45	19.53	0.79		0.604 ± 0.072
DESI-002.9359+01.0175	REX	22.18	20.63	19.61	0.15	0.7402	
DESI-003.0228-44.3054	REX	22.24	20.48	19.54	0.62		0.853 ± 0.057
DESI-003.2647-32.9648	REX	22.35	20.53	19.55	0.50		0.482 ± 0.086
DESI-003.8795+24.4528	DC	22.26	20.48	19.56	0.94	0.5970	
DESI-003.9009-29.8221	DC	20.90	19.47	18.57	0.99		0.873 ± 0.050
DESI-004.0093-13.4169	DC	20.11	18.90	18.14	0.95	0.4246	
DESI-004.2156-05.8182	DC	21.04	19.77	19.06	0.97	0.3293	
DESI-004.7352-31.8716	REX	20.88	20.13	19.62	0.13		0.288 ± 0.023
DESI-004.8732-31.1123	REX	21.11	19.91	19.19	0.15		0.323 ± 0.027
DESI-005.2856-39.3724	REX	22.46	20.68	19.69	0.30		0.342 ± 0.030
DESI-005.5523-04.4710	REX	20.95	19.57	18.77	0.12	0.6013	
DESI-006.0703+01.4212	DC	22.49	21.01	19.89	0.48	0.4951	
DESI-006.0848-64.9549	REX	22.03	20.64	19.86	0.12		0.860 ± 0.083
DESI-006.1955-57.9429	REX	20.12	19.52	19.13	0.14		0.751 ± 0.065
DESI-006.2199-01.8426	REX	20.17	19.54	19.06	0.21	0.6907	
DESI-006.3643+10.1853	DC	20.74	19.25	18.42	0.14	0.4579	
DESI-006.4166-27.4448	REX	19.71	18.83	18.23	0.68		0.821 ± 0.051
DESI-006.4448+03.6455	DC	22.13	20.39	19.42	0.25	0.4092	
DESI-006.5376-05.1005	DC	22.22	20.43	19.47	0.18	0.3694	

Table 6 continued on next page

Table 6 *(continued)*

Name	Type	mag_g	mag_r	mag_z	Probability	z_{spec}	z_{phot}
DESI-006.5454-60.8859	REX	22.83	21.02	19.99	0.17		0.470 ± 0.034
DESI-006.6039+04.3071	REX	21.64	20.62	19.96	0.22	0.7094	
DESI-006.9518-03.8141	DC	22.17	20.36	19.38	0.14	0.5883	
DESI-007.0770-27.5692	DC	21.11	19.62	18.90	0.22		0.881 ± 0.074
DESI-007.0848-52.1662	REX	20.77	19.57	18.92	0.25		0.870 ± 0.072
DESI-007.3282-25.6413	REX	21.03	19.80	18.95	0.16		0.630 ± 0.092
DESI-007.4408-02.3542	DC	23.53	21.56	19.77	0.99	0.6435	
DESI-007.6167-07.3598	REX	21.98	20.82	20.00	0.99	0.6851	
DESI-007.7074-31.8051	DC	21.43	19.68	18.53	0.22		0.221 ± 0.006
DESI-007.7552-24.4012	DC	22.88	20.95	19.39	0.99		0.623 ± 0.013
DESI-007.9602-00.6805[e]	DC	21.18	20.08	19.30	0.58	0.4808	
DESI-008.0561+11.4205	DC	22.26	20.89	19.62	0.69	0.3835	
DESI-008.6662-13.6007	DC	21.90	20.05	18.94	0.67		0.714 ± 0.040
DESI-008.8590-20.2624	REX	23.13	21.16	19.89	0.73	0.3017	
DESI-008.9856-31.0498	REX	21.18	20.36	19.70	0.15		0.416 ± 0.053
DESI-009.4655-11.1778	DC	18.50	17.63	16.98	1.00	0.6034	
DESI-009.4901-61.7741	REX	22.13	20.89	19.88	0.13		0.366 ± 0.095
DESI-009.5831-22.7369	DC	20.59	19.73	19.16	0.34		0.669 ± 0.037
DESI-009.6186-25.3693	REX	21.71	20.54	19.73	0.29		0.695 ± 0.068
DESI-009.6226-36.7634	REX	20.98	20.02	19.33	0.37		0.761 ± 0.121
DESI-009.6721-07.4138	DC	22.51	20.73	19.18	0.50	0.2798	
DESI-009.7395-07.7564	DC	20.34	19.32	18.57	0.84	0.4099	
DESI-010.3697-51.0101	REX	22.44	20.89	19.98	0.39		0.694 ± 0.038
DESI-010.4341-23.6515	DC	22.84	21.03	19.65	1.00	0.3905	
DESI-010.5365-09.9688	DC	22.77	20.90	19.83	0.17	0.4173	
DESI-010.5692-05.5844	DC	21.10	19.19	18.25	1.00	0.2764	
DESI-010.6237-15.1890	DC	20.29	19.09	18.07	0.49		0.407 ± 0.011
DESI-011.0120+28.5026	REX	23.17	21.31	19.87	0.55	0.6125	
DESI-011.1176-09.8211	DC	21.28	19.83	19.04	0.29	0.5485	
DESI-011.6128-26.6737	DC	22.05	20.14	19.08	0.76		0.399 ± 0.117
DESI-011.6341-32.5680	REX	20.72	19.74	19.09	0.27		0.734 ± 0.038
DESI-012.5414-15.3948	DC	19.18	18.06	17.27	0.10		0.458 ± 0.045
DESI-012.6879+05.1953	DC	22.18	20.35	19.12	0.95	0.3940	
DESI-012.7302-17.3424[d]	DC	21.40	19.73	18.88	0.94		0.683 ± 0.028
DESI-013.0309-62.2004	REX	22.09	20.64	19.83	0.28		0.751 ± 0.039
DESI-013.0826-21.4621	DC	15.22	14.30	13.60	0.82		0.533 ± 0.041
DESI-013.3666-16.0988	DC	22.81	21.00	19.94	0.63		0.680 ± 0.100
DESI-013.4834-25.7652	REX	20.92	19.44	18.62	0.72		0.605 ± 0.023

Table 6 continued on next page

Table 6 *(continued)*

Name	Type	mag_g	mag_r	mag_z	Probability	z_{spec}	z_{phot}
DESI-014.0464+00.1260	REX	21.51	20.52	19.95	0.37	0.4563	
DESI-014.1862-18.9657	DC	20.95	19.36	18.50	0.96		0.410 ± 0.029
DESI-014.2189-16.4016	DC	20.20	18.67	17.86	0.97		0.359 ± 0.013
DESI-014.2352-25.7746	DC	20.90	19.55	18.74	0.97		0.606 ± 0.010
DESI-014.2478-14.0421	DC	21.20	19.92	19.04	0.94		0.426 ± 0.036
DESI-014.2970-13.2907	DC	20.52	18.97	18.11	0.57		0.388 ± 0.026
DESI-014.3439-25.1811	DC	20.05	18.49	17.64	0.97		0.535 ± 0.037
DESI-014.4115-29.9751	DC	22.64	20.83	19.95	0.97		0.723 ± 0.023
DESI-014.6510-23.5443	DC	23.61	21.53	19.90	0.73		0.513 ± 0.051
DESI-014.6810-05.0260	DC	22.04	20.20	19.14	0.88	0.5929	
DESI-014.8630-23.2117	DC	21.89	20.29	19.54	0.37		0.852 ± 0.076
DESI-014.9525-24.7056	DC	17.72	17.01	16.42	0.69		0.210 ± 0.021
DESI-014.9575-05.5838	DC	16.53	15.71	15.07	0.99	0.5091	
DESI-014.9799-18.4828	REX	22.64	20.75	19.79	0.19		0.850 ± 0.056
DESI-015.4277-15.0401	DC	20.72	19.75	19.14	0.98		0.646 ± 0.029
DESI-015.6197-20.2297	DC	21.74	19.83	18.73	1.00		0.414 ± 0.033
DESI-015.6786-23.9439	DC	23.34	21.70	19.92	0.82		0.799 ± 0.270
DESI-015.9876-07.1360	DC	22.31	20.57	19.73	1.00	0.4384	
DESI-016.3301-16.4985	DC	22.16	20.28	19.26	0.52		0.507 ± 0.062
DESI-016.4628-05.0324	DC	21.55	20.10	19.29	0.98	0.5998	
DESI-016.9846-14.6625	DC	18.93	17.94	17.26	0.97		0.610 ± 0.034
DESI-017.1638-08.3884	DC	22.35	20.40	19.16	0.91	0.5754	
DESI-017.3346-07.3951	DC	21.64	20.09	19.19	0.72	0.5312	
DESI-017.6727-14.7914	DC	22.45	20.68	19.72	1.00		0.668 ± 0.104
DESI-017.7799+13.7789	DC	21.14	19.51	18.66	1.00	0.6632	
DESI-017.8640+10.9845[a]	REX	21.42	20.39	19.72	0.40	0.2782	
DESI-017.8812+08.9282	DC	21.75	20.22	19.28	0.97	0.4062	
DESI-018.0610-21.6113	REX	22.58	20.71	19.73	0.63		0.577 ± 0.031
DESI-018.2042-02.9176	DC	22.04	20.25	19.21	0.52	0.3623	
DESI-018.5346-19.7225	DC	23.16	21.22	19.95	0.95		0.373 ± 0.048
DESI-019.1019-00.1335	REX	20.49	19.37	18.65	0.23	0.1824	
DESI-019.3417-30.0427	REX	22.65	20.80	19.46	0.53		0.328 ± 0.051
DESI-019.4619-29.9677	REX	22.09	20.72	19.94	0.92		0.812 ± 0.083
DESI-019.4701-11.0283	REX	21.44	20.35	19.65	0.78		0.796 ± 0.072
DESI-019.7886-05.2190	REX	21.29	20.10	19.33	0.56	0.6607	
DESI-019.8252-22.6356	DC	23.14	21.46	19.91	1.00	0.1714	
DESI-019.8273+27.4840	REX	20.60	19.49	18.84	0.14	0.6357	
DESI-020.3300-00.3409	REX	20.29	19.91	19.62	0.29	0.6346	

Table 6 continued on next page

Table 6 *(continued)*

Name	Type	mag_g	mag_r	mag_z	Probability	z_{spec}	z_{phot}
DESI-020.3660+21.7344	DC	24.09	21.79	19.94	0.94	0.6365	
DESI-020.6044-08.5205	DC	22.54	21.03	19.84	1.00	0.5325	
DESI-020.7916-08.1086	DC	22.31	20.71	19.54	0.26	0.3590	
DESI-021.1220-21.4623	DC	22.56	20.74	19.76	0.37	0.5022	
DESI-021.5140-10.3682	DC	19.72	18.70	17.99	0.86	0.1752	
DESI-021.8652-36.8157	REX	21.27	20.47	19.89	0.22		0.689 ± 0.162
DESI-022.2506+00.1193	DC	19.46	18.41	17.72	0.93	0.3288	
DESI-022.2823-07.0851	DC	22.31	20.63	19.70	0.11	0.3398	
DESI-022.4814-02.6654	DC	18.90	17.76	17.02	0.42	0.4996	
DESI-022.6133-18.8672	DC	22.95	21.24	19.86	0.33	0.5414	
DESI-022.8470-16.8840	DC	18.73	17.68	16.99	0.23		0.807 ± 0.063
DESI-023.0128-02.3005	DC	21.02	19.49	18.58	0.63		0.464 ± 0.115
DESI-023.0583+03.4399	REX	20.22	19.16	18.46	0.75	0.5785	
DESI-023.4239-16.8390	DC	22.94	21.32	19.91	0.94		0.644 ± 0.061
DESI-023.5148-30.5414[g]	DC	19.37	18.48	17.87	0.78		0.325 ± 0.016
DESI-023.5329-07.4703	REX	21.80	20.60	19.80	0.48	0.2615	
DESI-023.6649-28.7320	DC	22.12	20.42	19.47	0.15		0.981 ± 0.084
DESI-023.8146-17.4043[d]	DC	20.25	19.23	18.45	0.97		0.768 ± 0.051
DESI-023.8165-32.6842	REX	21.85	20.47	19.72	0.56		0.446 ± 0.055
DESI-023.8193+04.8514	REX	22.54	21.36	19.99	0.32	0.6901	
DESI-023.9221-18.7413	DC	20.27	19.94	19.70	0.14	0.5278	
DESI-023.9840-20.7577	DC	22.72	20.89	19.75	0.76	0.3380	
DESI-024.1759-12.2872	DC	19.85	18.68	18.03	0.25		0.407 ± 0.071
DESI-024.1913-40.4779	REX	20.21	19.84	19.53	0.11		0.587 ± 0.026
DESI-024.2160-14.8162	DC	21.89	20.08	19.07	0.12		0.320 ± 0.014
DESI-024.2426+00.3033	REX	20.00	19.39	18.96	0.14	0.8093	
DESI-024.3635-27.6051	DC	22.43	20.65	19.67	0.35		0.410 ± 0.024
DESI-024.3717-08.3056	DC	22.34	20.61	19.59	0.19		0.778 ± 0.025
DESI-024.3726+05.7609	DC	20.48	19.13	18.24	0.46	0.3618	
DESI-024.4002-27.1526	DC	21.13	19.65	18.87	0.10		0.234 ± 0.067
DESI-025.0520-20.1055	DC	18.18	17.21	16.53	0.36		0.397 ± 0.015
DESI-025.1595-11.4143	DC	21.84	19.99	18.63	0.61		0.322 ± 0.021
DESI-025.4548-24.8641	DC	20.75	19.82	19.03	0.85		0.223 ± 0.005
DESI-025.4686-22.4962	DC	21.30	19.56	18.50	0.68		0.370 ± 0.025
DESI-025.5981+14.8037	DC	19.63	19.24	19.00	0.45		0.772 ± 0.063
DESI-025.7040-19.7717	DC	22.45	20.58	19.57	0.50		0.546 ± 0.033
DESI-025.7910+07.5022	DC	20.86	19.40	18.50	0.14	0.5569	
DESI-025.8360-27.2964	REX	21.25	19.94	19.16	0.19		0.303 ± 0.069

Table 6 continued on next page

Table 6 *(continued)*

Name	Type	mag_g	mag_r	mag_z	Probability	z_{spec}	z_{phot}
DESI-025.8949+05.3365	DC	18.84	17.68	16.94	0.17	0.5272	
DESI-026.0431-28.9067	REX	20.54	19.38	18.64	0.94		0.375 ± 0.036
DESI-026.2418+00.8017	DC	22.09	20.49	19.44	0.15	0.4773	
DESI-026.3453+04.8579	DC	21.63	20.20	19.18	0.98	0.3351	
DESI-026.5508+22.6087	DC	19.65	18.57	17.75	0.73	0.6790	
DESI-026.7267-11.4066	DC	22.42	20.78	19.90	0.14		0.453 ± 0.038
DESI-026.7490-22.6820	DC	21.04	19.42	18.47	0.92		0.346 ± 0.053
DESI-026.7792-40.1610	REX	22.83	20.98	19.93	0.93		0.224 ± 0.096
DESI-026.9591-26.6311	DC	20.11	19.29	18.74	0.97		0.562 ± 0.018
DESI-027.3253-30.3055[g]	DC	21.72	19.92	18.94	0.99		0.450 ± 0.025
DESI-027.3698-08.7626	DC	21.31	20.12	19.39	0.98	0.6772	
DESI-027.3879+00.4647	DC	21.70	19.78	18.67	0.77	0.4892	
DESI-027.4775+21.7988	DC	21.06	19.58	18.71	0.17	0.5552	
DESI-027.4849-11.5108	DC	22.23	20.47	19.56	0.87		0.402 ± 0.036
DESI-027.5959-17.6114	DC	21.90	20.60	19.71	0.34		0.442 ± 0.175
DESI-027.6346-18.3062	DC	22.30	20.44	19.40	0.15		0.770 ± 0.067
DESI-027.8170-19.1052	REX	21.59	20.08	19.17	0.10		0.321 ± 0.067
DESI-027.8888-26.8005	DC	21.61	19.81	18.88	0.97		0.689 ± 0.061
DESI-027.9976-08.3646	DC	21.29	19.84	19.09	0.34	0.6218	
DESI-028.0192-29.3878	DC	22.22	20.42	19.38	0.64		0.367 ± 0.041
DESI-028.1435-21.6420	REX	22.67	20.91	19.89	0.99		0.369 ± 0.104
DESI-028.1494-31.3430	DC	20.55	18.69	17.72	0.14		0.354 ± 0.032
DESI-028.1997+03.2624	DC	18.87	18.46	18.26	0.97	0.3493	
DESI-028.4669-11.2551	DC	22.33	20.57	19.40	0.18		0.816 ± 0.057
DESI-028.5320-08.1000	DC	22.56	20.75	19.81	0.35	0.3346	
DESI-028.5715-16.2374	DC	20.86	20.23	19.81	0.23	0.3979	
DESI-028.7845-25.8463	DC	21.75	19.94	18.98	1.00		0.554 ± 0.038
DESI-029.1389-02.4224	REX	21.61	20.47	19.79	0.52		0.616 ± 0.118
DESI-029.1423-15.5876	REX	21.69	20.54	19.50	0.74	0.3950	
DESI-029.3642+22.9216	DC	22.04	20.51	19.48	0.24	0.2454	
DESI-029.3687-05.2778[e]	DC	21.98	20.12	19.09	0.82	0.5985	
DESI-029.4504-01.1535[e]	DC	22.90	20.92	19.33	0.12	0.5416	
DESI-029.4673-27.8568	DC	21.86	20.66	19.90	0.89		0.782 ± 0.027
DESI-029.5569-11.2721	DC	20.11	19.81	19.62	0.99		0.368 ± 0.022
DESI-029.7821-32.2109	REX	21.22	20.27	19.59	0.33		0.631 ± 0.079
DESI-029.7900-18.9500[d]	DC	20.38	18.87	18.03	0.99	0.3393	
DESI-029.9230+29.5992	DC	20.97	19.32	18.50	0.14	0.3444	
DESI-029.9687-27.8439	DC	22.02	20.21	19.12	1.00		0.789 ± 0.276

Table 6 continued on next page

Table 6 *(continued)*

Name	Type	mag_g	mag_r	mag_z	Probability	z_{spec}	z_{phot}
DESI-030.1018-10.7692	DC	18.99	17.92	17.19	0.62		0.272 ± 0.029
DESI-030.1108-08.6449	DC	21.72	20.25	19.43	0.23	0.3965	
DESI-030.1551+14.4092	DC	20.93	19.24	18.38	0.75	0.5040	
DESI-030.1743-11.0445	DC	21.75	20.36	19.50	0.99		0.176 ± 0.011
DESI-030.2531-36.7018	REX	21.97	20.60	19.81	0.92		0.487 ± 0.107
DESI-030.3065-26.0892	REX	20.86	19.83	19.12	0.20		0.855 ± 0.125
DESI-030.7600-06.6024	DC	20.76	19.47	18.72	0.98	0.4935	
DESI-030.7806-22.7856	DC	19.35	18.64	18.24	0.99		0.347 ± 0.038
DESI-030.8121-15.9384	DC	20.38	19.12	18.39	0.99		0.685 ± 0.070
DESI-030.9153-31.0823	DC	23.13	21.26	19.64	0.93		0.474 ± 0.052
DESI-031.1304-19.3899	REX	22.13	20.69	19.82	0.26		0.780 ± 0.046
DESI-031.2607-21.8603	REX	14.54	14.02	13.77	0.16		0.858 ± 0.077
DESI-031.3554-16.4083	DC	22.16	20.66	19.63	0.21		0.770 ± 0.075
DESI-031.3590-24.5664	REX	21.60	20.43	19.57	0.30		0.592 ± 0.053
DESI-031.4976-21.1722	DC	18.90	17.79	17.08	0.14		0.716 ± 0.090
DESI-031.6715-02.0052	DC	15.30	14.42	13.70	0.82	0.7005	
DESI-031.7319-31.7726	DC	21.23	19.93	19.32	0.25		0.607 ± 0.014
DESI-031.8616-27.2286	DC	21.92	20.41	19.37	0.62		0.820 ± 0.029
DESI-032.0005-17.7739	DC	18.57	17.68	17.02	0.88		0.908 ± 0.056
DESI-032.1245-18.3429	DC	19.94	18.97	18.26	0.16	0.5606	
DESI-032.1994+01.7689	DC	22.89	21.35	19.80	0.58	0.4722	
DESI-032.2091-25.0391	REX	21.33	20.00	19.14	0.41		0.449 ± 0.019
DESI-032.2674+03.6995	REX	20.20	19.63	19.22	0.81	0.2888	
DESI-032.2667+04.8088	REX	22.01	20.69	19.85	0.21	0.5005	
DESI-032.4773-30.3485	REX	20.03	19.46	19.03	0.20		0.881 ± 0.043
DESI-032.6664-00.6421[e]	REX	20.16	19.73	19.43	0.26	0.2544	
DESI-032.8213+00.3402	REX	21.92	20.46	19.55	0.14	0.6059	
DESI-032.8584-16.2274	DC	21.78	20.34	19.60	0.60		0.483 ± 0.014
DESI-033.0297+00.2472	DC	23.56	21.36	19.54	0.85	0.2135	
DESI-033.0825+30.5530	DC	21.91	20.65	19.38	0.71	0.5477	
DESI-033.1994-05.9312[i]	REX	20.34	19.31	18.55	0.73	0.5022	
DESI-033.2069-20.7412	DC	22.25	20.57	19.73	0.72		0.272 ± 0.008
DESI-033.5356-12.8859	DC	20.93	19.41	18.58	0.27	0.5551	
DESI-033.7026-24.8797	DC	22.66	20.84	19.82	0.92		0.803 ± 0.035
DESI-033.7174+19.5413[a]	REX	22.63	20.77	19.67	1.00	0.6180	
DESI-033.8312-22.6154	DC	22.05	20.88	19.81	0.90		0.390 ± 0.014
DESI-034.1856-00.3860	DC	20.77	19.27	18.43	1.00	0.4583	
DESI-034.2874-09.2052	DC	21.39	19.93	19.01	0.82	0.1872	

Table 6 continued on next page

Table 6 *(continued)*

Name	Type	mag_g	mag_r	mag_z	Probability	z_{spec}	z_{phot}
DESI-034.3096-10.0969	REX	21.11	19.77	18.91	0.12	0.6085	
DESI-034.3830+20.9523	REX	20.43	19.65	19.03	0.71	0.5886	
DESI-034.5247+26.6007	DC	19.93	18.71	17.99	0.98		0.460 ± 0.040
DESI-034.5314-27.6291	DC	19.87	18.78	18.10	0.32		0.214 ± 0.060
DESI-034.6677-24.8466	REX	21.32	19.93	19.16	0.12		0.752 ± 0.100
DESI-034.7239-16.8684	DC	18.71	17.74	17.09	0.75		0.805 ± 0.051
DESI-034.8554+05.6438	DC	19.60	18.48	17.63	0.13	0.6784	
DESI-034.9126-17.6882	DC	20.35	19.09	18.36	0.95		0.538 ± 0.014
DESI-034.9597-05.9518	DC	19.43	18.00	16.72	0.50	0.6726	
DESI-035.0412-28.1798	DC	23.26	21.23	19.46	0.81		0.305 ± 0.008
DESI-035.1949+05.8853	REX	22.31	20.68	19.88	0.37	0.6358	
DESI-035.2949-23.0878	DC	20.44	18.89	18.08	0.68		0.267 ± 0.011
DESI-035.4007-26.6592	DC	22.64	20.88	19.74	0.96		0.525 ± 0.027
DESI-035.7407-25.1018	DC	20.66	19.57	18.80	0.68		0.225 ± 0.013
DESI-036.0382-16.3869	DC	21.45	20.45	19.82	0.67	0.4718	
DESI-036.0573+19.8696	DC	19.84	18.69	17.96	0.16		0.847 ± 0.144
DESI-036.0992+02.4337	DC	21.22	19.83	18.78	0.84	0.4826	
DESI-036.1196-25.0390	DC	22.28	20.57	19.56	0.15		0.534 ± 0.013
DESI-036.3834-04.8500	REX	21.80	20.47	19.67	0.15	0.6087	
DESI-036.7384-29.3340	DC	22.70	20.83	19.61	0.98		0.567 ± 0.046
DESI-036.8066+29.5796	DC	20.56	19.82	19.34	0.96	0.4507	
DESI-037.2442-17.2723	REX	22.33	20.91	19.87	1.00		0.868 ± 0.064
DESI-037.3509+10.2791	DC	23.29	21.28	19.66	0.77		0.695 ± 0.035
DESI-037.5061-20.9108	DC	18.91	17.97	17.31	0.98		0.536 ± 0.031
DESI-037.6345-24.1463	DC	23.20	21.73	19.94	0.62		0.622 ± 0.015
DESI-037.6589-01.8803[k]	DC	23.69	21.97	19.77	0.67	0.2507	
DESI-037.7099-17.5029	REX	22.63	20.70	19.69	0.92		0.816 ± 0.051
DESI-038.0192-17.6864	DC	23.05	21.15	19.91	0.47	0.4523	
DESI-038.3831-03.4670[e]	DC	20.58	19.52	18.57	0.51	0.5494	
DESI-038.7280-30.9373	REX	20.90	19.47	18.59	0.99		0.794 ± 0.183
DESI-038.8158-17.1581	REX	21.94	20.57	19.92	0.27	0.6773	
DESI-039.2176-31.8548	DC	21.51	20.00	18.89	0.31		0.401 ± 0.010
DESI-039.3484-30.2921	DC	22.08	20.27	19.04	0.97		0.545 ± 0.019
DESI-039.6138-15.5779	DC	21.75	20.12	19.26	0.11		0.732 ± 0.032
DESI-039.8085-03.7403	DC	21.72	19.85	18.65	0.81		0.686 ± 0.046
DESI-039.9312-24.9308	DC	22.46	20.61	19.37	0.78		0.661 ± 0.016
DESI-039.9863-27.1208	DC	21.03	20.08	19.50	0.88		0.521 ± 0.033
DESI-040.0268-11.4252	REX	21.46	19.80	18.96	0.98		0.696 ± 0.041

Table 6 continued on next page

Table 6 *(continued)*

Name	Type	mag_g	mag_r	mag_z	Probability	z_{spec}	z_{phot}
DESI-040.1730-21.4503	DC	18.40	17.22	16.46	0.91		0.327 ± 0.012
DESI-040.6738-21.1358	REX	20.46	19.98	19.68	0.14		0.317 ± 0.026
DESI-041.1156-28.6150	DC	22.42	20.75	19.60	1.00		0.476 ± 0.012
DESI-041.4712-05.9667	DC	23.04	21.15	19.27	0.92	0.5731	
DESI-042.0215-18.9309	DC	21.71	20.15	19.37	0.46		0.417 ± 0.036
DESI-042.0939+02.7825	REX	22.71	20.85	19.88	0.96	0.3859	
DESI-042.1344-12.1016	REX	21.84	20.45	19.56	0.98		0.835 ± 0.102
DESI-042.1475-12.1625	DC	20.02	19.44	18.98	0.86		0.405 ± 0.016
DESI-042.2120-27.3537	DC	18.38	17.19	16.40	0.76		0.234 ± 0.008
DESI-043.3406-05.1544	DC	18.87	17.71	16.81	0.34	0.5834	
DESI-043.3785-12.6509[d]	DC	19.18	17.90	17.07	0.87		0.746 ± 0.048
DESI-043.8215-16.6815	DC	19.35	18.36	17.65	1.00	0.5032	
DESI-044.0165+00.3311	REX	22.41	20.61	19.69	0.25	0.6462	
DESI-044.2789-16.7736	DC	19.74	18.73	18.08	0.41		0.368 ± 0.010
DESI-044.3388-28.8952	DC	22.49	20.98	19.70	0.36		0.939 ± 0.108
DESI-044.4764-23.3071	REX	21.85	19.96	18.97	0.33		0.283 ± 0.046
DESI-044.5307-13.8106	DC	23.06	21.08	19.51	0.35		0.672 ± 0.082
DESI-044.7621-07.8029	DC	19.40	18.15	17.37	0.75	0.6841	
DESI-044.9661-38.8328	REX	19.89	19.07	18.49	0.41		0.660 ± 0.089
DESI-044.9857-26.8724[g]	DC	21.30	19.79	19.00	1.00		0.445 ± 0.009
DESI-044.9848-10.2476	REX	19.91	18.98	18.33	0.95		0.433 ± 0.027
DESI-045.0813+04.4270	REX	21.51	20.41	19.64	0.23	0.3044	
DESI-045.2324-10.9787	DC	20.44	19.22	18.36	0.95		0.474 ± 0.152
DESI-045.5432-22.6720	DC	24.08	21.87	19.97	1.00		0.465 ± 0.055
DESI-045.8553-22.9291	DC	22.24	20.45	19.46	1.00		0.531 ± 0.038
DESI-045.8714+03.7781	DC	21.62	19.82	18.91	0.97	0.5305	
DESI-046.5824-13.5938	DC	23.55	21.29	19.54	0.86		0.708 ± 0.032
DESI-046.6654-27.6075[g]	DC	21.59	20.88	19.87	1.00		0.421 ± 0.062
DESI-046.6785-28.5384	DC	21.80	20.29	19.46	0.18		0.544 ± 0.021
DESI-046.7377-23.3925	DC	22.32	20.60	19.35	0.91		0.555 ± 0.042
DESI-046.8383-24.2794	DC	19.03	18.11	17.44	0.27		0.484 ± 0.036
DESI-047.7104-21.2200	DC	20.87	19.48	18.75	0.61		0.571 ± 0.059
DESI-047.9174-07.5180	DC	22.38	20.58	19.51	0.42	0.4410	
DESI-048.2870-16.4246	DC	20.66	19.22	18.47	0.91		0.358 ± 0.066
DESI-048.6940-13.7434	DC	22.82	21.06	19.80	0.77	0.6225	
DESI-048.8942-27.2465	DC	22.16	20.21	18.95	0.50		0.633 ± 0.084
DESI-049.0800-28.8885	DC	16.30	15.69	15.20	0.68		0.426 ± 0.010
DESI-049.1543-26.8148	DC	20.24	19.79	19.54	0.44		0.690 ± 0.036

Table 6 continued on next page

Table 6 *(continued)*

Name	Type	mag_g	mag_r	mag_z	Probability	z_{spec}	z_{phot}
DESI-049.2052-18.0014	DC	20.75	19.21	18.43	0.80		0.208 ± 0.047
DESI-049.3327-30.1661	DC	23.00	21.09	19.88	0.94		0.523 ± 0.017
DESI-049.3356-26.6664	DC	22.70	20.99	19.84	1.00		0.310 ± 0.012
DESI-049.4146-27.3320	REX	20.90	19.80	19.13	0.10		0.501 ± 0.172
DESI-049.4239-21.3050[d]	DC	22.43	20.67	19.76	0.97		0.475 ± 0.011
DESI-049.7786-27.6615	DC	22.72	20.86	19.67	1.00		0.678 ± 0.079
DESI-049.7855-07.5011	DC	22.13	20.37	19.22	1.00	0.4757	
DESI-049.9132-21.1511	DC	20.74	19.88	19.35	0.65		0.628 ± 0.026
DESI-050.1173-29.0147	DC	20.97	19.69	18.85	0.77		0.740 ± 0.064
DESI-050.2069-21.4455	DC	22.61	20.72	19.16	0.52		0.700 ± 0.018
DESI-050.3265-22.2543	DC	22.59	20.57	19.07	0.27		0.535 ± 0.046
DESI-051.0021-27.1917	DC	20.94	19.48	18.71	0.99		0.704 ± 0.039
DESI-051.2450-11.5876	DC	19.98	18.99	18.20	1.00		0.424 ± 0.045
DESI-051.4778-17.1685	REX	22.07	20.25	19.26	0.83		0.867 ± 0.122
DESI-051.5965-25.8119	REX	21.39	19.86	18.82	0.37		0.713 ± 0.036
DESI-051.6476-25.0483	DC	19.85	18.38	17.65	0.31		0.668 ± 0.056
DESI-051.7081-00.7311	DC	21.82	20.03	19.09	0.86	0.1742	
DESI-052.0458-31.5770	DC	19.81	18.83	18.06	0.76		0.641 ± 0.059
DESI-052.3736-18.6378	DC	22.31	20.50	18.97	0.16		0.636 ± 0.016
DESI-052.4307-32.1849	REX	21.62	20.54	19.83	0.23		0.816 ± 0.074
DESI-052.5899+00.6691	DC	22.48	20.61	19.61	0.34	0.4920	
DESI-052.6889-29.4983	REX	21.73	20.56	19.87	0.85		0.645 ± 0.086
DESI-052.7565-09.4508	DC	22.20	20.33	19.22	0.97		0.860 ± 0.053
DESI-052.9149-18.2136	REX	22.80	20.95	19.41	0.50		0.334 ± 0.036
DESI-053.1504-39.1976	REX	19.46	18.74	18.24	0.14		0.532 ± 0.082
DESI-053.7471-26.5755[d]	DC	22.22	20.58	19.53	0.44		0.332 ± 0.008
DESI-053.9519-29.9771	DC	21.37	19.59	18.59	0.99		0.318 ± 0.010
DESI-054.1741-20.3531[d]	DC	22.43	20.60	19.61	0.55		0.597 ± 0.013
DESI-054.2674-04.8785	REX	21.60	20.21	19.37	0.17		0.386 ± 0.033
DESI-054.4002-15.7893	REX	22.44	20.65	19.73	0.63		0.410 ± 0.075
DESI-054.4115-21.0294	DC	17.67	16.53	15.81	0.83		0.782 ± 0.050
DESI-054.6271-05.6708	DC	23.13	21.30	19.93	0.69	0.6146	
DESI-054.6308-24.6332	DC	21.95	20.07	19.03	0.83		0.582 ± 0.021
DESI-054.7432-28.2190	REX	21.69	20.65	19.60	0.35		0.422 ± 0.077
DESI-054.7788-12.2879	REX	21.52	20.60	19.98	0.92	0.3747	
DESI-054.8226-38.9498	REX	22.18	20.39	19.45	0.99		0.715 ± 0.044
DESI-055.0105-27.3081	DC	19.79	18.61	17.90	0.89		0.761 ± 0.066
DESI-055.4130-13.4363	REX	22.15	20.45	19.58	0.78		0.790 ± 0.142

Table 6 continued on next page

Table 6 *(continued)*

Name	Type	mag_g	mag_r	mag_z	Probability	z_{spec}	z_{phot}
DESI-055.4365-31.6484	DC	23.21	21.19	19.78	0.92		0.796 ± 0.047
DESI-055.6364-20.0025	DC	16.79	15.97	15.34	0.27		0.650 ± 0.049
DESI-055.7686-10.8819	DC	22.28	20.56	19.38	0.23		0.583 ± 0.023
DESI-055.8961-29.9218	DC	22.19	20.25	18.94	0.20		0.409 ± 0.054
DESI-056.3743-33.2010	REX	21.72	20.82	19.72	0.49		0.879 ± 0.102
DESI-056.4484-30.3933	DC	20.41	19.23	18.53	0.87		0.455 ± 0.049
DESI-056.5384-26.4042	DC	21.76	19.92	18.52	0.88		0.601 ± 0.053
DESI-056.5861-09.6696	REX	17.74	17.40	17.20	0.90		0.699 ± 0.045
DESI-056.6788-09.2313	DC	20.51	18.94	18.09	0.99		0.427 ± 0.021
DESI-056.8707-25.7853	DC	21.91	20.20	19.32	0.12		0.611 ± 0.028
DESI-056.8839-20.4636	DC	21.05	19.53	18.65	0.39		0.298 ± 0.010
DESI-057.0469-25.5083	REX	22.88	21.03	19.97	0.13		0.654 ± 0.075
DESI-057.2082-22.3314	DC	19.76	18.78	18.13	0.87		0.499 ± 0.031
DESI-057.3298-26.9437	DC	21.77	19.94	18.99	0.40		0.690 ± 0.127
DESI-057.4192-19.9070	REX	22.70	20.86	19.88	0.29		0.824 ± 0.127
DESI-057.7531-19.8013	DC	23.04	21.33	19.79	0.32		0.681 ± 0.030
DESI-057.8307-15.1796	DC	21.31	19.90	19.11	0.46		0.455 ± 0.022
DESI-057.9593-22.2418	REX	22.61	20.96	19.98	0.97		0.753 ± 0.050
DESI-058.1777-19.3799	DC	21.48	20.13	19.20	0.95		0.631 ± 0.040
DESI-058.3477-30.5941	REX	22.35	20.71	19.86	0.51		0.867 ± 0.056
DESI-058.3547-02.8941	DC	15.43	14.76	14.25	0.82		0.483 ± 0.027
DESI-059.9626-26.5819	DC	21.72	20.25	19.47	0.36		0.276 ± 0.030
DESI-060.0000-27.7231	DC	22.70	20.79	19.24	0.70		0.700 ± 0.052
DESI-060.1170-15.1166	DC	18.33	17.28	16.58	0.12		0.355 ± 0.033
DESI-060.5532-27.5316	REX	21.33	19.80	18.99	0.17		0.454 ± 0.077
DESI-060.5575-32.2606	DC	22.35	20.85	19.82	0.24		0.912 ± 0.063
DESI-060.6043-22.0993	DC	20.43	19.97	19.82	0.15		0.804 ± 0.063
DESI-060.7510-18.9797	DC	21.89	20.24	19.40	0.14		0.238 ± 0.013
DESI-060.7611-18.5019	DC	19.98	18.99	18.35	0.97		0.731 ± 0.097
DESI-061.0473-16.8863	DC	20.89	19.53	18.68	0.21		0.649 ± 0.030
DESI-061.1936-08.7636	DC	19.73	18.20	17.39	0.48		0.466 ± 0.150
DESI-061.3000-15.6132	DC	23.07	21.23	19.63	0.99		0.426 ± 0.026
DESI-061.3613-25.6735	DC	22.26	20.68	19.84	0.96		0.280 ± 0.010
DESI-061.5534-22.9034	DC	23.17	21.15	19.64	0.69		0.802 ± 0.021
DESI-061.6860-14.6132	DC	21.31	20.53	19.90	0.12		0.437 ± 0.014
DESI-061.9786-31.8631	DC	21.44	20.10	19.25	0.81		0.953 ± 0.087
DESI-062.2880-32.0960	DC	22.85	21.06	19.81	0.83		0.385 ± 0.021
DESI-062.3942-31.5637	DC	22.77	20.82	19.59	0.23		0.869 ± 0.041

Table 6 continued on next page

Table 6 *(continued)*

Name	Type	mag_g	mag_r	mag_z	Probability	z_{spec}	z_{phot}
DESI-062.4692-32.1910	DC	21.94	20.05	18.88	0.29		0.614 ± 0.023
DESI-062.5854-03.6132	DC	21.32	19.76	18.95	0.60		0.696 ± 0.049
DESI-062.6288-14.8934[a]	DC	22.29	20.41	19.21	0.99		0.568 ± 0.044
DESI-062.6611-19.4171	DC	22.80	21.04	19.89	0.91		0.556 ± 0.090
DESI-063.2031-01.8160	DC	22.75	20.92	19.77	0.80		0.296 ± 0.021
DESI-063.2873-35.0175	REX	21.57	20.62	19.89	0.14		0.769 ± 0.033
DESI-063.4434-29.6321	DC	21.82	20.42	19.53	0.44		0.873 ± 0.080
DESI-064.0540-30.3893	REX	19.95	19.07	18.51	1.00		0.627 ± 0.060
DESI-064.1560-20.0800	DC	21.82	20.01	18.94	0.79		0.404 ± 0.052
DESI-064.5125-19.1295	DC	19.76	18.59	17.83	0.81		0.476 ± 0.022
DESI-064.5883-31.2553	DC	20.35	19.20	18.50	0.99		0.514 ± 0.019
DESI-064.6062-24.9971	DC	21.19	20.13	19.47	0.11		0.324 ± 0.051
DESI-064.8599-09.5649	DC	23.04	21.15	19.84	0.61		0.574 ± 0.032
DESI-064.8752-37.1532	REX	22.23	20.50	19.57	0.15		0.366 ± 0.041
DESI-065.1328-21.1219	DC	21.59	19.81	18.81	0.30		0.694 ± 0.027
DESI-065.2204-24.1023	DC	20.95	19.86	19.20	0.25		0.592 ± 0.094
DESI-065.2768-20.9997	DC	23.20	21.35	19.90	0.67		0.812 ± 0.046
DESI-065.4182-22.9294	DC	22.64	20.69	19.52	0.16		0.620 ± 0.030
DESI-065.4574-11.0477	DC	21.64	19.75	18.77	0.96		0.576 ± 0.032
DESI-065.5424-29.0529	REX	20.91	19.62	18.91	0.14		0.505 ± 0.168
DESI-065.5591-28.8002	DC	21.84	19.94	18.79	0.19		0.416 ± 0.051
DESI-065.6339-26.1299	DC	21.11	20.04	19.38	0.11		0.773 ± 0.016
DESI-065.7967-01.3515	DC	20.00	19.27	18.78	0.37		0.387 ± 0.021
DESI-065.8473-03.3572	DC	21.35	19.32	18.37	0.88		0.603 ± 0.008
DESI-066.5255-13.2436	DC	20.33	19.24	18.54	1.00		0.749 ± 0.054
DESI-067.6651-25.8495	DC	18.80	17.74	17.05	0.93		0.596 ± 0.101
DESI-067.8196-31.4630	DC	22.17	20.53	19.65	0.30		0.489 ± 0.057
DESI-068.1022-20.0038	DC	20.94	19.08	18.15	1.00		0.555 ± 0.009
DESI-068.8475-22.0006	REX	21.62	20.66	19.80	0.45		0.712 ± 0.047
DESI-068.9055-25.3337[a]	DC	17.37	16.47	15.79	0.81		0.544 ± 0.053
DESI-068.9980-21.6384	DC	21.65	20.48	19.83	0.11		0.517 ± 0.035
DESI-069.3619-23.0974	DC	21.44	19.78	18.86	0.13		0.384 ± 0.027
DESI-069.5641-32.3475	DC	22.15	20.35	19.37	0.97		0.506 ± 0.017
DESI-069.6110-27.1239	DC	21.92	20.28	19.43	0.83		0.757 ± 0.031
DESI-069.6660-28.5525	DC	22.54	20.68	19.46	0.71		0.592 ± 0.024
DESI-070.0841-06.3394	DC	22.26	19.99	18.86	0.14	0.1599	
DESI-070.1117-24.5699	DC	22.60	20.72	19.70	0.25		0.672 ± 0.221
DESI-070.2650-27.0995	REX	22.16	20.76	19.94	0.13		0.389 ± 0.127

Table 6 continued on next page

Table 6 *(continued)*

Name	Type	mag_g	mag_r	mag_z	Probability	z_{spec}	z_{phot}
DESI-070.8793-32.1335	DC	22.74	21.06	19.92	0.28		0.317 ± 0.068
DESI-071.3350-22.0787	DC	21.94	20.54	19.51	0.97		0.434 ± 0.026
DESI-071.5515-28.6470	REX	22.03	20.68	19.84	0.20		0.810 ± 0.120
DESI-071.9694-29.1854	DC	21.91	20.05	19.05	0.90		0.552 ± 0.059
DESI-072.0873-19.4173	DC	17.79	17.57	17.41	0.50		1.021 ± 0.061
DESI-072.1089-29.1347	DC	21.46	19.52	18.20	0.28		0.341 ± 0.059
DESI-072.1777-05.0516	DC	22.03	20.33	19.44	0.22	0.2951	
DESI-072.8336-18.7814	DC	20.53	19.10	18.22	0.43		0.601 ± 0.032
DESI-072.8845-01.0118	DC	22.70	20.95	19.29	0.88	0.6166	
DESI-072.9124-08.0276	DC	22.91	21.04	19.87	0.29		0.720 ± 0.070
DESI-073.5270-24.5988	DC	21.94	20.04	18.85	0.72		0.793 ± 0.057
DESI-073.6913-29.8156	DC	23.33	21.43	19.84	0.22		0.690 ± 0.026
DESI-074.2036-00.8212	DC	22.07	20.43	19.46	0.49	0.6326	
DESI-074.3280-04.4293	DC	22.29	20.47	19.48	1.00	0.7333	
DESI-074.4224-18.7934	DC	22.91	20.87	19.10	0.48		0.671 ± 0.030
DESI-074.4853-23.1579	DC	21.48	19.77	18.88	0.34		0.549 ± 0.031
DESI-074.6542-27.1065	DC	22.82	21.18	19.70	0.52		0.558 ± 0.024
DESI-075.3911-03.2937	DC	22.30	20.86	19.47	0.25		0.770 ± 0.065
DESI-075.4100-18.6007	DC	22.79	21.06	19.90	0.58		0.279 ± 0.011
DESI-075.5665-31.0876	DC	22.13	20.31	19.20	0.92		0.765 ± 0.023
DESI-075.9545-26.6809	REX	19.94	19.01	18.39	0.10		0.650 ± 0.050
DESI-076.3503-24.3444	DC	21.93	20.52	19.69	0.58		0.781 ± 0.101
DESI-076.4074-36.0651	REX	22.02	20.84	20.00	0.54		0.590 ± 0.059
DESI-076.7517-25.6907	REX	22.10	20.24	19.25	0.61		0.624 ± 0.030
DESI-077.2638-21.5958	DC	23.07	21.31	19.85	0.35		0.637 ± 0.012
DESI-077.3886-30.6005	DC	20.77	19.38	18.61	0.77		0.626 ± 0.158
DESI-077.6960-26.5395	DC	21.16	19.95	19.14	0.81		0.726 ± 0.054
DESI-077.7769-51.1904	REX	20.73	19.54	18.83	0.32		0.305 ± 0.075
DESI-078.4202-28.2351	DC	22.24	20.49	19.60	0.41		0.713 ± 0.045
DESI-079.4502-23.2598	DC	22.48	20.79	19.87	0.60		0.521 ± 0.050
DESI-079.7106-32.3011	DC	22.08	20.39	19.43	0.12		0.545 ± 0.010
DESI-080.2860-18.3170	DC	23.26	21.35	19.83	0.63		0.803 ± 0.034
DESI-080.6361-24.9674	DC	23.21	21.39	19.90	0.41		0.525 ± 0.012
DESI-080.6724-24.0688	DC	22.59	20.82	19.74	0.37		0.446 ± 0.012
DESI-080.9091-21.0160	DC	20.33	18.60	17.72	0.84		0.758 ± 0.014
DESI-081.2511-26.2779	DC	21.14	19.40	18.53	0.97		0.753 ± 0.020
DESI-081.5917-27.3214	REX	21.45	20.39	19.77	0.21		0.634 ± 0.154
DESI-082.4980-19.9199	DC	22.43	20.97	19.59	0.55		0.544 ± 0.025

Table 6 continued on next page

Table 6 *(continued)*

Name	Type	mag_g	mag_r	mag_z	Probability	z_{spec}	z_{phot}
DESI-083.1991-29.3017	REX	21.85	20.55	19.67	0.65		0.675 ± 0.027
DESI-083.4490-22.2658	DC	20.97	19.88	19.18	0.98		0.731 ± 0.016
DESI-083.7580-31.1953	REX	21.05	20.00	19.34	0.74		0.822 ± 0.094
DESI-083.9416-27.0088	DC	20.69	18.90	17.99	1.00		0.541 ± 0.013
DESI-084.2051-21.8332	REX	22.46	20.65	19.70	0.93		0.307 ± 0.074
DESI-084.7962-28.0211	DC	21.14	19.38	18.48	0.20		0.994 ± 0.027
DESI-085.5750-21.8217	DC	22.42	20.73	19.86	0.87		0.549 ± 0.029
DESI-085.7339-31.4431	DC	22.08	20.91	19.64	0.92		0.508 ± 0.039
DESI-086.5017-24.7015	REX	21.01	19.51	18.65	0.98		0.760 ± 0.034
DESI-086.5815-27.7223	DC	21.96	20.32	19.41	0.51		0.830 ± 0.054
DESI-086.8986-28.1308	DC	19.81	18.55	17.80	0.12		0.348 ± 0.014
DESI-087.1209-25.5251	DC	23.61	21.83	19.53	0.90		0.319 ± 0.028
DESI-087.2700-23.9175	DC	21.60	19.92	19.01	0.98		0.514 ± 0.040
DESI-087.4139-30.4661	DC	21.46	19.90	18.99	0.74		0.467 ± 0.038
DESI-087.9077-25.1400	DC	20.46	18.78	17.90	1.00		0.724 ± 0.066
DESI-088.3590-23.0945	REX	22.46	20.95	20.00	0.28		0.567 ± 0.299
DESI-088.5024-29.7013	DC	21.12	19.43	18.52	0.96		0.603 ± 0.026
DESI-088.6111-44.9258	REX	21.25	19.60	18.69	0.44		0.339 ± 0.063
DESI-089.5700-30.9485	DC	22.06	20.32	19.45	0.72		0.711 ± 0.046
DESI-089.6163-27.0385	REX	20.73	20.16	19.97	0.98		0.727 ± 0.044
DESI-090.4566-39.9871	REX	22.15	20.44	19.51	0.80		0.464 ± 0.026
DESI-094.5639+50.3059	DC	21.50	20.09	19.28	1.00		0.522 ± 0.020
DESI-095.7736+58.8572	DC	21.99	20.57	19.84	0.98		0.610 ± 0.029
DESI-103.0258+33.1167	DC	21.20	19.74	18.84	0.24		0.264 ± 0.029
DESI-104.3289+45.1488	DC	22.03	20.57	19.77	0.26		0.274 ± 0.189
DESI-104.3594+32.5562	DC	21.34	20.22	19.38	0.64		0.556 ± 0.023
DESI-106.9992+50.2149	DC	22.08	20.41	19.55	0.17		0.629 ± 0.027
DESI-107.9746+28.3465	DC	23.62	21.52	19.88	0.91		0.697 ± 0.095
DESI-109.4348+42.7031	DC	20.54	18.82	17.95	0.17		0.227 ± 0.014
DESI-112.0041+47.9631	DC	21.15	19.65	18.83	0.17		0.703 ± 0.039
DESI-112.0551+31.6799	DC	20.88	19.16	18.24	0.63	0.6745	
DESI-112.1757+38.2037	DC	19.64	18.35	17.57	0.55	0.5956	
DESI-112.6173+38.3732	DC	20.72	20.09	19.72	0.81	0.5263	
DESI-113.2567+51.5755	DC	21.71	20.09	19.25	0.93		0.360 ± 0.042
DESI-113.5048+34.7261	REX	20.82	19.60	18.75	0.16	0.6162	
DESI-114.0195+21.3041	DC	22.06	20.36	19.50	0.97	0.4533	
DESI-115.4473+34.9407	DC	20.80	19.24	18.39	1.00	0.5287	
DESI-116.4388+09.6096	DC	22.37	20.84	19.96	0.39	0.5022	

Table 6 continued on next page

Table 6 *(continued)*

Name	Type	mag_g	mag_r	mag_z	Probability	z_{spec}	z_{phot}
DESI-117.2449+53.7774	DC	23.07	21.06	19.99	0.80		0.601 ± 0.043
DESI-117.7803+11.1984	DC	21.07	19.69	18.96	0.24	0.3592	
DESI-118.2474+52.6265	DC	21.05	19.62	18.86	0.13	0.8186	
DESI-118.3583+10.5130	DC	20.42	18.92	18.07	0.60	0.5655	
DESI-118.4566+25.8080	DC	21.50	20.21	19.43	0.33	0.5024	
DESI-118.7209+31.4647	REX	21.75	20.69	19.95	0.29	0.6156	
DESI-118.7654+12.3763	DC	20.50	19.57	18.96	0.97	0.6674	
DESI-119.0587+30.2350	DC	20.89	19.90	19.29	1.00	0.3813	
DESI-119.3016+24.1528	DC	21.32	19.60	18.73	0.12	0.5161	
DESI-119.5864+12.3470	DC	19.05	18.07	17.36	0.40	0.5794	
DESI-120.0515+43.4978	DC	18.87	17.70	16.96	0.55		0.989 ± 0.086
DESI-120.3991+54.8115	DC	18.89	17.84	17.12	1.00	0.5286	
DESI-120.8544+37.7610	DC	20.48	19.96	19.61	0.27	0.7049	
DESI-121.6989+77.2344	DC	21.31	19.64	18.79	0.94		0.738 ± 0.139
DESI-122.5113+33.7794	DC	21.66	20.33	19.56	1.00	0.3136	
DESI-122.5445-01.9522	DC	23.24	21.23	19.82	0.60	0.6349	
DESI-122.8280+00.5908	DC	18.77	17.78	17.10	0.91	0.3799	
DESI-122.8819+41.6140	DC	22.69	20.95	19.80	0.59	0.2815	
DESI-123.5420+11.5365	REX	21.12	20.16	19.55	0.38	0.1198	
DESI-123.6121+27.3335	DC	18.96	17.76	16.96	0.98	0.3383	
DESI-124.3100+74.1113	DC	18.89	17.70	16.92	0.88		0.859 ± 0.072
DESI-124.8181+31.4990	DC	18.27	17.10	16.35	1.00	0.5819	
DESI-124.9193+19.2529	DC	18.94	17.81	17.09	0.78	0.6060	
DESI-125.3638+69.4352	REX	21.34	20.38	19.79	0.11		0.349 ± 0.042
DESI-125.6309+75.0251	DC	22.11	20.13	18.90	0.12		0.366 ± 0.027
DESI-125.9350+04.6293	DC	20.97	19.95	19.23	0.10	0.6567	
DESI-126.0499+04.7936	DC	19.24	17.96	17.09	0.93	0.3896	
DESI-128.1456+11.5864	DC	21.35	19.53	18.61	0.97	0.6133	
DESI-129.9505+30.6284	DC	22.38	20.91	19.58	0.35	0.6653	
DESI-130.0214+11.8118	DC	22.77	21.18	19.86	0.43	0.4064	
DESI-130.5312+27.2618	DC	20.90	20.12	19.64	0.16	0.4179	
DESI-130.6033+10.4171	REX	20.44	19.73	19.23	0.45	0.4848	
DESI-131.5647+51.9315	DC	22.47	20.56	19.39	0.10		0.646 ± 0.163
DESI-131.9068+13.5143	DC	21.46	20.90	19.91	0.90	0.4707	
DESI-132.2802+22.0446	DC	21.05	19.38	18.57	0.86	0.2895	
DESI-132.8111+24.4868	DC	21.57	19.99	19.15	0.40	0.6765	
DESI-133.1155+26.4614	DC	23.03	21.23	19.72	0.49	0.5363	
DESI-134.3978+21.5059	REX	20.66	19.70	19.09	0.12	0.2608	

Table 6 continued on next page

Table 6 *(continued)*

Name	Type	mag_g	mag_r	mag_z	Probability	z_{spec}	z_{phot}
DESI-134.8207+06.2549	DC	22.84	20.93	19.84	1.00	0.2479	
DESI-136.0956+45.0733	DC	21.38	20.25	19.41	0.99	0.2974	
DESI-136.8675+42.5504[a]	REX	21.43	20.30	19.61	0.95	0.2413	
DESI-137.0261+01.3321[e]	DC	21.76	20.14	19.30	0.30	0.6752	
DESI-137.1509+54.2055	DC	17.31	16.49	15.88	0.99		0.715 ± 0.076
DESI-137.4500+07.3521	DC	22.56	20.99	19.97	1.00	0.6459	
DESI-137.9497+28.4536	DC	22.91	20.98	19.58	1.00	0.5653	
DESI-138.5115+16.5394	DC	21.95	20.02	18.68	0.12	0.8691	
DESI-139.3411+62.4459	DC	22.41	20.50	19.21	0.47	0.4060	
DESI-139.4885+64.4473	DC	18.66	17.68	17.03	0.91	0.5243	
DESI-140.1299+02.7830[e]	DC	22.27	20.68	19.56	0.20	0.2527	
DESI-141.5275+07.8090	DC	21.17	19.80	18.92	0.96	0.5715	
DESI-141.8108+73.2823	DC	21.56	20.11	19.23	0.22		0.392 ± 0.032
DESI-142.7762+17.7152	REX	21.27	20.26	19.61	0.14	0.5243	
DESI-143.7713+18.2787	DC	22.25	20.41	19.11	0.19		0.921 ± 0.073
DESI-144.0261+12.8391	DC	22.56	20.67	19.35	0.68	0.2845	
DESI-144.7849+00.6228	DC	20.21	19.08	18.39	0.14	0.4395	
DESI-145.1485+13.1356	DC	22.37	20.83	19.94	0.82	0.4702	
DESI-145.2603+38.7152	REX	19.60	18.81	18.25	0.91	0.6208	
DESI-146.0028-01.8290[l]	DC	21.00	19.52	18.63	0.32	0.5804	
DESI-146.0983-08.1021	DC	22.30	20.84	19.02	0.94		0.989 ± 0.089
DESI-146.2199+40.2997	DC	19.24	18.07	17.28	0.99	0.4601	
DESI-146.5442+13.9284	DC	22.72	20.85	19.67	0.80	0.5040	
DESI-146.6840+19.4528	DC	22.44	20.65	19.40	0.10	0.4963	
DESI-147.1576-02.5598[a]	REX	21.63	20.60	20.00	1.00	0.6511	
DESI-148.2095+10.7169	DC	20.53	19.56	19.03	0.79	0.3750	
DESI-148.3840+10.5475	DC	21.77	19.75	18.56	0.11	0.3446	
DESI-150.2941+46.1759	DC	19.93	18.84	18.04	0.11	0.6315	
DESI-150.5232+15.3083	DC	22.11	20.27	19.32	0.94	0.5493	
DESI-151.2523+10.4499	DC	22.81	20.98	19.57	0.58	0.6799	
DESI-151.4072+67.5076	DC	23.37	21.47	19.95	0.63		0.431 ± 0.017
DESI-151.8455-05.3863	DC	21.92	20.15	19.00	0.25		0.743 ± 0.089
DESI-152.2710+43.7279	DC	21.43	19.93	19.14	0.98	0.5751	
DESI-152.3889-05.6017	DC	22.67	20.79	19.63	1.00		0.425 ± 0.057
DESI-153.0776+44.3831	DC	20.07	18.99	18.31	0.84	0.4569	
DESI-153.2654+10.1926[a]	REX	21.78	19.99	19.14	0.70	0.4228	
DESI-154.5759+74.5812	DC	23.77	21.71	19.96	0.94		0.772 ± 0.040
DESI-155.2571+53.8914	DC	22.22	20.46	19.50	0.51	0.6023	

Table 6 continued on next page

Table 6 *(continued)*

Name	Type	mag_g	mag_r	mag_z	Probability	z_{spec}	z_{phot}
DESI-157.8915+18.5814	DC	23.37	21.46	19.98	0.98	0.5702	
DESI-157.9520+43.7158[a]	DC	19.71	19.13	18.77	1.00	0.4414	
DESI-158.0901+31.8835	DC	21.19	19.67	18.64	0.56	0.3334	
DESI-158.1287+46.3340	DC	20.59	19.79	19.55	0.62	0.6389	
DESI-158.1868+08.6779	DC	16.92	16.01	15.32	0.11	0.6930	
DESI-158.2260+39.8507	DC	23.21	21.44	19.81	0.11	0.4079	
DESI-159.1096+12.9958	REX	21.89	20.55	19.78	0.40	0.3015	
DESI-160.0017+56.5219	REX	21.93	20.55	19.53	0.16	0.2363	
DESI-160.0232+01.9838[g]	DC	22.09	20.43	19.30	0.81	0.3753	
DESI-160.1817+44.8942	DC	20.41	19.49	18.86	0.53	0.5807	
DESI-160.5973+00.2559	DC	22.49	20.58	19.33	0.91	0.5598	
DESI-160.6171+32.9365	DC	22.00	20.08	18.83	0.45	0.5335	
DESI-160.7046+62.6611	DC	21.35	19.80	18.99	0.99	0.3573	
DESI-160.7978+37.3601	DC	22.11	20.53	19.42	0.93	0.5615	
DESI-161.5784+46.2302	DC	21.80	20.04	19.16	0.21	0.5755	
DESI-161.8519-03.2118	REX	22.21	20.56	19.74	0.14	0.3404	
DESI-161.8653+23.9568	DC	21.13	19.69	18.86	1.00	0.5448	
DESI-162.0174+31.6472	DC	22.27	20.40	19.12	1.00	0.5825	
DESI-162.5961+20.0916	REX	20.69	19.82	19.25	0.73	0.4948	
DESI-162.7849-07.1816	DC	21.03	19.55	18.78	0.26		0.327 ± 0.038
DESI-163.3484+09.6864	REX	22.49	20.86	19.41	0.34	0.5301	
DESI-163.5448+05.8739	DC	22.09	20.16	18.87	0.31	0.4434	
DESI-163.7019+27.5697	DC	18.64	17.60	16.93	1.00	0.5270	
DESI-164.0099+22.8302	REX	22.57	20.83	19.91	0.13	0.5996	
DESI-164.1866+16.3070	DC	22.53	20.91	19.87	1.00	0.2531	
DESI-164.3198-08.2676	DC	21.77	20.52	19.76	1.00		0.335 ± 0.024
DESI-165.0321+10.9706	REX	21.46	20.59	19.69	0.23	0.6193	
DESI-165.1459+23.2635	DC	19.23	18.21	17.50	0.15	0.4366	
DESI-165.2130-00.8810	REX	21.29	19.55	18.68	0.81	0.4508	
DESI-165.2321+64.9414	DC	21.90	20.24	19.28	0.41		0.567 ± 0.033
DESI-165.2764+20.4527	DC	18.94	18.08	17.43	0.51	0.2910	
DESI-165.7828-00.6598	DC	21.95	20.47	19.31	0.18	0.4963	
DESI-166.7196+07.6232	DC	23.11	21.22	19.97	0.14	0.2991	
DESI-167.2393+37.8604	DC	22.83	21.01	19.90	0.94	0.2053	
DESI-167.7733+26.7798	DC	18.13	16.98	16.19	0.51	0.2765	
DESI-168.5731+08.7634	REX	22.19	20.74	19.85	0.83	0.7123	
DESI-168.9620+57.8315	DC	20.26	19.51	18.91	1.00	0.4893	
DESI-169.1444+19.0986	DC	21.22	19.69	18.68	0.13	0.5931	

Table 6 continued on next page

Table 6 *(continued)*

Name	Type	mag_g	mag_r	mag_z	Probability	z_{spec}	z_{phot}
DESI-169.6106-03.6275	REX	21.08	20.11	19.48	0.66	0.3945	
DESI-170.4254+36.9636	DC	20.17	19.28	18.74	0.93	0.5815	
DESI-170.8944+12.5591	DC	21.31	19.97	19.05	1.00	0.5305	
DESI-171.1047+71.1948	DC	22.31	20.73	19.79	0.27		0.754 ± 0.037
DESI-172.4891+32.1637	DC	20.39	19.53	18.86	0.30	0.5193	
DESI-172.6002+05.7333	DC	19.32	18.25	17.57	0.64	0.2636	
DESI-172.6730+11.3081	DC	21.14	20.10	19.47	0.24	0.6632	
DESI-173.5198+09.5846	DC	21.21	19.73	19.05	1.00		0.638 ± 0.069
DESI-173.5474+17.0433	DC	23.47	21.55	19.90	0.57	0.6664	
DESI-174.0108+52.2363[a]	REX	21.39	20.46	19.89	0.18	0.5404	
DESI-174.1285+21.7754	DC	22.52	20.64	19.32	0.98	0.4636	
DESI-174.2820+14.7811	DC	22.69	20.87	19.64	1.00	0.5951	
DESI-174.4592+46.6094	DC	21.32	19.49	18.47	0.25	0.3134	
DESI-174.8727-02.3072[e]	DC	21.91	20.24	19.38	0.99	0.5190	
DESI-175.1662+14.3254	REX	20.07	19.56	19.24	0.61	0.3711	
DESI-175.1752-00.7266	DC	21.88	20.15	19.28	1.00	0.6160	
DESI-175.7321+43.1339	DC	19.60	18.50	17.65	0.91	0.4782	
DESI-175.7329+22.2232	REX	20.50	19.53	18.89	0.74	0.6900	
DESI-176.6399-06.1812	DC	21.88	20.09	19.15	0.99		0.386 ± 0.028
DESI-176.9273+67.7222	DC	22.88	21.01	19.97	0.94	0.5990	
DESI-176.9311+26.1644[a]	DC	20.05	18.58	17.79	0.82	0.6131	
DESI-177.0183+29.4844	DC	20.57	19.29	18.52	0.96	0.5151	
DESI-177.0319+29.0869	DC	21.76	20.13	19.21	1.00	0.6224	
DESI-178.5091+14.0868	DC	19.86	18.93	18.23	0.70	0.7410	
DESI-178.7212+21.4151	DC	22.63	20.84	19.66	0.99	0.5466	
DESI-179.4811+22.9115	REX	21.61	20.07	19.14	0.36	0.7805	
DESI-181.0043+47.5381	DC	22.68	20.92	19.64	1.00	0.4861	
DESI-181.3974+41.1790	DC	20.14	18.41	17.42	1.00	0.4764	
DESI-182.5596+28.7243[a]	REX	20.68	19.95	19.53	1.00	0.2960	
DESI-182.7337-02.2276	DC	19.62	18.40	17.66	0.66	0.5326	
DESI-183.0990-01.5510[e]	DC	20.33	19.13	18.35	0.70	0.4034	
DESI-183.1167-08.5941	DC	23.29	21.25	19.85	0.63		0.212 ± 0.012
DESI-184.4375+31.5263	DC	21.70	19.66	18.45	1.00	0.6967	
DESI-185.2581+21.8900	DC	20.18	18.76	17.97	0.41	0.5735	
DESI-185.6190+23.9709	DC	20.32	19.10	18.26	0.80	0.5869	
DESI-185.6850+70.6065	DC	20.49	19.17	18.41	0.64		0.568 ± 0.035
DESI-185.9848+19.7177	DC	19.56	18.39	17.62	0.45	0.4966	
DESI-186.0916+02.2030	DC	21.47	20.16	19.39	0.47	0.3481	

Table 6 continued on next page

Table 6 *(continued)*

Name	Type	mag_g	mag_r	mag_z	Probability	z_{spec}	z_{phot}
DESI-187.1282+09.6881	REX	21.43	20.27	19.61	0.16	0.7398	
DESI-189.2482+25.3442	DC	20.09	19.31	18.81	0.48	0.6128	
DESI-190.4855+03.7332	DC	21.79	20.07	19.17	0.52	0.3586	
DESI-190.5769+27.8629	DC	22.35	20.76	19.83	0.93	0.5112	
DESI-190.5981+31.4848	DC	21.03	19.30	18.40	0.16	0.2420	
DESI-191.8527+36.7353[a]	DC	21.32	19.47	18.54	0.98	0.6986	
DESI-192.8317-01.2219	REX	20.55	19.89	19.54	0.94	0.2631	
DESI-193.6682+18.9533	REX	22.23	20.45	19.40	0.81	0.6412	
DESI-194.1102+04.6703	DC	22.24	20.54	19.55	0.28	0.2292	
DESI-195.4842+11.1801	DC	19.08	18.07	17.30	0.30	0.6066	
DESI-196.3635+26.7520	DC	19.50	18.07	17.32	0.17	0.3611	
DESI-196.6232-05.6670	DC	21.67	20.59	19.93	0.36		0.405 ± 0.011
DESI-196.8233+23.1565	DC	22.81	21.01	19.83	1.00	0.3819	
DESI-198.2028+30.6423	DC	21.48	19.88	19.08	0.27	0.5037	
DESI-198.4925+31.0493	REX	22.43	20.81	19.95	0.18	0.3212	
DESI-199.9412+01.5311	DC	19.19	17.99	17.24	0.91	0.5803	
DESI-200.5670+04.3460	DC	19.91	18.53	17.66	0.51	0.4027	
DESI-200.7983+38.2180	DC	22.47	20.63	19.57	0.12	0.5085	
DESI-202.5096+47.8919	DC	23.92	21.72	19.82	0.71	0.2674	
DESI-202.7745+07.4491	DC	21.75	20.00	19.09	0.49	0.1929	
DESI-203.2912+06.9014	REX	20.38	19.49	18.92	0.63	0.4303	
DESI-203.5927-09.2837	DC	21.87	20.48	19.71	0.53		0.333 ± 0.016
DESI-203.7084-08.7623	DC	20.03	18.83	17.97	0.63		0.721 ± 0.045
DESI-203.8962+40.3315	DC	22.64	20.91	19.90	0.96	0.3087	
DESI-204.0300+25.6164	DC	20.28	19.14	18.30	0.46	0.4939	
DESI-204.2365+12.0278	DC	21.76	20.33	19.54	0.20	0.5327	
DESI-204.3113+42.3813	DC	20.67	19.44	18.75	0.39	0.2802	
DESI-205.4375+04.1861	DC	20.73	19.28	18.51	0.97		0.598 ± 0.059
DESI-205.8655+21.7388	DC	21.17	19.50	18.65	0.20	0.5585	
DESI-206.0993-01.6071	DC	20.70	19.53	18.73	0.49	0.4681	
DESI-206.7000+28.6985	DC	21.84	20.37	19.53	0.47	0.4410	
DESI-207.4187+38.5022	DC	21.48	19.94	19.12	0.22	0.5818	
DESI-207.4889+34.2732	DC	21.95	20.36	19.50	0.84	0.4911	
DESI-207.5513+31.5862	DC	22.83	21.08	19.39	0.34	0.5095	
DESI-207.7049+52.9559	DC	22.14	20.48	19.42	0.66	0.2877	
DESI-207.8335-06.3831[a]	DC	20.61	18.87	17.92	1.00	0.6211	
DESI-208.4386+31.8650	DC	22.96	21.21	19.99	0.15	0.5292	
DESI-208.6688+19.1370	DC	21.00	19.27	18.38	0.50	0.5852	

Table 6 continued on next page

Table 6 *(continued)*

Name	Type	mag_g	mag_r	mag_z	Probability	z_{spec}	z_{phot}
DESI-208.9997+19.7239	REX	21.42	20.39	19.80	0.24	0.3816	
DESI-209.0944+03.6524	DC	21.80	20.20	19.33	0.75	0.2686	
DESI-209.7020-04.3961	DC	22.60	21.17	19.87	0.72		0.417 ± 0.097
DESI-211.6546+38.7004	DC	22.04	20.43	19.59	0.43	0.4952	
DESI-212.5306+62.1634	DC	23.50	21.43	19.84	0.99	0.5431	
DESI-212.7709+23.2324[a]	DC	22.01	20.19	19.17	0.82	0.2873	
DESI-214.7102+19.9447	DC	21.51	19.93	19.08	0.88	0.3740	
DESI-215.1638+12.9717[a]	DC	20.87	19.40	18.55	0.74	0.5937	
DESI-216.0618+45.0242	DC	21.89	20.23	19.34	1.00		0.819 ± 0.100
DESI-217.0936+03.3000	DC	22.25	20.50	19.53	1.00	0.6108	
DESI-217.0950+22.9130	DC	22.06	20.24	19.24	0.82	0.3242	
DESI-217.2090+51.6467	DC	22.21	20.60	19.56	0.22		0.664 ± 0.033
DESI-217.7996+03.0093	DC	22.10	20.73	19.87	0.23	0.1665	
DESI-218.1147+28.7213	DC	21.78	20.50	19.69	0.91	0.3280	
DESI-218.4468+18.7098	DC	22.32	20.67	19.81	1.00	0.2820	
DESI-218.4780+03.0039[g]	DC	23.31	21.47	19.98	0.97	0.6438	
DESI-219.1501+21.1453	DC	22.13	21.10	19.75	0.99	0.6024	
DESI-219.5680+25.0994	DC	19.24	18.28	17.66	0.75	0.3854	
DESI-219.9040+07.3502[a]	DC	22.92	21.18	19.94	0.60	0.5608	
DESI-220.0226+23.8599	DC	21.10	19.74	19.02	0.96	0.4126	
DESI-220.3113+04.4308	REX	21.55	20.49	19.82	0.50	0.3293	
DESI-220.3862-00.8996[k]	DC	22.62	20.80	19.35	0.84	0.5167	
DESI-221.4063+04.9046	DC	19.61	18.58	17.96	0.37	0.3224	
DESI-221.6054+21.6944	DC	19.37	18.21	17.47	0.54		0.071 ± 0.029
DESI-221.9368+23.4043	DC	23.03	21.19	19.99	0.76	0.2818	
DESI-222.2403-07.4558	DC	21.20	19.49	18.56	0.23		0.518 ± 0.147
DESI-222.4812-06.8463	DC	20.82	19.28	18.43	0.30	0.3110	
DESI-222.7391+03.5562	REX	21.11	20.28	19.73	0.13	0.2866	
DESI-223.0001-01.0752[g]	DC	20.42	19.51	18.89	0.86	0.2712	
DESI-223.2085+58.0265	DC	20.18	18.86	18.00	0.11	0.3785	
DESI-223.2358+58.0531	DC	19.46	18.28	17.50	0.86	0.3319	
DESI-223.4373-06.5203	REX	20.08	19.42	18.99	0.20	0.1862	
DESI-224.3832-08.0150	DC	22.55	20.91	19.82	1.00		0.429 ± 0.044
DESI-225.1316+62.7228	REX	21.97	20.67	19.83	0.21		0.421 ± 0.101
DESI-225.5679+15.1661	DC	19.74	18.61	17.88	0.11	0.5515	
DESI-226.1397+28.0320	DC	23.07	21.14	19.91	0.93	0.4815	
DESI-226.2950+17.3451	DC	21.62	20.57	19.88	0.32	0.4836	
DESI-226.3130+41.7447	DC	19.12	18.01	17.31	0.15		0.446 ± 0.100

Table 6 continued on next page

Table 6 *(continued)*

Name	Type	mag_g	mag_r	mag_z	Probability	z_{spec}	z_{phot}
DESI-226.9254+29.9560	REX	20.85	19.68	18.91	0.13	0.1851	
DESI-226.9378+70.1215	DC	20.22	19.76	19.44	0.96		0.509 ± 0.026
DESI-226.9381+05.3823	DC	21.23	19.55	18.64	0.98	0.6187	
DESI-227.7518+10.5556	DC	21.80	20.38	19.63	0.91	0.3586	
DESI-227.9059+05.6220	DC	21.18	20.32	19.75	0.49	0.6132	
DESI-227.9362+06.5090[b]	DC	20.87	19.55	18.65	0.67	0.5379	
DESI-228.4624-03.4634	DC	17.81	16.71	15.91	0.98		0.648 ± 0.019
DESI-228.4698+14.1675	REX	21.38	20.30	19.61	0.11	0.5766	
DESI-228.6370+68.4893	DC	21.64	20.60	19.68	0.18		0.521 ± 0.023
DESI-229.2637+10.0569	DC	22.19	20.94	19.91	0.87	0.5636	
DESI-229.7213+09.2304	REX	20.58	19.59	18.89	0.57	0.6645	
DESI-229.7448+27.3746	DC	21.16	19.44	18.57	0.10	0.6638	
DESI-230.5321+32.8538	DC	22.38	20.52	19.55	1.00	0.6249	
DESI-230.6318-00.7509[g]	DC	21.08	19.69	18.79	0.89	0.5028	
DESI-230.9520+10.2717	REX	21.28	20.09	19.40	0.94	0.4470	
DESI-230.9711+04.9138	DC	21.57	20.39	19.44	0.36	0.6340	
DESI-230.9776+67.6248	DC	20.49	18.70	17.76	0.73		0.752 ± 0.020
DESI-231.0060+49.1881	DC	22.32	20.83	19.64	0.84	0.5332	
DESI-232.6507+80.8392	DC	22.71	20.89	19.89	0.25		0.556 ± 0.087
DESI-233.2341+50.1953	DC	22.13	20.49	19.63	0.97	0.5655	
DESI-234.8063+11.7178	DC	22.23	20.38	19.13	0.91	0.5713	
DESI-235.0039+32.6092	DC	21.94	20.14	19.25	0.41	0.2990	
DESI-235.2734+07.5424	DC	22.77	21.09	19.78	0.58	0.2481	
DESI-235.5208+40.3319	DC	20.81	19.58	18.80	0.87	0.4568	
DESI-235.7400+14.8762	REX	21.39	20.54	19.74	0.99	0.4532	
DESI-236.5762+48.3642	DC	20.31	19.35	18.60	0.24	0.2110	
DESI-236.5969+23.9051	DC	22.49	20.50	19.23	0.52	0.3051	
DESI-237.7649+06.8422	DC	22.88	21.09	19.98	0.46	0.4967	
DESI-238.0854+61.6594	DC	19.49	18.55	17.87	0.37	0.4605	
DESI-238.4959+16.3935	DC	18.90	17.99	17.34	1.00	0.3838	
DESI-238.5690+04.7276	DC	19.87	18.96	18.32	1.00	0.5394	
DESI-238.6455+44.3415	DC	21.58	19.83	18.91	0.22	0.5738	
DESI-238.6575+46.1560	DC	22.49	20.89	19.68	0.53	0.7298	
DESI-239.7952+07.5133	DC	18.83	17.72	17.02	0.12	0.4492	
DESI-241.7346+42.1102[k]	REX	21.65	20.08	19.24	1.00	0.8924	
DESI-241.7375+18.1017	DC	21.94	20.25	19.02	0.98	0.2258	
DESI-241.8696+05.8963	DC	19.73	19.08	18.62	0.87	0.5909	
DESI-242.2528+04.4242	DC	20.89	19.65	18.94	0.41	0.2835	

Table 6 continued on next page

Table 6 *(continued)*

Name	Type	mag_g	mag_r	mag_z	Probability	z_{spec}	z_{phot}
DESI-244.5857+54.5052[e]	DC	17.42	16.56	15.84	0.55	0.3616	
DESI-246.0592+10.6100	DC	22.75	21.19	19.62	0.99	0.6235	
DESI-246.4202+33.2659	DC	21.81	20.41	19.51	0.75		0.992 ± 0.120
DESI-246.6316+49.1584	DC	22.47	20.65	19.57	0.63	0.2777	
DESI-247.9945-01.6681	DC	18.82	17.84	17.17	0.72		0.733 ± 0.150
DESI-248.9636+46.8071	DC	21.28	19.49	18.47	0.39	0.5405	
DESI-249.0881+27.7159	DC	19.07	18.08	17.40	0.99	0.3342	
DESI-249.3569+31.6652	REX	21.41	20.45	19.99	0.99	0.4376	
DESI-250.4830+66.2103	DC	21.90	20.13	19.17	0.58		0.543 ± 0.066
DESI-250.8015+21.3635	DC	22.08	20.47	19.43	0.50	0.4826	
DESI-251.4915+22.9241	DC	23.64	21.37	19.71	0.53	0.3371	
DESI-251.7677+11.2970[a]	REX	21.45	20.27	19.41	1.00		0.220 ± 0.141
DESI-251.8574+09.6103	DC	20.87	19.56	18.88	0.99		0.319 ± 0.014
DESI-252.1292+63.7872	DC	22.82	20.82	19.35	0.99	0.5302	
DESI-253.0914+55.0867	REX	22.34	20.67	19.83	1.00		0.462 ± 0.114
DESI-253.2568+30.8665	DC	19.62	18.52	17.81	0.37	0.5169	
DESI-254.2942+31.8480[a]	REX	21.24	20.19	19.27	1.00	0.3915	
DESI-255.9749+41.6783	DC	18.96	17.52	16.03	0.29	0.4128	
DESI-256.1498+08.2505	REX	21.86	20.60	19.85	0.10		0.485 ± 0.093
DESI-256.2179+07.8065	DC	21.10	19.51	18.66	0.37		0.400 ± 0.017
DESI-256.7414+25.8919	DC	19.25	18.34	17.67	0.21	0.5953	
DESI-257.0428+11.8169	DC	22.14	20.36	19.46	0.94	0.5460	
DESI-259.6311+23.7908	REX	20.35	19.76	19.30	0.99	0.6059	
DESI-259.8396+24.6880	DC	22.42	20.93	19.80	1.00	0.4894	
DESI-261.7825+13.0155	DC	21.68	19.96	18.94	0.30		0.507 ± 0.015
DESI-264.2946+26.8373	DC	19.21	18.08	17.33	0.96	0.4208	
DESI-266.3918+27.2260	DC	21.66	19.84	18.77	0.19		0.751 ± 0.054
DESI-267.9412+43.5847	DC	22.09	20.31	19.28	0.28	0.7418	
DESI-267.9501+43.5780	DC	21.11	19.93	19.13	0.74		0.559 ± 0.268
DESI-270.2102+35.8525	DC	20.67	19.37	18.46	0.94		0.807 ± 0.034
DESI-270.4979+48.3192	DC	22.81	21.03	19.81	0.88	0.4020	
DESI-270.5244+35.2017	DC	21.08	20.39	19.92	0.99		0.343 ± 0.025
DESI-273.3831+34.2652	DC	20.26	18.89	18.02	0.10		0.217 ± 0.011
DESI-273.6883+54.7764	DC	20.58	19.09	18.31	0.52		0.510 ± 0.016
DESI-274.3781+42.3118	DC	21.55	19.68	18.69	0.51	0.5793	
DESI-275.2007+40.0650	DC	20.27	18.86	18.04	0.77		0.848 ± 0.067
DESI-276.8661+51.8599	DC	21.45	20.17	19.33	0.77		0.783 ± 0.023
DESI-277.7776+57.3732	DC	22.05	20.24	19.24	0.13		0.789 ± 0.068

Table 6 continued on next page

Table 6 *(continued)*

Name	Type	mag_g	mag_r	mag_z	Probability	z_{spec}	z_{phot}
DESI-279.6919+47.5645	DC	23.08	21.07	19.81	0.97		0.388 ± 0.015
DESI-281.6950+76.1017	DC	22.51	20.56	19.35	1.00		0.721 ± 0.054
DESI-282.8164+66.4911	DC	22.09	20.22	19.09	0.83		0.667 ± 0.018
DESI-283.8139+45.1750	DC	23.67	21.71	19.72	0.81		0.692 ± 0.172
DESI-286.9816+69.1405	DC	22.95	21.01	19.79	0.36		0.181 ± 0.014
DESI-290.9468+61.3182	DC	21.51	20.25	19.37	0.91		0.575 ± 0.018
DESI-291.7549+66.7310	DC	21.53	20.29	19.10	0.30		0.695 ± 0.037
DESI-291.8967+54.2998	DC	22.30	20.78	19.86	0.49		0.588 ± 0.026
DESI-296.6448+60.3651	DC	21.13	19.35	18.48	0.93	0.2854	
DESI-308.6348-47.1690	REX	21.58	20.48	19.85	0.87		0.729 ± 0.062
DESI-308.8072+00.7818	DC	21.26	19.62	18.77	0.59	0.3933	
DESI-310.9666+03.2223	DC	22.76	21.02	19.89	0.15	0.3051	
DESI-313.3618-09.2758	DC	19.59	18.49	17.70	0.45		0.419 ± 0.016
DESI-313.5823-41.4077	REX	22.18	20.33	19.03	0.28		0.406 ± 0.224
DESI-314.7376+04.7259	DC	18.52	17.68	17.05	0.42	0.5939	
DESI-315.3295+02.2958	DC	16.15	15.22	14.53	0.67	0.7481	
DESI-316.8445-00.9920	REX	21.44	20.42	19.71	0.13	0.5142	
DESI-319.1672-01.5035	DC	22.81	21.80	19.92	0.26	0.1627	
DESI-319.4948-00.7468	REX	22.56	21.44	19.99	1.00	0.3865	
DESI-319.5281+16.9379	DC	20.46	20.06	19.80	0.73	0.6610	
DESI-319.7068-63.3875	REX	21.80	20.62	19.88	0.33		0.656 ± 0.053
DESI-320.1446-11.1251	DC	22.85	21.04	19.98	0.47	0.5877	
DESI-320.8584+01.8867	DC	23.33	21.39	19.91	0.39	0.5249	
DESI-321.3061-00.0295	DC	21.94	20.18	19.29	0.15		0.618 ± 0.199
DESI-321.5604+09.8332	DC	20.04	18.53	17.73	0.51	0.5691	
DESI-322.6011-61.9086	REX	21.95	20.06	19.18	0.74		0.828 ± 0.056
DESI-324.8366-63.7250	REX	21.75	20.50	19.81	0.74		0.512 ± 0.086
DESI-326.2881+19.8848	REX	20.94	20.24	19.79	0.99	0.6892	
DESI-326.7119-43.0078	REX	23.08	21.30	19.48	1.00		0.831 ± 0.078
DESI-327.4249-44.1038	REX	21.23	20.20	19.56	1.00		0.628 ± 0.038
DESI-327.4427-00.3822	REX	21.18	20.33	19.80	0.36	0.5660	
DESI-328.0860-43.5877	REX	19.91	19.01	18.39	0.38		0.582 ± 0.047
DESI-328.7427+16.3475	REX	21.08	19.97	19.35	0.52	0.5108	
DESI-329.5066+06.6401	DC	21.02	19.67	18.80	0.67	0.5044	
DESI-330.1481+23.6703	DC	20.68	19.25	18.44	0.11	0.6629	
DESI-330.1499+07.1124	DC	22.36	20.64	19.66	0.17	0.3633	
DESI-330.4536+01.8039	DC	21.54	20.20	19.34	0.89	0.4534	
DESI-330.5620+10.6918	REX	21.89	20.49	19.49	0.13	0.3004	

Table 6 continued on next page

Table 6 *(continued)*

Name	Type	mag_g	mag_r	mag_z	Probability	z_{spec}	z_{phot}
DESI-331.9712-00.6607	DC	20.92	20.29	19.84	0.10	0.5372	
DESI-333.8922-46.6457	REX	20.51	19.91	19.50	0.34		0.336 ± 0.049
DESI-334.2188-08.9595	DC	21.84	20.06	19.13	1.00	0.3127	
DESI-334.5268+20.8617	DC	22.61	20.70	19.22	0.89	0.1981	
DESI-334.7964+08.9935	DC	21.25	19.50	18.61	0.16		0.440 ± 0.176
DESI-335.2071-11.9607	DC	22.04	20.18	19.23	0.36		0.366 ± 0.013
DESI-336.7102+15.1795	DC	19.06	18.15	17.51	0.59	0.5059	
DESI-338.1775+01.6182	DC	18.27	17.27	16.50	0.35	0.4101	
DESI-338.9341+07.7338	DC	20.87	19.37	18.56	0.70	0.4919	
DESI-339.3998-12.0424	REX	20.46	20.04	19.86	0.60		0.432 ± 0.028
DESI-340.0966+26.9614	DC	21.44	19.83	18.99	1.00	0.2671	
DESI-340.6218+03.2048	DC	22.13	20.27	18.93	0.94	0.5738	
DESI-340.7868-55.1416	REX	19.82	19.05	18.52	0.99		0.780 ± 0.046
DESI-341.2747+00.6718	REX	20.95	20.06	19.54	0.37	0.6426	
DESI-341.8329+18.0226[a]	DC	22.56	20.61	19.36	0.63	0.3000	
DESI-342.0957+01.8350[j]	DC	21.29	19.39	18.18	0.27	0.5150	
DESI-342.2726+19.8035	DC	22.04	20.26	19.23	0.31	0.4892	
DESI-343.7432+03.9726	REX	21.30	20.40	19.85	0.10		0.237 ± 0.023
DESI-344.5905+05.0181	DC	19.96	18.87	18.12	0.95	0.6923	
DESI-344.9569+12.0924	DC	21.95	20.09	18.93	0.86	0.2568	
DESI-344.9861-02.7461	DC	20.91	19.49	18.64	0.97	0.4047	
DESI-345.8679+08.9273	DC	21.55	20.09	19.32	0.96	0.5559	
DESI-346.1290-60.6806	REX	21.75	20.64	19.98	0.95		0.619 ± 0.046
DESI-346.6288+27.4720	DC	18.37	16.79	15.78	0.47	0.5264	
DESI-346.7222-12.6443	DC	20.72	19.41	18.68	1.00		0.394 ± 0.014
DESI-346.7984-12.4431	DC	23.32	21.38	19.94	0.24		0.331 ± 0.014
DESI-347.1009+28.9983	DC	21.04	19.66	18.87	1.00	0.3953	
DESI-347.3571+28.3380[a]	DC	21.33	19.65	18.76	0.76	0.3061	
DESI-347.7996-09.4026	DC	22.44	20.76	19.87	0.94	0.6376	
DESI-347.9137-08.0379	REX	22.00	20.28	19.56	0.12	0.3190	
DESI-348.1504-03.4410	DC	22.28	20.55	19.43	1.00	0.3298	
DESI-348.2452+04.8615	DC	21.28	19.70	18.73	0.18	0.3382	
DESI-348.3888-00.0460	DC	20.38	19.96	19.63	0.12	0.5643	
DESI-349.3386+14.7537	DC	20.57	19.39	18.72	0.36	0.4549	
DESI-349.5061+13.3835	DC	20.90	19.34	18.49	0.74	0.5571	
DESI-349.8902-01.1028	DC	22.51	20.66	19.30	0.90	0.5712	
DESI-349.8938+11.8378[a]	DC	22.03	20.65	19.82	1.00	0.5206	
DESI-350.0271-12.0343	DC	18.48	17.61	16.98	0.83		0.400 ± 0.018

Table 6 continued on next page

Table 6 *(continued)*

Name	Type	mag_g	mag_r	mag_z	Probability	z_{spec}	z_{phot}
DESI-350.1155-00.5958	DC	17.40	17.75	18.45	0.72	0.4668	
DESI-350.2503-13.4958	DC	23.02	21.08	19.53	0.98		0.683 ± 0.067
DESI-350.8416+10.7701	DC	21.21	19.54	18.72	1.00	0.5166	
DESI-351.8760-10.4864	DC	22.50	20.69	19.68	0.54	0.3882	
DESI-352.1378-14.5816	REX	20.76	19.58	18.89	0.34		0.410 ± 0.049
DESI-352.2239+00.0936[e]	DC	23.16	21.35	19.99	0.71	0.4390	
DESI-352.6210-05.0038	REX	21.35	20.37	19.78	0.79	0.6345	
DESI-352.9172-10.0133	DC	23.79	21.54	19.76	1.00	0.2137	
DESI-353.1493-00.0513[e]	DC	23.78	21.72	19.94	0.97	0.5917	
DESI-353.2414+07.2878	DC	19.67	19.15	18.78	0.18	0.2956	
DESI-353.9228+00.6577	REX	21.17	20.20	19.46	0.61	0.4617	
DESI-355.1190+29.7964	DC	22.43	21.03	19.99	0.99	0.4956	
DESI-355.2734+24.1552	DC	23.17	21.24	19.78	0.37	0.2531	
DESI-355.7900-13.8140	DC	22.17	20.59	19.75	0.97		0.736 ± 0.014
DESI-356.4023+14.0221	DC	19.61	19.06	18.75	0.24	0.2247	
DESI-356.8749-00.1896	DC	21.70	20.02	19.19	0.59		0.768 ± 0.097
DESI-357.3211-04.4758	DC	22.82	20.90	19.47	0.43	0.7070	
DESI-358.0861+18.1055	DC	22.29	20.57	19.64	0.76	0.2761	
DESI-358.4109-13.2745	DC	20.57	20.04	19.76	0.68		0.501 ± 0.033
DESI-358.5111-10.0359	DC	21.26	19.80	18.85	0.22	0.4271	
DESI-358.6999+05.0447	DC	21.78	20.12	19.22	1.00	0.4691	
DESI-359.1421+02.6922	DC	22.22	20.63	19.09	0.57	0.7455	
DESI-359.7217+01.4018	DC	22.61	21.06	19.48	0.93	0.3398	
DESI-359.8831-02.2601	DC	22.32	20.53	19.64	0.45	0.6462	
DESI-359.9690+03.3971	REX	21.00	20.30	19.88	0.61	0.2749	

NOTE—Four hundred and fifty-six of the above 897 Grade C lens candidates have spectroscopic redshifts from SDSS DR16. All spectroscopic redshift uncertainties $< 3.9 \times 10^{-4}$. For references of known lenses, see NOTE for Table 4.